TAMPEREEN TEKNILLINEN YLIOPISTO
TAMPERE UNIVERSITY OF TECHNOLOGY

JOSHUA FILLION

DEVELOPMENT AND OPTIMIZATION OF CURTAIN WALL CONNECTION SYSTEM

Master of Science Thesis

Examiner: Assoc. Prof. Sami Pajunen
Examiner and topic approved on 24 September 2018

ABSTRACT

JOSHUA FILLION: DEVELOPMENT AND OPTIMIZATION OF CURTAIN WALL CONNECTION SYSTEM
Tampere University of technology
Master of Science Thesis, 73 pages, 43 Appendix pages
November 2018
Master's Degree Program in Civil Engineering
Major: Structural Engineering
Examiner: Associate Professor (tenure track) Sami Pajunen

Keywords: optimization, parametric modelling, curtain wall, connection, anchor, finite element

A total of 8 different connections (4 custom profiles and 4 L-profiles) for curtain wall systems are developed while investigating the benefits of applying modern numerical analysis, optimization and parametric design techniques to extruded aluminium alloy profile design. Investigations of modern connection designs offered by manufacturers is done. The connections are developed and designed according to relevant Eurocode and curtain walling standard specifications. Optimization algorithm results, material savings and connection designs are presented.

TIIVISTELMÄ

JOSHUA FILLION: JULKISIVUJÄRJESTELMÄN KIINNIKERATKAISUN KEHITYS JA OPTIMOINTI
Tampereen teknillinen yliopisto
Diplomityö, 73 sivua, 43 liitesivua
Lokakuu 2018
Rakennustekniikan diplomi-insinöörin tutkinto-ohjelma
Pääaine: Rakennesuunnittelu
Tarkastaja: Associate Professor (tenure track) Sami Pajunen

Avainsanat: optimointi, parametrinen mallinnus, julkisivujärjestelmä, kiinnike, elementti menetelmä

Työssä kehitetään yhteensä 8 kpl alumiiniselle julkisivujärjestelmälle sopivaa liitosta (4 kpl erikoisprofiilia ja 4 kpl L-profiilia). Kehityksen ohella tutkitaan modernien parametristen mallintamismenetelmien, optimointialgoritmien ja numeeristen laskentamenetelmien mahdollisia hyötyjä alumiinisten pursotettujen profiileiden suunnittelussa. Markkinoilla tarjolla olevia ratkaisuja selvitetään. Liitokset kehitetään ja suunnitellaan Eurokoodin ja asianmukaisten tuotestandardien vaatimusten mukaisesti. Lopuksi esitetään optimointialgoritmien tulokset, materiaalisäästöt ja liitosratkaisut.

PREFACE

I'd like to thank Jari Mäkinen for providing this interesting topic and the guidance and inspiration he has offered throughout my studies. I'd also like to thank Sami Pajunen and Vesa Knuutila for their guidance.

I'm also grateful for the support provided by my fiancée Julianna and two chihuahuas Ludvig and Schnappi.

Tampere, 21.11.2018

Joshua Fillion

CONTENTS

LIST OF FIGURES

LIST OF SYMBOLS AND ABBREVIATIONS

ACT	Application customization toolkit.
EC1	Eurocode 1
EC1-1-4	Part 1-4 of Eurocode 1
EC9-1-1	Part 1-1 of Eurocode 9
EC9-1-3	Part 1-3 of Eurocode 9
EC9-1-5	Part 1-5 of Eurocode 9
GMNA	Geometrically and materially non-linear analysis
GMNIA	Geometrically and materially non-linear analysis with imperfections
HAZ	Heat Affected Zone
IGU	Insulated glass unit
MNA	Materially non-linear analysis
NA	National Annex
A	Bolt nominal cross-section area
A_s	Bolt stress area
α	Coefficient of thermal expansion
α_b	Coefficient
α_v	Coefficient
$\beta_{p,Rd}$	Design punching resistance of fastener.
c_{dir}	Directional factor
$c_{p,net}$	Net pressure coefficient
c_r	Roughness factor
c_{season}	Seasonal factor
c_0	Orography factor
D_L	Total damage of Palmgren-Miner summation.
D_{lim}	Maximum permissible damage
d	Bolt diameter
d_m	Mean across the flats dimensions of the bolt head or washer diameter, whichever is smaller.
d_0	Bolt hole diameter
e_1	End distance
e_2	End distance
e_3	End distance for slotted holes
e_4	Edge distance for slotted holes
ϵ	Coefficient
$F_{b,Rd}$	Design bearing resistance of fastener
F_{Ed}	Design load
F_{Rd}	Design resistance
$F_{t,Rd}$	Design tension resistance of fastener

$F_{v,Rd}$	Design shear resistance of fastener
$f_{eq,Rd}$	Equivalent von Mises design strength
$f_{Fat1.4,Rd}$	Maximum permissible nominal principle stress for detail 1.4
$f_{Fat1.6,Rd}$	Maximum permissible nominal principle stress for detail 1.6
$f_{Fat15.2,Rd}$	Maximum permissible nominal principle stress for detail 15.2 when (R=-1)
$f_{Fat15.2,Rd2}$	Maximum permissible nominal principle stress for detail 15.2 when (R=0)
f_o	0.2 % proof strength
f_u	Ultimate material strength
f_{ub}	Ultimate strength of bolt material
$f(x)$	Objective function
G_d	Design load, self-weight
$g(x)$	Constraint function
γ_{Ff}	Partial factor for uncertainties in loading spectrum and analysis of Response.
γ_{Mf}	Partial factor for uncertainties in materials and execution.
γ_{M1}	Partial factor for resistance
γ_{M2}	Partial factor for bolted connections
$I_v(z)$	Turbulence intensity at height z
k_l	Turbulence factor
k_r	Terrain factor
k_1	Coefficient
k_2	Coefficient
m_1	Inverse slope of S-N curve $N \leq 5x10^6$ cycles
m_2	Inverse slope of S-N curve for $5x10^6 < N \leq 10^8$ cycles
N_g	Number of gust loads
N_i	Predicted number of cycles to failure of a stress range $\Delta\sigma_i$
n_i	Equivalent number of cycles
p_1	Spacing
p_2	Spacing
$Q_{d.sill}$	Design sill load
$Q_{d.wind}$	Design wind load
$Q_{k,wind}$	Characteristic wind reaction force.
q_k	Line load
q_p	Peak velocity pressure
R	Stress ratio

R_{load}	Load ratio
$R_{Self-weight}$	Design force reaction for self-weight
$R_{sill.load.\max}$	Design force reaction for sill loads
$R_{wind.load}$	Design force reaction for wind load
ρ	Air density
S_k	The effect due to 50 years return period wind action.
ΔS	A percentage of S_k
$\sigma_{eq,Ed}$	Design stress
σ_{max}	Maximum absolute stress.
σ_v	Standard deviation of turbulent wind component
$\Delta\sigma_c$	Reference value of fatigue strength at 2×10^6 cycles
$\Delta\sigma_i$	Stress range for principle stresses at constructional detail
T_L	Design life
T_S	Safe life
t	Thickness of the plate
t_p	Thickness of the plate under bolt head
$v_{b,0}$	Basic wind velocity
$v_m(z)$	Mean wind velocity
x	Variable
z_{min}	Minimum height
z_0	Roughness length
$z_{0,II}$	Roughness length for terrain category II

1 INTRODUCTION

A connection system comprising of two different sizes and types of connections for Purso Oy's aluminium alloy curtain walling system P50L will be developed while investigating the benefits of applying modern parametric modelling, analysis and optimization methods to the design process. The final designs must fulfil current Eurocode and product standard requirements. The connection system should be relatively simple and cost effective. Design limits need to be provided for ease of use in curtain wall design.

The design process is augmented by extensive application of parametric finite element analysis and optimization algorithms to find better designs of connection profiles and minimize material use. The finite element analysis (FEA) software Ansys Workbench R19.1 is used in conjunction with an application customization toolkit (ACT) extension; Sorvi Design Booster, provided by Sorvimo Optimointipalvelut Oy. The computer aided design (CAD) program used for modelling parametric geometry is Autodesk Inventor Professional 2018.

In theory, the number of possible curtain wall configurations is endless; however, the goal is for the connection system to be applicable to only the great majority of cases that Purso Oy encounters on a regular basis. Therefore, limits are set for defining governing design loads which have a large influence on the final designs of the connections. Special cases are not considered, as these are handled on a case by case basis. As agreed with Purso Oy, the maximum span possible between connections (simply supported) is taken as 3 m, glass width as 3 m and building height as 30 m. The connection design is limited to the connection profiles and fasteners; the underlying main structure is not considered. Mullion profile wall strengths must be investigated separately in conjunction with overall curtain wall design and analysis, as wall material thicknesses and stiffener profile use vary.

The research method used in this thesis was primarily literature investigation; comprising of investigation of design standards and modern connection designs and specifications. Information on methods of connection used by curtain wall manufacturers is commonly available on their websites; however, in many cases connections designs are presented without much information on load capacity. This is due to the bespoke nature of curtain walls. Details and guidance of connection methods often encountered in the industry were provided by Purso Oy.

2 CURTAIN WALLS

Curtain wall systems constructed from extruded aluminium alloy profiles and infill panels are a common sight in modern construction, particularly in high rise structures. These are complex systems which need to be designed with care to ensure structural integrity, insulation and air and water tightness under various loading conditions. Differential movements and building tolerances between the underlying load bearing structure and curtain wall system must be considered. The application of Eurocodes to curtain walls is supported by the curtain wall product standard [1].

Curtain walls consist primarily of vertical and horizontal frame members with infill panels and are designed as self-supporting structures which transmit imposed loads and self-weight to an underlying load bearing structure; however, they do not contribute to the load bearing or stability of the building [2].

Curtain wall mullions (primary vertical members) cannot be fabricated continuously for very tall walls due to manufacturing and logistical constraints. However, in many cases they can still be analysed as continuous beams. The joining profiles used to connect Purso Oy's mullion profiles at expansion joints are loose-fitting and therefore not thought to transfer bending moments. (see Figure 1). The mullions are only analysed as continuous beams up to a maximum length of 6.6 m; determined by Purso Oy's manufacturing constraints. Transoms (horizontal secondary members of frame) are analysed as single span beams.

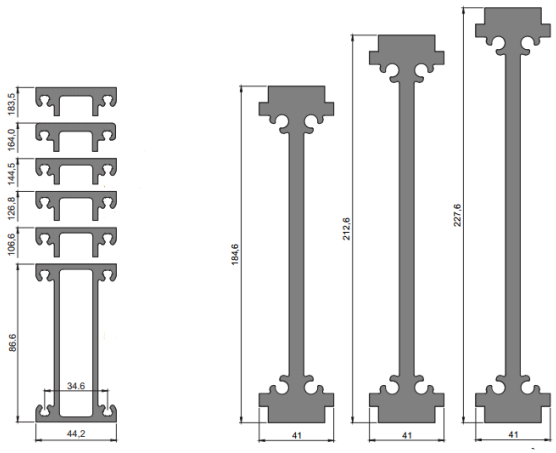

Figure 1 *P50L frame connection profiles. Figure adapted from [3].*

Wind loads act perpendicularly to the curtain wall surface. The load is transferred from the infill panels to the frame members, which then transfer loads to the underlying anchoring connections. In design situations, it is often enough to simplify the total wind

load transfer from the infill panels to the frame members as uniform distributed loading. Trapezoidal load patterns can be used if higher accuracy is required (see Figure 2). Anchoring connections are typically modelled as pinned supports [4].

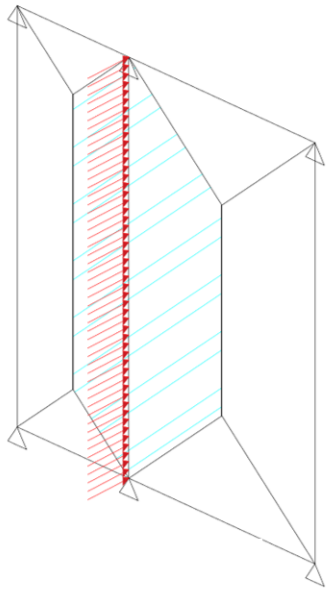

Figure 2 *Trapezoidal load distribution. The small triangles represent pinned supports.*

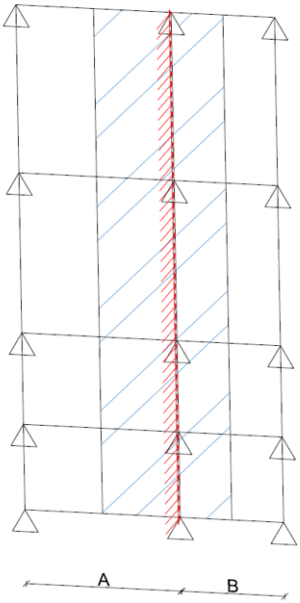

Figure 3 *Load area used for designing connections.*

The design forces in the connections can be solved for simply by analysing the mullions as beams under uniform distributed loading. The area from which wind pressure loading is collected for each mullion can be seen in Figure 3. Half of the loading from side A and half of the loading from side B is collected.

3 P50L SYSTEM

The P50L thermally insulated façade system by Purso Building Systems is CE marked according to the standard EN 13830. The frame width used in the system is 50 mm. Figure 4 shows an example of a basic frame profile. The specific dimensions vary depending on profile size. Other profile shapes are also available, but these special cases are not considered in the development of the connection system.

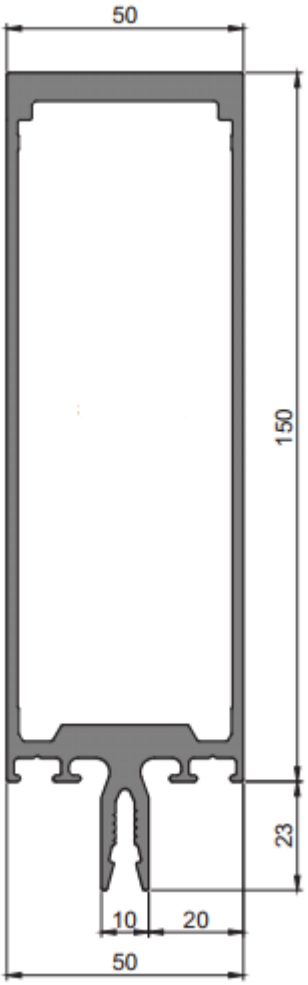

Figure 4 *P50L frame profiles. Figure Adapted from [3].*

Frame depths up to 250 mm are available. Up to 62 mm thick insulated glass units (IGU) can be accommodated. The glazing is held in place mechanically (dry-glazed) via rubber gaskets and pressure plates (glazing beads) fastened to the main frame structure via self-tapping stainless-steel screws.

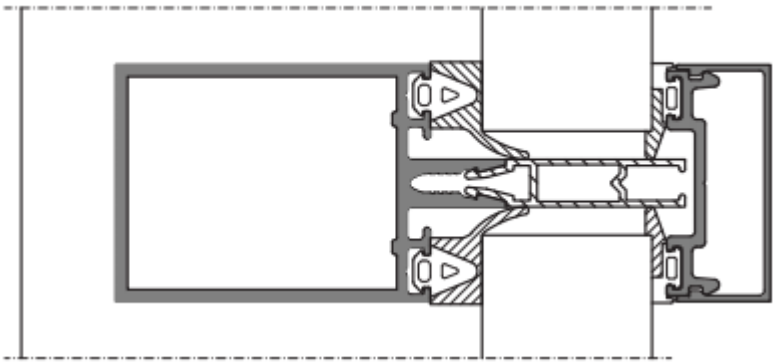

Figure 5 *P50L dry glazing assembly. Figure adapted from [3].*

Figure 5 depicts the dry glazing assembly. Notice the thermal break between the pressure plate and frame profile. The break reduces thermal conductivity between internal and external surfaces. Thermal breaks are often fabricated from high-performance poly-amide via an extrusion process [4].

The curtain wall frame profiles are typically manufactured from EN-AW 6063 T5 aluminium alloy via extrusion process with manufacturing tolerances according to EN 755-9 or EN 12020-2. The normal maximum delivery length of the profiles is 6.6 m, but longer lengths (up to 7.8 m with anodized surface treatment) are available on special agreement. The profiles can be finished with an anodized surface treatment or powder coating [3]. Figure 6 shows a complete P50L system façade.

Figure 6 *Revontuli shopping centre. Image courtesy of Purso Oy.*

4 MODERN ANCHORAGE METHODS

Curtain walls are generally anchored to the underlying load-bearing structure at floor lines by means of:

- Extruded aluminium anchor profiles;
- Steel anchor profiles with separator pads;
- Bolts and screws.

Other methods of anchorage are also used, such as self-tapping stainless-steel screws screwed directly through the side of the façade profile screw channel. This method has often been used for connecting strips of windows (such as stairwell glazing) to the load-bearing structure. An example of this connection can be seen in Figure 7.

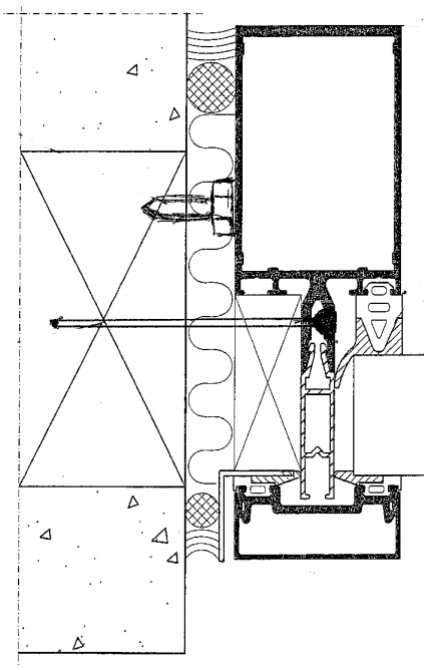

Figure 7 *Direct connection to wall via screw. Image provided by Purso Oy.*

The bolt seen in the Figure 7 beside the side wall of the profile is to prevent torsional deflection. The glazing is supported at the edge of the profile, which causes eccentric wind load transfer. The following subsections provide insight into what other solutions are generally available on the market. The amount of connections and solutions available on the market is wide-ranging; therefore, only a limited amount is presented here for sake of brevity. The load ranges supported by cast in channels will be considered in the design of the connection brackets for Purso Oy, as it is possible that they could also be used in the future.

4.1 HALFEN HCW

The company HALFEN based in Langenfeld, Germany produces an extensive range of curtain wall support systems. The systems include anchor channels, T-bolts, and curtain wall brackets (HALFEN HCW). Anchor channel designs are available for both top and edge embedding to concrete slabs. The curtain wall brackets connect the mullions to the anchor channels (see Figure 8).

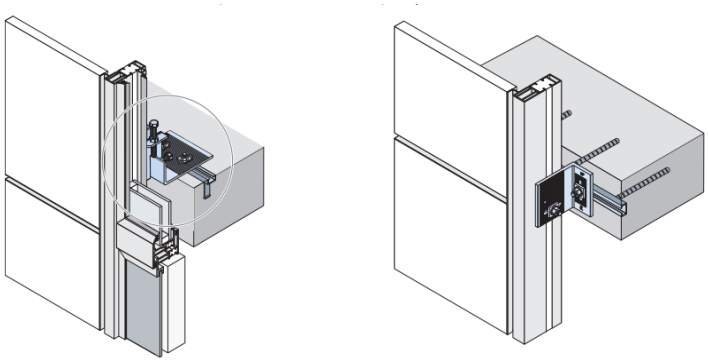

Figure 8 *HALFEN curtain wall support systems. Figure adapted from [5].*

There are two main types of anchor channel lip designs available: plain lipped channels (HALFEN HTA) and serrated lipped types (HALFEN HZA). Each lip type uses a serrated or non-serrated T-bolt type. The serrated model HALFEN HZA provides support to relatively large longitudinal (along channel) shear forces. M12, M16 and M20. The two different models can be seen in Figure 9.

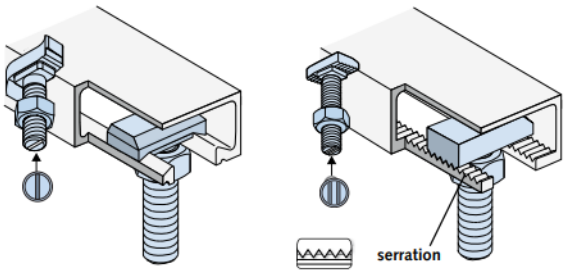

Figure 9 *HALFEN HTA and HZA anchor channels. Figure adapted from [5].*

There are three main types of brackets available; HCW-ED (three sizes available), HCW-EW (three sizes available), and HCW-B (7 sizes available). The brackets HCW-ED and HCW-EW (see Figure 9) are of the commonly seen L-profile types of brackets used for connecting post and beam façades directly to the edge of concrete slabs. HCW-ED carries horizontal and vertical loads (wind and self-weight), while HCW-EW is designed to carry

wind load only. Both types are made from “high strength aluminium alloy” (exact type not specified).

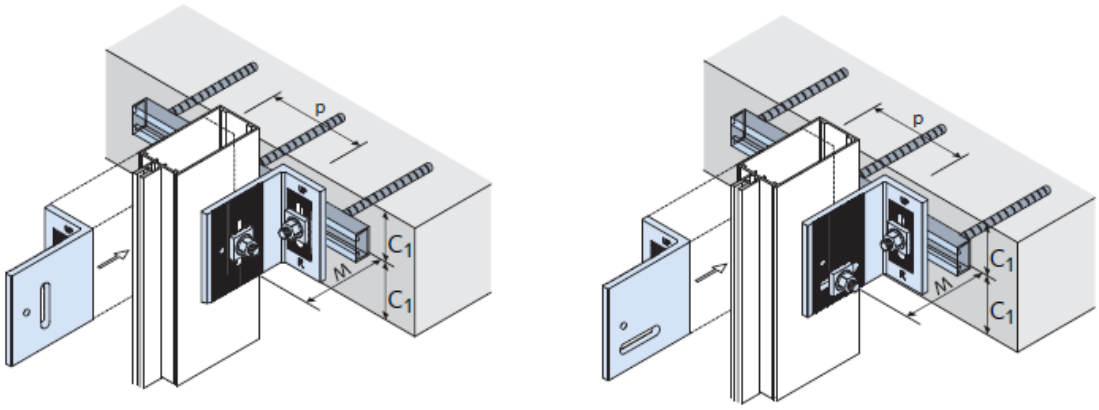

Figure 10 *HALFEN HCW-EW and HCW-ED brackets. Figure adapted from [5].*

Some of the key benefits of HCW-EW and -ED brackets according to HALFEN are:

- suitable for dynamic loads;
- adjustable;
- no welding;
- cost effective installation;
- no special tools required;
- many sizes available.

HCW-B brackets are designed for connection to the top of floor slabs. All sizes of brackets are fabricated from S355 grade steel. The benefits provided by these brackets according to HALFEN are largely the same as for -ED and -EW brackets. The brackets are easily adjustable in all three planes via adjustments screws. Many sizes are available. HCW-B1 provides 3 sizes for two load ranges and -B2 provides 4 different lengths of base plates for variable edge distances. Figure 11shows an HCW-B bracket.

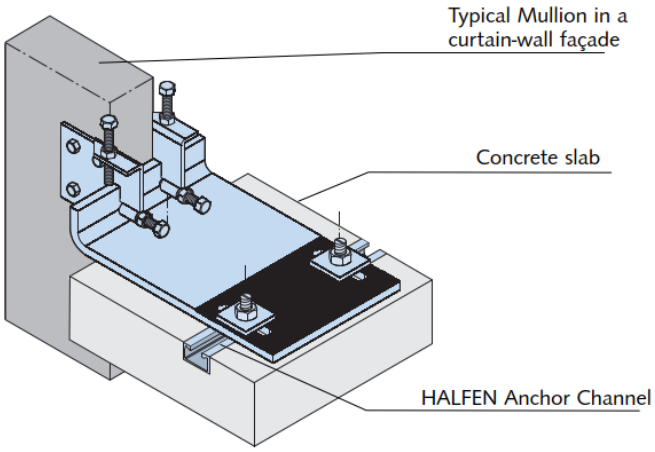

Figure 11 *HALFEN HCW-B1. Figure adapted from [5].*

HALFEN provides interaction diagrams for all their connection brackets. Table 1 shows the extreme values of the supported loads.

Table 1 *Extreme values of supported loads for HALFEN HCW brackets.*

Bracket	Vertical load [kN]	Horizontal load [kN]
HCW-ED 1 (small)	6.13	5.67
HCW-ED 2 (medium)	5.83	7.78
HCW-ED 3 (large)	5.61	9.31
HCW-EW 1(small)	-	5.67
HCW-EW 2 (medium)	-	7.78
HCW-EW 3 (large)	-	9.31
HCW-B 1	4.0 and 12.0	7.0 and 20.0
HCW-B 2	17.19	14.40

The adjustability ranges for each bracket type can be seen in Table 2. Horizontal adjustability depends on the method used to connect brackets to the underlying structure and profile width; therefore, values are not listed here. When using HALFEN anchor channels, adjustability greater than ± 25 mm is easily achievable.

Table 2 *Adjustability of HALFEN HCW brackets.*

Bracket	Height [mm]	Depth [mm]
HCW-ED 1 (small)	± 26 mm	± 26 mm
HCW-ED 2 (medium)	± 26 mm	± 26 mm
HCW-ED 3 (large)	± 26 mm	± 26 mm
HCW-EW 1(small)	± 26 mm	-
HCW-EW 2 (medium)	± 26 mm	-
HCW-EW 3 (large)	± 26 mm	-
HCW-B 1	± 13 mm	± 25 mm
HCW-B 2	± 24 mm	± 32 mm

The adjustability of the connections is in line with the tolerances defined in building standards for wood, steel, aluminium and concrete structures (see Section 6.4)

4.2 PEC Group Façade technology

PEC Group is a part of Hilti Group from Liechtenstein Germany. The company offers cast in channels and connections for various façade types, including curtain walls. Figure 12 shows two connection solutions from PEC; the one on the left is for top of slab installation, while the other is for edge of slab installation. Both connections can be adjusted in all three planes.

Figure 12 *PEC Curtain wall brackets. Figure adapted from [6].*

Standard connection solutions are not available in PEC Groups product catalogue. This is because most of the solutions they provide are not standard. The solutions are designed on a case by case basis according to project requirements. Brackets can be fabricated from hot dip galvanized steel and aluminium. All components are produced via casting process.

The cast in channel range PEC-TA consists of cold- and hot-rolled smooth and serrated cast in channels. Channels with European technical Approval are available. Figure 13 shows a general view of a channel specimen.

Figure 13 *PEC-TA cast-in channels. Figure adapted from [6].*

Table 3 *Channel sizes available from PEC.*

Channel Profile	Tension resistance of channel lips per bolt. [kN]	Shear resistance of channel lips per bolt. [kN]
PEC-TA 28/15 Cold rolled	5.0	5.0
PEC-TA 38/17 Cold rolled	10.0	10.0
PEC-TA 40/25 Cold rolled	11.1	11.1
PEC-TA 49/30 Cold rolled	17.2	17.2
PEC-TA 54/33 Cold rolled	30.6	30.6
PEC-TA 41/22 Cold rolled	6.9	6.9
PEC-TA 29/20 Hot rolled	11.2	11.2
PEC-TA 40/22 Hot rolled	19.4	14.4
PEC-TA 50/30 Hot rolled	20.0	22.4
PEC-TA 52/34 Hot rolled	36.1	39.7

The channel width and height in millimetres can be read from the profile names (PEC-TA width / height). The sizes of channels and loads that can be carried can be seen in Table 3. T-bolts are also available with sizes ranging from M8 to M20.

4.3 Various Other Connection Designs

This section contains various known connection types. Limited information on load bearing capacity is available on these connections; however, the overall designs are still useful in providing ideas for new connections. Figure 14 depicts one of Purso Oy's old connection models not currently manufactured.

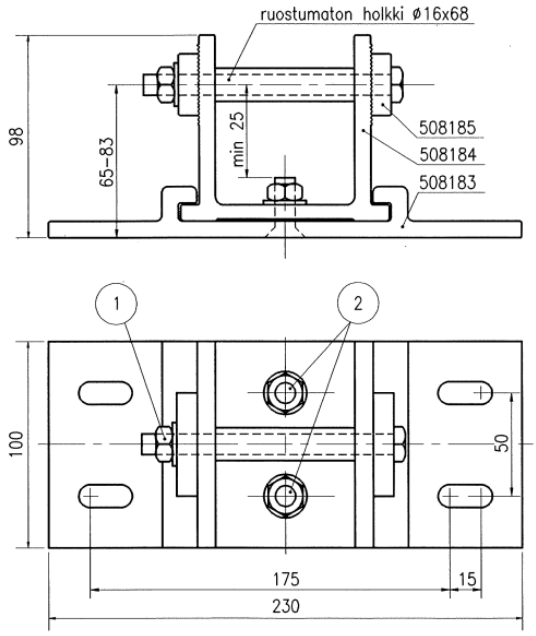

Figure 14 *Old Purso P50L 1.6 connection bracket. Not currently manufactured. Image courtesy of Purso Oy. Note the bushing used in conjunction with M10 bolt, this acts as a safeguard against overtightening and crushing mullion walls.*

The bracket in Figure 15 is not meant for transferring loads from the curtain wall to the underlying load bearing structure; it's used for connecting solar shading to the curtain wall itself.

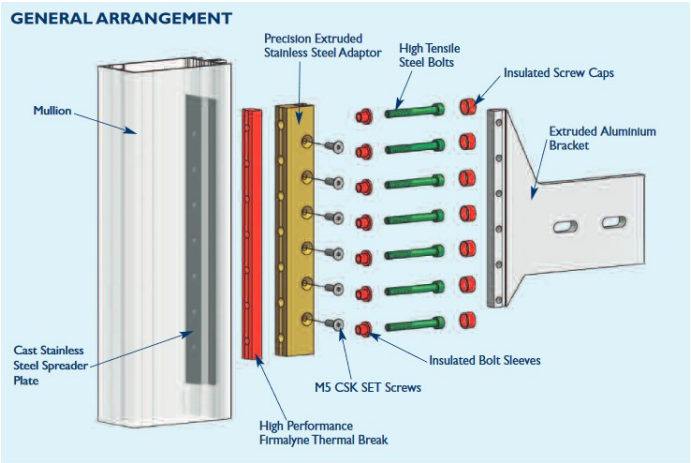

Figure 15 *Levolux TRINITI® Bracket. This connection type is used to support solar shading. Figure adapted from [7].*

Figure 16 *Welded bracket encountered in the field. Image courtesy of Purso Oy.*

The connection in Figure 16 and 17 is a connection type commonly encountered; to simple plates welded to the underlying steel structure and bolted to the mullion. This connection type provides limited adjustability; furthermore, welding onsite is undesirable due to the risks involved. Nevertheless, this type of connection is often encountered as it's relatively cheap and simple.

Figure 17 *Welded bracket encountered in the field. Image courtesy of Purso Oy.*

By observing the connection types presented a trend is noticed: most connections rely on some form of fastening via bolts through holes in the mullion sidewalls. The reason for this choice is obvious; drilling holes into the rear of the mullion would cause significant loss in local mullion bending stiffness. Furthermore, holes in high stress regions are undesirable when fatigue is considered; particularly in areas of large tension stress, such as the front and rear walls of the mullion under bending caused by wind loading. This will be taken into account in the design of the new connections.

5 LOADS

Loading conditions and combinations must be investigated to design the connection system. There are many possible load combinations that the curtain wall system can come under in practice, but only the relevant loading combinations with regards to maximum force reactions at the connections need to be examined. In particular; self-weight, sill and wind loads must be considered. Thermal expansion will be considered in the connection design to ensure it takes place in an unrestricted manner; thus, it does not act as a load in this case. Earthquake, explosion and other accidental loads are not considered here as these are special cases not often encountered by Purso Oy. Eurocode 1 (EC1) provides methods to define these loadings along with load combinations [8]. Guidance on the use of Eurocodes for defining resistance to actions is available in the curtain walling product standard [1]. A newer version of this standard has been released [2], but it is yet to be published in the Official Journal of the European Union, so it cannot be used for CE marking. The older version is used while conservatively considering the newer versions possible updates.

5.1 Self-Weight

EC1 defines the density of glass in sheets as 25 $\mathrm{kN/m^2}$ which is approximately 2.54 $\mathrm{kg/mm{\cdot}m^2}$.The guideline [9] defines the weight of glass as 2.5 $\mathrm{kg/mm{\cdot}m^2}$ which is approximately the same as EC1. IGU elements are frequently used due to Nordic environmental conditions. Double glazing (2K) and triple glazing (3K) IGU panels are the most common types used, however quadruple glazing (4K) units are also available. Some roughly calculated IGU weights based on nominal glass density can be seen in Table 4. The weight values are rounded up to the nearest kilogram.

Table 4 *Weight of glass per area of various IGU configurations.*

IGU	kg/m^2	IGU	kg/m^2	IGU	kg/m^2
2K4	21	3K4	31	4K4	41
2K5	26	3K5	39	4K5	51
2K6	31	3K6	46	4K6	61

In practice, IGU weights per area are often much larger due to the use of special glazing such as laminates; therefore, an assumed maximum IGU weight of $70\ \mathrm{kg/m^2}$ is used. This assumption is based on Purso Oy's experience and requirements. The maximum self-weight is taken as

$$G_d = 1.15 \times 70\mathrm{kg/m^2} \times 9.81\mathrm{m/s^2} \times 3\mathrm{m} \times 3\mathrm{m} \approx 7.0\ \mathrm{kN}. \tag{5.1}$$

The self-weight of the curtain wall frame is of minimal significance when compared to the weight of the glass units and is therefore not considered in the calculation of these connection design loads. However, the weight of the frame must be considered when using these connections.

5.2 Wind Loads

Wind loads are modelled in EC1 as simplified pressures or force resultants which have an effect that is equivalent to the extreme effects of turbulent wind [10]. The resultant forces are often used to evaluate the entire buildings resistance to wind loading. The design of curtain walls requires the simplified pressure approach to depict the local effects of wind loading. To define the simplified pressures, one must first calculate an expected peak velocity pressure. The peak velocity pressure is based on wind velocity and is comprised of a mean and fluctuating component. The basis for calculation is as follows.

The basic wind velocity is calculated as

$$\mathrm{v}_b(z)=\mathrm{c}_{dir}c_{season}v_{b,0}\,, \tag{5.2}$$

where c_{dir} is the directional factor, c_{season} the season factor (with recommended value 1.0) and $v_{b,0}$ the fundamental value of the basic wind velocity (see [10]: 4.2 Clause (1)P for definition). The fundamental value of basic wind velocity is given in the Finnish National Annex (NA) [11] as $v_{b,0}=21$ m/s. The seasonal factor c_{season} and directional factor may also be given in the NA; however, in the Finnish case the recommended values of 1.0 are used.

The mean wind velocity $v_m(z)$ is calculated by

$$v_m(z)=c_r(z)c_0(z)v_b\,, \tag{5.3}$$

where c_r roughness factor and c_0 is the orography factor, taken as 1.0 unless otherwise specified. Notice that the mean wind velocity is a function of height z. The factor c_0 considers the effects of terrain orography, which effect wind loads; however, the effects of orography may be neglected when the average slope of upwind terrain is less than 3 degrees. For simplicity, the value of 1.0 is used in this case. The roughness factor also depends on terrain conditions and is defined using equations

$$c_r(z)=k_r\ln\left(\frac{z}{z_0}\right)\text{ for } z_{min}\le z\le z_{max}\,, \tag{5.4}$$

$$c_r = c_r(z_{min}) \text{ for } z \le z_{min}, \tag{5.5}$$

where k_r is a terrain factor that depends on terrain roughness length z_0 and z_{min} the minimum height. Both are defined in Table 5 and both are dependent on terrain category. The terrain categories categorize different types of terrain in a range from 0 to IV, where 0 type terrain has the least number of obstacles (e.g. open sea and coastal area), and type IV the most (e.g. heavily built areas). The reader is referred to [10] Annex A, for further details.

Table 5 *Terrain categories and terrain parameters as defined in EC1.*

Terrain Category	z_0 $[m]$	$z_{\min}$ $[m]$
0	0.003	1
I	0.01	1
II	0.05	2
III	0.3	5
IV	1.0	10

The terrain factor k_r is calculated from the equation

$$k_r = 0.19\left(\frac{z_0}{z_{0,II}}\right)^{0.07}, \tag{5.6}$$

where $z_{0,II}$ is the roughness length for terrain category II ($z_{0,II} = 0.05$). Equation 5.5 is not used when the terrain category is 0 according to the Finnish NA; $k_r = 0.18$ in this case. Using the designated equations above, the mean value of wind velocity is calculated.

Now, the turbulent part must also be solved. The turbulence intensity $I_v(z)$ at height z is defined in EC1 as the standard deviation of turbulence divided by mean wind velocity. The turbulent part has a standard deviation of σ_v and mean value of 0. The standard deviation is calculated by

$$\sigma_v = k_r k_l v_b, \tag{5.7}$$

where k_l is the turbulence factor that may be given in the NA. The recommended value $k_l = 1.0$ is used. Subsequently, the turbulence intensity can be solved for using

$$I_v(z) = \frac{\sigma_v}{v_m(z)} \text{ for } z_{min} \le z \le z_{max}, \tag{5.8}$$

$$I_v = I_v(z_{min}) \text{ for } z \leq z_{min}\,. \tag{5.9}$$

Finally, the peak velocity pressure can be solved for by

$$q_p = \left[1 + 7I_v(z)\right]\frac{1}{2}\rho {v_m}^2(z)\,, \tag{5.10}$$

where ρ is the air density taken as 1.25 kg/m^3 according to the Finnish NA. Figure 18 shows the peak velocity pressures for heights 0 to 200 m solved using the given equations. The maximum velocity pressure at height 30 m, terrain class 0 is approximately 1.33 kN/m^2. Note the relatively large difference between terrain classes 0 and I.

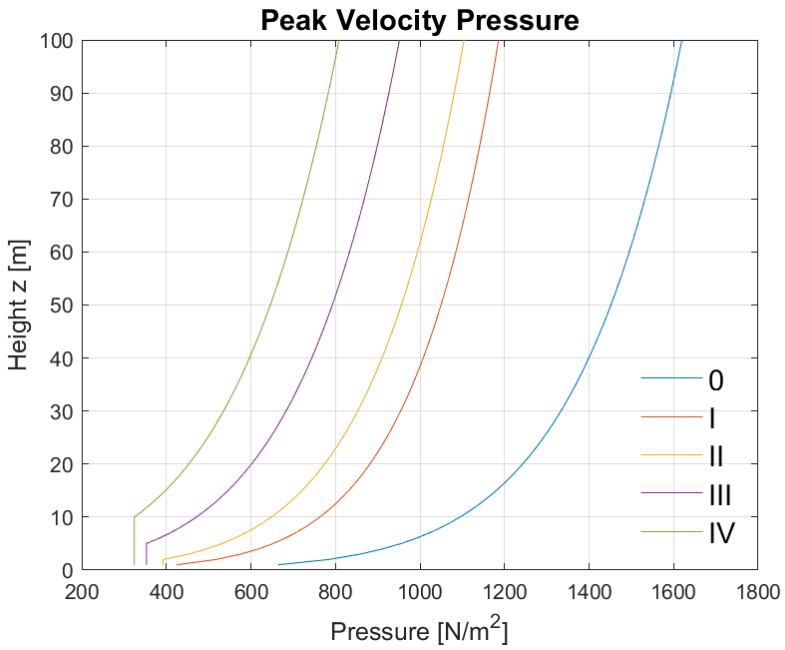

Figure 18 *Peak velocity pressures calculated according to EC1 specifications.*

Considering these results, the peak velocity pressure of 1.33 kN/m^2 is taken as the largest peak wind velocity pressure (30 m high building). This velocity pressure as multiplied by a net pressure coefficient $c_{p,net}$ to get the design wind load. The net pressure coefficient depends greatly on the building under consideration. To cover most cases, a simplified approach is used; the net pressure coefficient is taken as $c_{p,net} = 1.5$ [12]. This value will be used for defining the permissible wind reaction force for the largest connection design size: $Q_{k.wind} \approx 2.0$ kN.

5.3 Sill Loads

According to SFS-EN 1991-1-1, a sill load is applied at height 1.2 m (from floor level) to the curtain wall structure. The sill load is modelled as a line load q_k. Values for this load can be defined in the NA. The values of sill loads depending on category of use can be seen in Table 6.

Table 6 *Sill loads according to the Finnish NA.*

Loaded Area	q_k [kN/m]
A	0.5
B	0.5
C1…C4 & D	1.0
C5	3.0
E	1.0

The typical categories of use encountered by Purso Oy are A (domestic/residential), B (office areas), C (public areas where people may congregate) and D (shopping areas). The sill load is taken as 1.0 kN/m.

5.4 Thermal Expansion

Aluminium alloys coefficient of thermal expansion is defined as $\alpha = 23 \times 10{-}6$ 1/°C in EN 1999-1-1. In a fully fixed connection, the resulting stress from thermal expansion restriction under a temperature delta of 60 °C (conservative estimate encountered in Purso Oy's cases) would be approximately 97 MPa, resulting in relatively large force reactions (e.g. 150 kN for 200 mm deep profile size). Therefore, a fixed connection is undesirable. Thermal expansion will be considered in the connection design by use of slotted holes to allow for free expansion. Furthermore, a nylon shim placed between mullion and connection profile will be used to ensure that the aluminium mullion is not damaged over time. The maximum amount of thermal movement possible for a 6.6 m long profile is calculated to be approximately 8.3 mm.

5.5 Design Loads

Theoretically, there are an infinite amount of different combinations of loads and frame configurations. To solve the largest force reaction expected to be encountered in most design situations, we solve the simple case of a 3 m long single span simply supported beam under uniform distributed wind loading (UDL) and single point load (sill load). As mentioned earlier, the glass width is taken as 3 m. The design loads used according to EC1 are thus:

- $G_d = 1.15 \cdot K_{FI} \cdot G_k = 1.15 \cdot 3\ \text{m} \cdot 3\ \text{m} \cdot 70\ \text{kg/m}^2 \cdot 9.81\ \text{m/s}^2 \approx 7.0\text{kN}$
- $Q_{d.sill} = 1.5 \cdot \Psi_0 \cdot b_{window} \cdot Q_{k.sill} = 1.5 \cdot 0.7 \cdot 3\ \text{m} \cdot 1\ \text{kN/m} \approx 3.2\ \text{kN}$
- $Q_{d.wind} = 1.5 \cdot b_{window} \cdot Q_{k.wind} = 1.5 \cdot 3\ \text{m} \cdot 2.0\ \text{kN/m}^2 \approx 9\ \text{kN/m}$

The force reactions can be solved for by basic statics formulae found in handbooks (not presented here) such as [13] and the method of superposition. The governing reactions are:

- $R_{sill.load.\max} = 3.2\ \text{kN} \cdot (3\ \text{m} - 1.2\ \text{m})/3\ \text{m} \approx 2.0\ \text{kN}$
- $R_{wind.load} = 9\ \text{kN/m} \cdot 3\ \text{m} / 2 \approx 14\ \text{kN}$
- $R_{Self-weight} = 7.0\ \text{kN}$

Notice that only the lower support is designed to carry self-weight. The top support functions as a wind tie only. The maximum horizontal and vertical loads have been solved. Based on these results, design loads of the connections are decided upon.

Table 7 *Summary of design loads.*

Connection size	Horizontal load [kN]	Vertical load [kN]
Heavy	16	7.0
Light (~60% Large)	10	4.0

Table 8 *Summary of fatigue loads (wind only).*

Connection size	Horizontal load [kN]	Vertical load [kN]
Heavy	9	0
Light (~60% Large)	6	0

A summary of the loads to be used in the designing of the connection system can be seen in Table 7. These design loads are mostly in line with the design loads of many of connection brackets currently offered on the market (see Section 4) and what is mentioned in [14]. As noted earlier, the profile sizes under consideration are limited to 40-200mm. Under 9 kN/m wind loading the 200 mm P50L profile (simply supported 3 m span) would deflect approximately 15 mm, which is the deflection allowed according to [2]

6 DESIGN TO EUROCODE 9

Part 8 of EC9-1-1 handles the design of joints for aluminium structures. Provisions are provided for bolted, riveted, pinned, welded and adhesive joints. In the designs developed, a bolted connection is used; specifically type A (bearing type connection, see Table 8.4 of EC9-1-1), applicable for connections subject to reversal of shear load caused by wind according to EC9 (clause 8.3 (3)).

Part 8.1.4 provides design assumptions that may be used in the design of connections. It is stated that connections may be designed by distributing internal forces in any rational way, provided that the internal forces are in equilibrium with the external loads and each part of the joint is able to resist the loads applied to it. This is clearly based on the well-known static theorem (lower bound theorem) of theory of plasticity [15], which states that an external load computed based on assumed internal forces (which are bound by a yield criteria) is less than or equal to the true failure load. By requiring that the external load calculated from the internal force distribution must be the external load applied, we arrive at the statement given in EC9.

To solve the internal load distribution in a rational way which considers the different relative stiffness properties of parts comprising the joint, linear-elastic analysis is carried out by means of the finite element method (see Section 6.2). Residual stresses from tightening fasteners are omitted from the analysis. Eccentricity present in the connection design is considered (see Section 9). This approach is supported by clauses 8.1.3 (2), 8.1.4 (3) and 8.2 (2) of EC9-1-1

6.1 Bolts

EC9-1-1 requires that bolted connections be checked for bolt hole spacing and edge distances, block tearing, shear, tension, combined shear and tension, bearing, punching and net section resistance.

Bolt hole spacing requirements are specified in Table 8.2 of EC9. Relevant spacing requirements as functions of bolt hole diameter d_0 or bolt diameter d are presented in Table 9. It is worth noting that maximum values for spacings and edge distances are unlimited except for compression members (to restrict local buckling) and exposed tension members. Due to the complexity of the internal load distribution, simplifying local buckling calculations by limiting maximum spacing is not adequate in this case; the most compressed zones of the connections do not reside inside bolt groups. Therefore, local buckling is considered numerically according to the guidance provided by EC9-1-5 (see Section 6.2). Figures 19 and 20 show the graphic definitions of the distance and spacing symbols.

Table 9 *Edge distances and spacing required by EC9.*

Distances	Minimum [mm]	Regular [mm]
End distance e_1	$1.2d_0$	$2.0d_0$
End distance e_2	$1.2d_0$	$1.5d_0$
Spacing p_1	$2.2d_0$	$2.5d_0$
Spacing p_2	$2.4d_0$	$3.0d_0$
End distance e_3 for slotted holes	$1.5(d+1)$	-
Edge distance e_4 for slotted holes	$d+1$	-
Length between extreme edges (short slotted hole)	-	$1.5(d+1)$ (max allowed)
Length between extreme edges (long slotted hole)	-	$2.5(d+1)$ (max allowed)

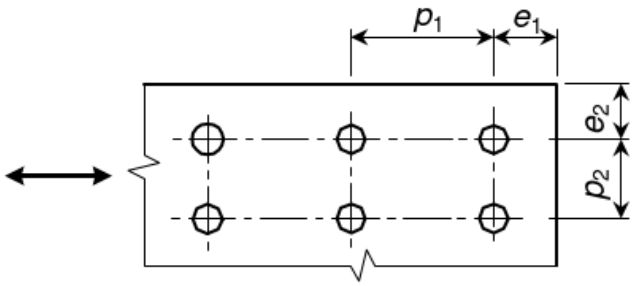

Figure 19 *Bolt spacing and edge distances. Figure adapted from [16].*

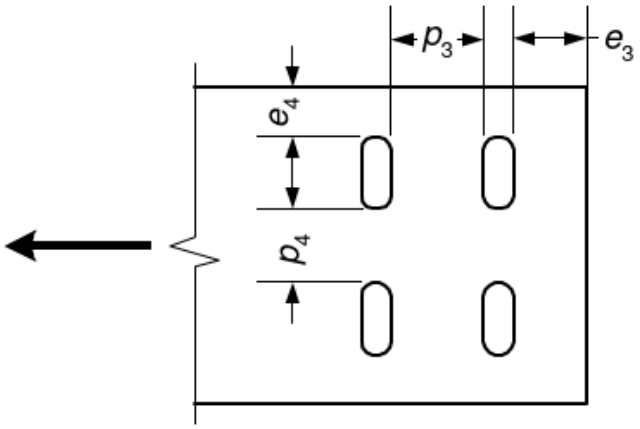

Figure 20 *Bolt spacing and edge distances for slotted holes. Figure adapted from [16].*

The shear resistance per shear plane of a bolt is calculated as

$$F_{v,Rd} = \frac{\alpha_v f_{ub} A}{\gamma_{M2}}, \tag{6.1}$$

where α_v is a factor that considers the bolt type used, A is the stress area of the bolt, f_{ub} is the characteristic ultimate strength of the bolt material and γ_{M2} the partial factor for bolted connections (recommended value of 1.25). The tensile stress area of the bolt is used in cases where the shear plane is situated at the threaded portion of the bolt; the gross cross section is used otherwise. For a steel bolt of class 8.8 $\alpha_v = 0.6$.

The bearing resistance of a bolt hole is calculated as

$$F_{b,Rd} = \frac{k_1 \alpha_b f_u d\, t}{\gamma_{M2}}, \tag{6.2}$$

where f_u is the characteristic ultimate strength of the material of the connected part and t is the thickness of the connected part.

The factor k_1 is calculated by

$$\begin{aligned} &\min\{2.8\frac{e_2}{d_0}-1.7, 2.5\}, \text{ for edge bolts} \\ &\min\{1.4\frac{p_2}{d_0}-1.7, 2.5\}, \text{ for inner bolts} \end{aligned} \tag{6.3}$$

and the factor α_b is calculated by

$$\begin{aligned} &\min\{\frac{e_1}{3d_0}, \frac{f_{ub}}{f_u}, 1.0\}, \text{ for end bolts; } \le 0.66 \text{ for slotted holes} \\ &\min\{\frac{p_1}{3d_0}-\frac{1}{4}, \frac{f_{ub}}{f_u}, 1.0\}, \text{ for inner bolts; } \le 0.66 \text{ for slotted holes} \end{aligned} \tag{6.4}$$

The spacing measurements and edge distances used in calculating α_b are taken with respect to the direction of the load transfer; the direction perpendicular to the load transfer is used in the case of k_1 .Slotted holes require special consideration with regards to bolt spacings and edge distances. The hole diameter d_0 is replaced by $(d+1)$, e_1 is replaced by $(e_3 + d/2)$, e_2 by $(e_4 + d/2)$, p_1 by $(p_3 + d)$ and p_2 by $(p_4 + d)$. Furthermore, slotted hole bearing resistance is reduced on a basis of slot length; the bearing strength of short and long slotted holes are reduced to 80 % and 65 % respectively.

Tension resistance is calculated according to

$$F_{t,Rd} = \frac{k_2 f_{ub} A_s}{\gamma_{M2}}, \tag{6.5}$$

Where k_2 is a factor that considers the bolt material ($k_2 = 0.9$ for steel bolts) and A_s is the tensile area of the bolt. Combined shear and tension resistance can thus be calculated accordingly;

$$\frac{F_{v,Ed}}{F_{v,Rd}} + \frac{F_{t,Ed}}{1.4F_{t,Rd}} \le 1.0\,. \tag{6.6}$$

Finally, punching shear is checked by the formula

$$\beta_{p,Rd} = \frac{0.6\,\pi\, d_m\, t_p\, f_u}{\gamma_{M2}}, \tag{6.7}$$

Where t_p is the thickness of the plate under the bolt head, f_u the characteristic ultimate strength of the material and d_m the mean across the flats dimensions of the bolt head or washer diameter, whichever is smaller.

In addition to the strength requirements showed, the design of connections using different metal types requires consideration of durability with regards to galvanic corrosion. In certain exposure conditions galvanic corrosion may occur. Table D.2 of Annex D EC9-1-1 provides guidance for different metals and exposure conditions. According to the table, the conditions most encountered by Purso Oy do not require any special treatment when zinc coated bolts are used (dry, unpolluted rural and non-industrial conditions).

6.2 Application of Numerical Analysis

Part 5 of Eurocode (EC9-1-5) provides guidance on designing and numerically analysing shell structures fabricated from aluminium alloy. This includes guidelines for the application of different analysis types, stress limits and buckling resistance. Table 5.2 and 5.3 of EC9-1-5 contain lists of the different types of analyses applicable in the design of these structures and their descriptions.

In the case of linear elastic analysis or geometrically non-linear elastic analysis, von Mises stress can be used as the equivalent design stress. Clause 6.1.3 of EC9-1-5 states that every verification of the ultimate limit state should require the design stress $\sigma_{eq,Ed}$ to satisfy the equation

$$\sigma_{eq,Ed} \leq f_{eq,Rd}, \tag{6.8}$$

where $f_{eq,Rd}$ is the equivalent von Mises design strength defined as

$$f_{eq,Rd} = \frac{f_0}{\gamma_{M1}}. \tag{6.9}$$

The characteristic value of 0.2% proof strength f_0 depends on alloy choice and is provided in Section 3 of EC9-1-1 (Materials) for various types, tempers and thicknesses of aluminium alloys. The partial factor for resistance γ_{M1} is given in clause 2.1 (3) of EC9-1-5 (recommended value 1.10).

According to clause 6.1.4 (1), the design plastic limit state should be determined as

$$R = \frac{F_{Rd}}{F_{Ed}} \geq 1.0 \ , \tag{6.10}$$

Where F_{Rd} is the design resistance, F_{Ed} is the design load and R_{load} the load ratio.

Materially (MNA) or geometrically and materially non-linear analysis (GMNA) may also be applied (if applicable). If MNA is used, the design load ratio is defined according to the load level of plastic limit observation. In the case of GMNA, a load-displacement path with a maximum load followed by sudden drop in stiffness may be observed; in these cases, the maximum load is taken as the load level for design load ratio definition. Naturally, if GMNA does not differ in behaviour from MNA, the definition used in MNA applies.

In addition to material resistance requirements, local buckling resistance must also be considered. The design for compression and shear is handled in Section 6.2.3 of EC9-1-5; analytical solutions are presented, but the application is limited; particularly in cases with irregular geometry and local softening of material due to welding (HAZ). As an alternative approach to the analytical methods provided, clause 6.2.5 (1) states that a geometrically and materially non-linear analysis with imperfections (GMNIA) may be applied. Initial geometrical imperfections with amplitudes according to maximum values of tolerances given in Section 6.2.2 of EC9-1-5 are used.

To ensure local buckling resistance is met, GMNIA is performed on all final designs with apparent slenderness in addition to the linear analyses performed during optimization. GMNIA is relatively expensive computationally; therefore, it is not used during the optimization procedure. Stability is not expected to be a limiting factor in the designs; however, if stability problems arise slender parts can easily be thickened.

6.3 Fatigue

The principles of part 1-3 of Eurocode 9 (EC9-1-3) require that structures subjected to frequently fluctuating service loads be checked for the limit state of fatigue [17]. The standard provides two methods for designing aluminium structures against this limit state: the safe life design method and damage tolerant design method. Both methods can be replaced or supplemented by design assisted by testing. In this case, we use the safe life design method.

The safe life design method provides a conservative estimate of fatigue life. The damage accumulated over the structures design life is calculated by means of an upper bound estimate of fatigue loading and lower bound endurance data. EC9-1-3 Annex A presents the basic procedure for safe life design. Simply put, the method consists of the following steps:

1. Obtain upper bound estimate for service load sequence over the structures design life.
2. Categorize the constructional detail in accordance with the given set of categories (provided in EC9-1-3) and determine the appropriate $\Delta\sigma - N$ relationship. This relationship determines design stress ranges $\Delta\sigma_i$ along with permissible endurance limits N_i.
3. Calculate resulting stress history in structure at potential failure initiation sites, typically highly stressed points.
4. Reduce the stress history to an equivalent number of cycles n_i of different stress ranges $\Delta\sigma$. In other words, define the stress history spectrum.
5. Calculate the total damage D_L for all cycles of service loading by using Palmgren-Miner summation where

$$D_L = \sum \frac{n_i}{N_i}. \tag{6.11}$$

6. Calculate the safe life T_S as

$$T_S = \frac{T_L}{D_L}, \tag{6.12}$$

where T_L is the design life.

To clarify, Step 4 of the method requires "an equivalent number of cycles n_i of different stress ranges $\Delta\sigma$" to be defined. Essentially, this means one must first determine the stress history in the structure caused by the upper bound estimate service load sequence. Then, one must extract stress cycles along with the corresponding number of each cycle encountered.

Stress histories often have a large range of different sizes of stress cycles. Therefore, it is often convenient to conservatively group stress cycles as bands; the largest stress cycle in a bands range defines the bands stress range, while the total number of cycles for all stress cycles in the range sets the bands width (see Figure 21). A well-known method used for the extraction of these cycles is the rainflow-counting algorithm, typically implemented in software [18]. This is particularly useful for design by testing. Figure 21 shows an example of a simplified stress spectrum given in EC9-1-3.

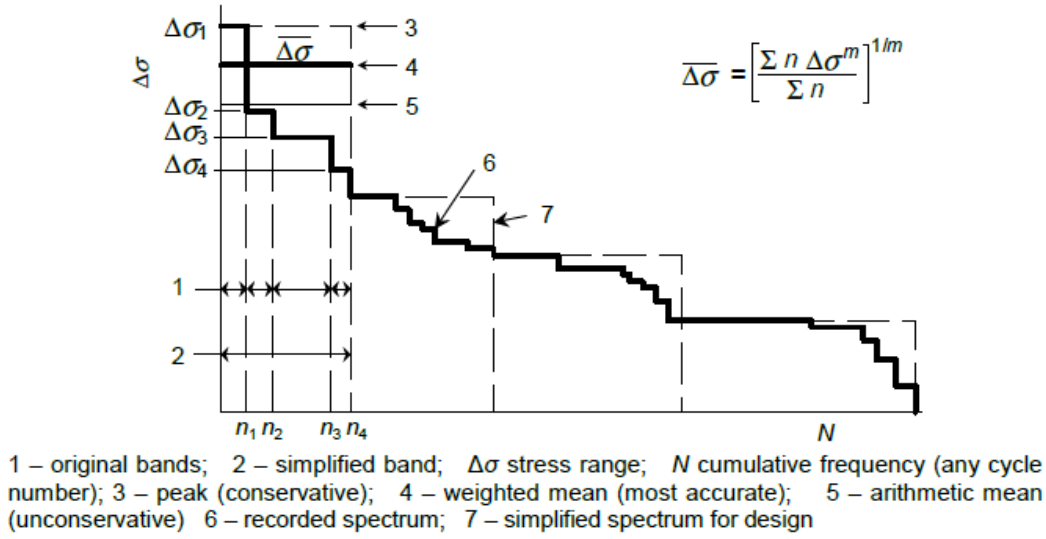

1 – original bands; 2 – simplified band; $\Delta\sigma$ stress range; N cumulative frequency (any cycle number); 3 – peak (conservative); 4 – weighted mean (most accurate); 5 – arithmetic mean (unconservative) 6 – recorded spectrum; 7 – simplified spectrum for design

Figure 21 *Simplified stress range spectrum. Figure adapted from [17].*

EC9-1-3 requires all sources causing fluctuating stress to be identified. The standard lists the following typical sources which should be considered:

- superimposed moving loads, including vibrations from machinery in stationary structures;
- loads due to exposure conditions such as **wind**, waves, etc;
- acceleration forces in moving structures;
- dynamic response due to resonant effects;
- temperature changes.

The effects of wind are considered in the design of the developed connection system. Temperature changes are irrelevant in this case, as they are dealt with by allowing for free expansion of the curtain wall mullions via slotted connection; no induced stresses arise. Dynamic response due to resonant effects is occasionally relevant in curtainwall design. However, due to the nearly endless amount of possible curtain wall configurations, dynamic response and resonance of these systems is not considered in the connections developed in this thesis. Dynamic considerations are deemed mostly irrelevant for the majority of Purso Oy's cases and will thus be considered only on a case by case basis.

Fatigue loads should be described by means of design load spectrums. A design load spectrum defines multiple ranges of intensities for a loading, along with corresponding number of cycles per intensity. EC1-1-4 defines a load spectrum for wind loading in Annex B, which can be used for fatigue calculations [19]. This spectrum is defined by the equation

$$\frac{\Delta S}{S_k} = 0.7\left(\log\left(N_g\right)\right)^2 - 17.4\left(\log\left(N_g\right)\right) + 100\,, \tag{6.13}$$

where S_k is the effect due to a 50 years return period wind action, ΔS a percentage of S_k and N_g the number of gust loads for an effect of **at least** $\Delta S / S_k$. Figure 22 gives a graphic representation of the load spectrum. The use of this spectrum in the context of analysing fatigue of façade elements with emphasis on the discrepancies caused by omitting dynamic response is examined in [20].

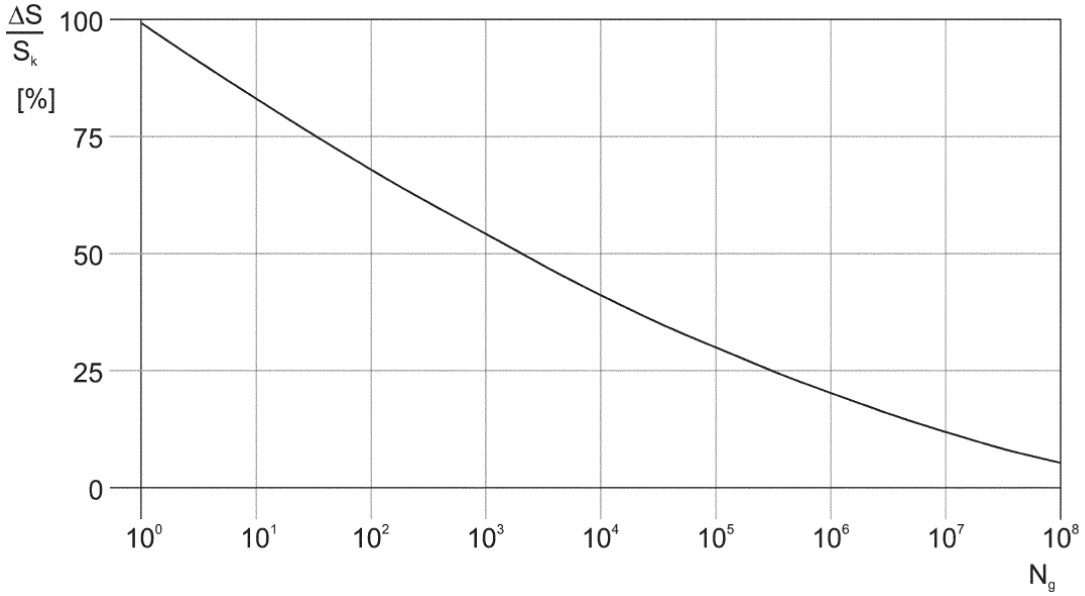

Figure 22 *Number of gust loads N_g for an effect $\Delta S / S_k$ during a 50 years period. Figure adapted from [10].*

This equation is particularly useful if the stress calculations are carried out linearly; instead of analysing stress histories for each gust load size separately, it is possible to analyse a single load case; the other stress bands can be solved for on a basis of proportionality. The stresses encountered in the solved load case are scaled accordingly for other gust load levels of the spectrum.

The largest wind loading expected to be encountered is used for defining the gust load spectrum (characteristic loads used). A single stress range limit is defined as a reference fatigue load level. This level is chosen such that the resulting summation of damage for the total loading spectrum doesn't exceed the damage limit. Therefore, if this stress range limit is not exceeded, the fatigue limit state is not exceeded. This greatly reduces the computational cost needed to perform fatigue limit state calculations for wind loads; however, this simplification is only valid if proportionality holds for the stresses induced in the structure and the principle stress axes angles do not change when the wind load direction is reversed.

EC9-1-3 defines resistance values for numerous standardised detail categories. A detail category comprises of one or more frequently used structural details; for example, welded attachments or notches and holes. The factors that affect fatigue strength of a detail category in EC9-1-3 are:

- the direction of fluctuating stress in the constructional detail;
- the location of initiating crack in the constructional detail;
- the geometric arrangement and proportions of the constructional detail;
- the product form;
- the material (unless welded);
- execution method;
- quality level;
- connection type.

Each detail category provides corresponding values of reference fatigue strength and inverse slope of the main part of the linearized $\Delta\sigma - N$ relationship. Research has shown that the inverse slope values generally lie in the range of 3 - 10 and that $\Delta\sigma - N$ curves are approximately parallel for a specified detail. Therefore, this efficient way of providing design curves via detail categorisation is possible [18].

The standardised $\Delta\sigma_c$ values can be seen in Table 10.

Table 10 *Standardized* $\Delta\sigma_c$ *values (N/mm2)*

140, 125, 112, 100, 90, 80, 71, 63, 56, 50, 45, 40, 36, 32, 28, 25, 23, 20, 18, 16, 14, 12

Depending on exposure conditions and alloy type, $\Delta\sigma_c$ may need to be reduced. For example, a detail type provided in one of the many detail category tables in EC9-1-3 gives the values of $\Delta\sigma = 125$ MPa and $m_1 = 7$. The structure is fabricated from the alloy 7020 and it is immersed in fresh water. The reference value of fatigue must therefore be reduced by one standardised step to $\Delta\sigma = 112$ MPa. The inverse slope m_1 remains the same.

$$N_i = 2\times10^6 \left(\frac{\Delta\sigma_c}{\Delta\sigma_i} \frac{1}{\gamma_{Ff}\gamma_{Mf}} \right)^{m_1} \tag{6.14}$$

where N_i is the predicted number of failure cycles for the stress range $\Delta\sigma_i$ of the principle stresses encountered at the constructional detail; $\Delta\sigma_c$ the reference value of fatigue for 2×10^6 cycles (depends on detail category); m_1 the inverse slope of the $\Delta\sigma - N$ curve (depends on detail category); γ_{Ff} the partial factor allowing for uncertainties in the loading spectrum and analysis of response (recommended value 1.0, but may be defined in NA) and γ_{Mf} the partial factor for uncertainties in materials and execution (recommended value 1.0, but may be defined in NA). The partial factor γ_{Mf} is set to 1.2 according to the Finnish NA [21] for consequence class 2 (CC2). The partial factor γ_{Ff} is set to 1.0.

$$N_i = 5\times10^6 \left(\frac{\Delta\sigma_c}{\Delta\sigma_i} \frac{1}{\gamma_{Ff}\gamma_{Mf}} \right)^{m_2} \left(\frac{2}{5} \right)^{\frac{m_2}{m_1}} \tag{6.15}$$

The relevant detail types and categories along with corresponding figures are listed in Table 11. The detail categories provided in the standard are applicable to all mean stress values (unless stated otherwise) and are based on high tensile mean stress values.

The inverse of functions (6.15) and (6.14) can be solved for by considering that the values being raised to the powers of the inverse slopes are always positive in the detail categories presented. Furthermore, the values of the inverse slopes are also positive. Therefore, we can simply declare that the inverse functions are of the form

$$\Delta\sigma_i = \left(\frac{2\times10^6}{N_i} \right)^{1/m_1} \cdot \frac{\Delta\sigma_c}{\gamma_{Ff}\gamma_{Mf}} \tag{6.16}$$

$$\Delta\sigma_i = \frac{\Delta\sigma_c}{\gamma_{Ff}\gamma_{Mf}} \cdot \left(\frac{5\times10^6 \cdot \left(\frac{2}{5} \right)^{m_1/m_2}}{N_i} \right)^{1/m_2} \tag{6.17}$$

for equations (6.15) and (6.14) respectively. These equations are not explicitly given in EC9 but may prove to be useful in some cases; such as when decisions on material thicknesses need to be made in situations where the loading spectrum is known.

Table 11 *Detail types used in connection designs.*

Detail	Detail category $\Delta\sigma - m_1$	Figure depicting detail types. Adapted from [17].
1.4	71-7	Sheet, plate, extrusions, tubes, forgings 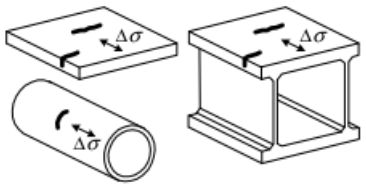 Surface irregularity
1.6	100-7	Notches, holes 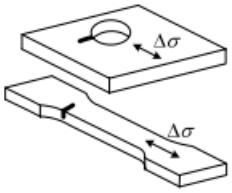 Surface irregularity
15.2	56-4	Non-preloaded (bearing type) steel bolt 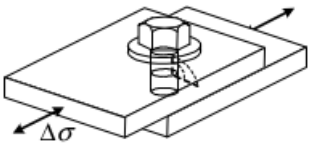 At edge of hole

Figures 23 to 25 show the graphs corresponding to the details shown in Table 11. Note the wind stress levels are also depicted. Each step on the wind graph depicts a band used for Palmgren-Miner summation. We assume fully reversed stress cycles per gust and a stress ratio (minimum stress / maximum stress) R = -1. Bolt hole detail categories are also calculated for R = 0. In other words, the max wind loading only causes a maximum tensile stress; the stress delta is therefore shifted from a mean of 0 to a mean of $\sigma_{max}/2$. Depending on profile geometry, it is possible that high tensile stresses arise in the surrounding bolt hole material, but compression stresses do not arise when the load is reversed as the internal load path changes significantly.

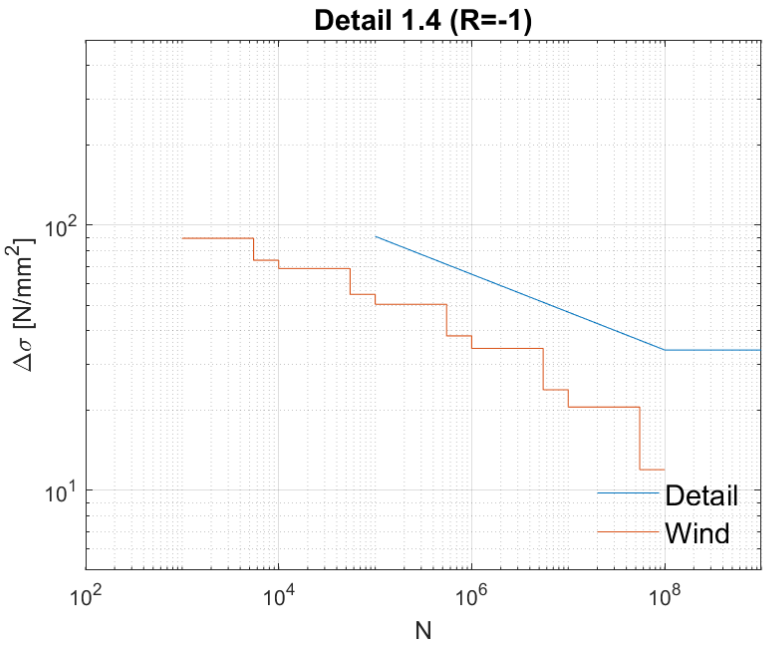

Figure 23 *S-N Curve of detail 1.4*

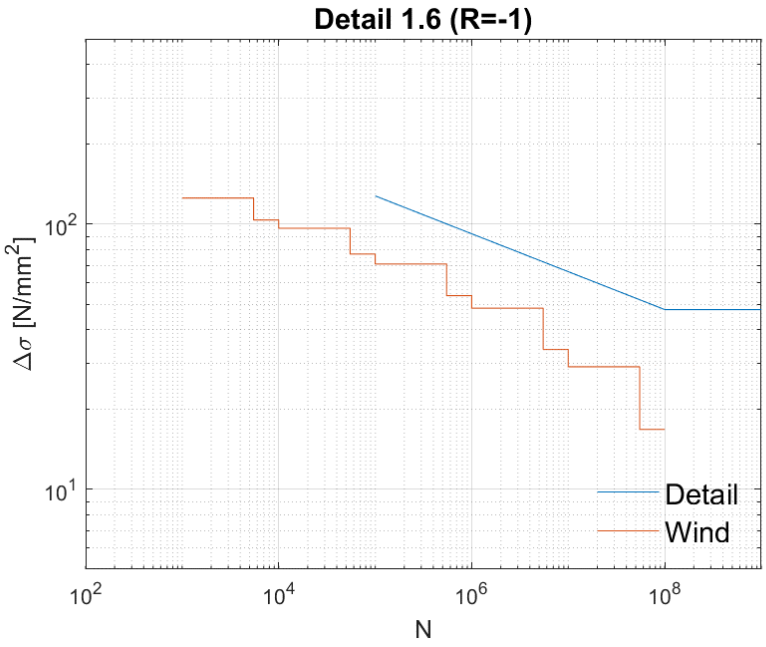

Figure 24 *S-N Curve of detail 1.6*

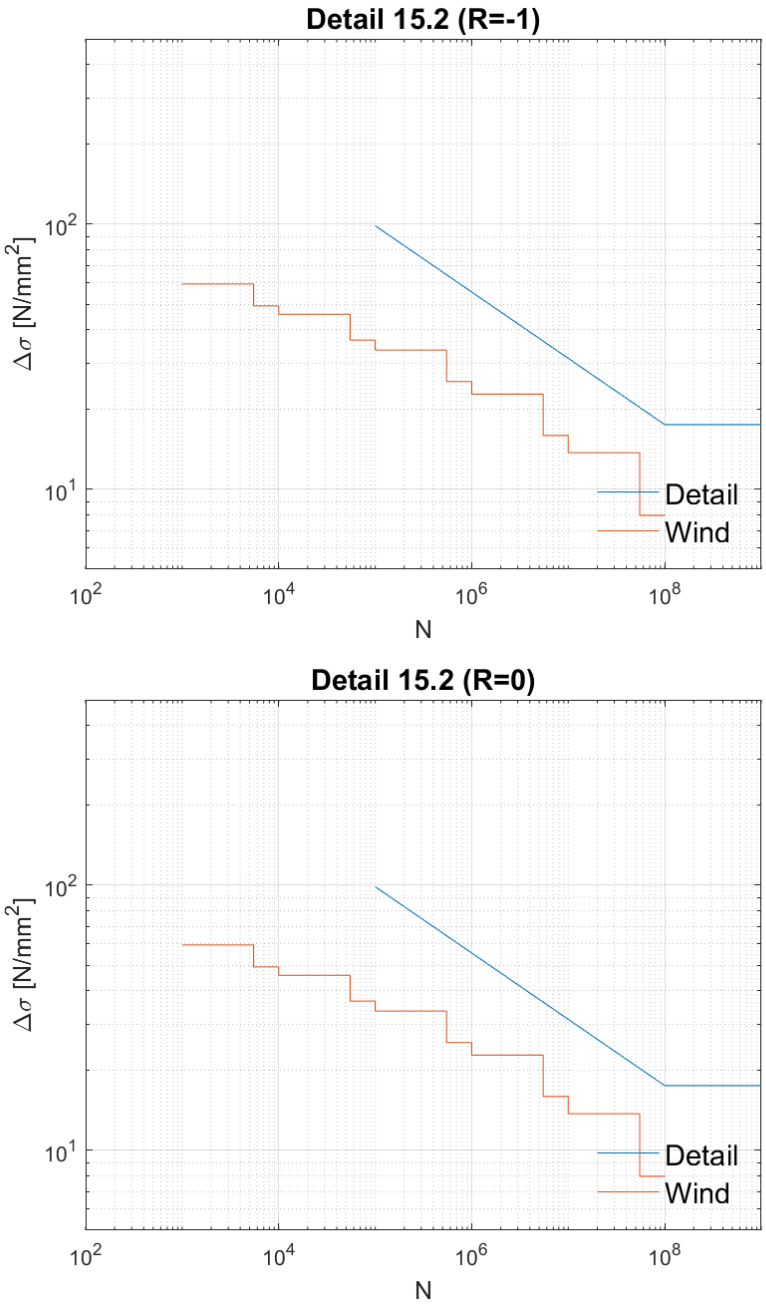

Figure 25 *S-N Curve of detail 15.2*

The results of Palmgren-Miner summation and corresponding maximum permissible stress levels for each detail type can be seen in Tables 12 to 14. In the tables, $\Delta\sigma_i$ is the maximum stress delta of the band, n_i the number of gust cycles, N_i the cycle limit for the stress range, D_L the total damage result and D_{lim} (NA) the maximum permissible damage according to Finnish National Annex specifications. The damage limit is for each detail is limited to the range specified as

$$\left(\frac{1}{\gamma_{Ff}\cdot\gamma_{Mf}}\right)^{m2} \le D_{lim} \le \left(\frac{1}{\gamma_{Ff}\cdot\gamma_{Mf}}\right)^{m1}$$

in Amendment A1 of the aluminium fatigue standard, according to the Finnish NA.

Table 12 *Detail 1.4, maximum permissible nominal principle stress at detail* $f_{Fat1.4,Rd} = 82.5$ MPa *(R=-1).*

i	$\Delta\sigma_i$ [N/mm^2]	n_i	N_i	n_i / N_i	Cum.Sum
1	89.3	4.50E+03	1.12E+05	0.040	0.04
2	73.8	4.50E+03	4.27E+05	0.011	0.05
3	68.6	4.50E+04	7.07E+05	0.064	0.11
4	54.9	4.50E+04	3.40E+06	0.013	0.13
5	50.3	4.50E+05	6.21E+06	0.072	0.20
6	38.3	4.50E+05	4.24E+07	0.011	0.21
7	34.3	4.50E+06	9.05E+07	0.050	0.26
8	24.0	4.50E+06	1.12E+09	0.004	0.26
9	20.6	4.50E+07	3.20E+09	0.014	0.28
10	12.0	4.50E+07	1.44E+11	0.000	0.28
				D_L	**0.28**
				D_{lim} (NA)	**0.28**

Table 13 *Detail 1.6, maximum permissible nominal principle stress at detail* $f_{Fat1.6,Rd} = 116$ MPa *(R=-1).*

i	$\Delta\sigma_i$ [N/mm^2]	n_i	N_i	n_i / N_i	Cum.Sum
1	125.5	4.50E+03	1.14E+05	0.040	0.04
2	103.7	4.50E+03	4.32E+05	0.010	0.05
3	96.5	4.50E+04	7.16E+05	0.063	0.11
4	77.1	4.50E+04	3.44E+06	0.013	0.13
5	70.8	4.50E+05	6.28E+06	0.072	0.20
6	53.8	4.50E+05	4.29E+07	0.010	0.21
7	48.3	4.50E+06	9.16E+07	0.049	0.26
8	33.7	4.50E+06	1.13E+09	0.004	0.26
9	29.0	4.50E+07	3.24E+09	0.014	0.28
10	16.8	4.50E+07	1.46E+11	0.000	0.28
				D_L	**0.28**
				D_{lim} (NA)	**0.28**

Table 14 *Detail 15.2, maximum permissible nominal principle stress at detail* $f_{Fat15.2,Rd} = 55$ MPa *(R=-1).*

i	$\Delta\sigma_i$ [N/mm^2]	n_i	N_i	n_i / N_i	*Cum.Sum*
1	59.5	4.50E+03	7.56E+05	0.006	0.01
2	49.2	4.50E+03	1.62E+06	0.003	0.01
3	45.8	4.50E+04	2.16E+06	0.021	0.03
4	36.6	4.50E+04	5.30E+06	0.008	0.04
5	33.6	4.50E+05	7.49E+06	0.060	0.10
6	25.5	4.50E+05	2.24E+07	0.020	0.12
7	22.9	4.50E+06	3.46E+07	0.130	0.25
8	16.0	4.50E+06	1.46E+08	0.031	0.28
9	13.8	4.50E+07	2.65E+08	0.170	0.45
10	8.0	4.50E+07	2.34E+09	0.019	0.47
				D_L	**0.47**
				D_{lim} (NA)	**0.48**

Table 15 *Detail 15.2, maximum permissible nominal principle stress at detail* $f_{Fat15.2,Rd2} = 110$ MPa *(R=0).*

i	$\Delta\sigma_i$ [N/mm^2]	n_i	N_i	n_i / N_i	*Cum.Sum*
1	59.5	4.50E+03	7.56E+05	0.006	0.01
2	49.2	4.50E+03	1.62E+06	0.003	0.01
3	45.8	4.50E+04	2.16E+06	0.021	0.03
4	36.6	4.50E+04	5.30E+06	0.008	0.04
5	33.6	4.50E+05	7.49E+06	0.060	0.10
6	25.5	4.50E+05	2.24E+07	0.020	0.12
7	22.9	4.50E+06	3.46E+07	0.130	0.25
8	16.0	4.50E+06	1.46E+08	0.031	0.28
9	13.8	4.50E+07	2.65E+08	0.170	0.45
10	8.0	4.50E+07	2.34E+09	0.019	0.47
				D_L	**0.47**
				D_{lim} (NA)	**0.48**

We note that detail 1.4 and 1.6 give significantly different fatigue strengths. Both could be interpreted as the detail category to be used for analysing the fatigue life of irregularities of extruded connection profiles; particularly at corner fillets. A conservative choice is made and, detail 1.4 is used.

6.4 Tolerances

Curtain walling must accommodate specified building movements and thermal movements according to [4]. The movement and tolerance specifications vary between projects. To design the connection system to accommodate most cases, an investigation of the normative tolerances generally used in construction was done. These are used to define a suitable range of tolerance and movement accommodation to use in the designs. It would be impractical to list all the tolerance requirements given in the standards. Therefore, only the largest and most relevant are shown in the following.

The standard [22] defines permitted geometrical tolerances for aluminium structures. By the standards definition; a permitted tolerance is the difference between the upper limit size and the lower limit size. The permitted deviations do not include elastic deformations and the dimensions specified in drawings are dimensions referring to room temperature (20 °C). Two types of geometrical tolerances are defined; essential tolerances and functional tolerances. Essential tolerances are essential for the mechanical resistance and stability of the completed structure. Functional tolerances are required to satisfy other criteria, such as aesthetics and fit-up criteria. Annexes G, H and provide values for the permitted deviations of these two types of tolerances.

The most relevant tolerances with respect to the design of the connection system can be seen in Table 16. The relevant tolerances for steel construction are provided in [23] and are approximately the same as for aluminium or tighter. Therefore, steel tolerances are not presented here. Manufacturing tolerances for extruded aluminium alloy profiles vary with profile dimensions [24]. An assumed tolerance of approximately 0.1 mm is assumed in the designs and final dimensions are rounded accordingly.

Tolerances for other building materials (reinforced concrete and timber structures) were investigated. The standard [25] provides guidance on geometrical tolerances for concrete structures. Tolerance guidance for the execution of timber structures can be found in [26]. The tolerances listed in the tables are based on the choice of tolerance class 1 for both timber and concrete structures, as the tolerance classes 2 and 3 are tighter. The most relevant tolerances with respect to the design of the connection system can be seen in Table 17 and 18.

.

Table 16 *Geometrical tolerances for aluminium structures [22].*

	Parameter	**Permitted**	**Adapted from**
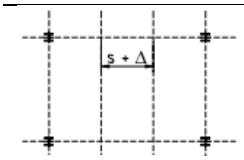	Distance between adjacent beams	$\Delta = \pm 10$ mm	Table H.7
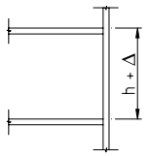	Levels at adjacent floors	$\Delta = \pm 10$ mm	Table H.7
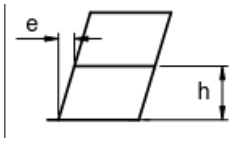	Inclination of a column between adjacent storey levels	$e = \pm \frac{h}{500}$	Table G.8
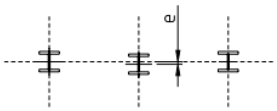	Location of a column at base and storey level compared to a line joining adjacent columns:	$e = \pm 10$ mm	Table H.6

Table 17 *Geometrical tolerances for concrete structures [25].*

	Parameter	**Permitted deviation**	**Adapted from**
	Distance between adjacent beams	$\Delta = \pm 20$ mm or $\pm$ L/600 no more than 40 mm	G.10.5
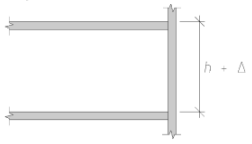	Levels at adjacent floors	$\Delta = \pm 20$ mm	G.10.5
	Inclination of a beam or a slab	$\pm(10 + L/500)$ mm	G.10.5
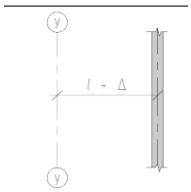	Position in plane of a wall relative to the secondary line	$\Delta = \pm 25$ mm	G.10.4

Table 18 *Geometrical tolerances for timber structures [26]. No images provided in standard.*

Parameter	Permitted deviation	Adapted from
Column base deviation	$\Delta = \pm 20$ mm	Table 8.1
Beam deviation from secondary line	$\Delta = \pm 20$ mm	Table 8.1
Max deviation of wall frame from vertical.	$\Delta = \pm 8$ mm	Table 8.1
Deviation between floor connections.	$\Delta = \pm 10$ mm	Table 8.1

Based on these tolerance investigations, the connection system should accommodate for around $\pm 20 - 25$ mm of deviation in each direction (x, y, z). This is approximately the same as what is generally provided by other connection types available on the market (see Table 2).

We note that EC9 does not permit slotted holes of this size for the bolt sizes most likely to be used (see Section 6.1). Consequently, this amount of tolerance is not achievable in the designs presented in this thesis. In most of Purso Oy's cases, the connection fit-up is measured and holes are drilled on site. Furthermore, as mentioned above, tolerances can be specified on a case by case basis; tighter requirements are possible. If desired, the designs presented could be improved in the future by longer bolt slots; however, this will require physical testing with statistical analysis to be done according to the provisions of Eurocode 0 (EC0) Annex D [27].

7 PRELIMINARY DESIGNS AND DIMENSIONING

The designs to be developed were discussed with Purso Oy; it was thought necessary to develop a simple L-profile design (such as presented in Section 4.1) and a custom design. The reason for this is that mullion placement varies between projects; sometimes it is necessary to have a gap between the mullion and underlying structure, while sometimes there is no gap at all. The custom profile shape was partly inspired by the solar shading connection (Figure 15) and basic L-profiles. The triangular part of the profile was developed out of necessity; without the hypotenuse plate, large stresses would be present (see Figure 26 for the triangular shapes situated at the rear of the mullion). The terminology hereon used in discussion of the L- and custom profiles are shown in Figure 31 and 32 respectively.

The aluminium alloy chosen to be used in the connection profiles is EN-AW 6082-T6. Strength properties of this alloy for different plate thicknesses are presented in EC9-1-1 Table 3.2b. The conservative choice to use strength properties for plate thicknesses $t \leq 5$ mm was made. The 0.2 % proof strength is $f_o = 250$ MPa and the ultimate strength is $f_u = 290$ MPa .

The custom profiles allow for the mullion to be connected to an underlying load bearing plate (fin plate connection). Plate thickness is chosen according to the bolt force reactions; the thickness is parameterized to be twice the thickness of the connection profile rear legs, which ensures bearing resistance. The plate material used must be at least as strong as the connection profile material. Stability of the plate should not be limiting. Overall plate resistance must be checked separately as plate design is beyond the scope of the connection design.

Two connection sizes are desired for each connection type. The sizes of P50L mullions range from 40-200 mm depths. This range was divided into two design ranges; 40-80mm and 100-200 mm for the small and large connection types respectively. The large profiles must therefore accommodate up to 200 mm deep mullion profiles, while the small sized profiles must accommodate up to 80 mm. Based on the mullion accommodation requirements, connection profile outstand lengths were fixed at 100 mm for the large custom profiles and 40 mm for the small profiles. This choice was made to reduce eccentric prying forces by situating bolts near the neutral axes of the largest mullions. The outstand lengths of the L-profiles were set to 40 and 120 mm for the small and large sizes respectively. The rear leg lengths of the custom profiles were also fixed to a length of 57 mm to provide adjustability.

The minimum bolt size used (M10) was chosen to accommodate the relatively thin mullion wall thicknesses (bearing forces); furthermore, most anchor channels use this size of bolt and future use of these may be necessary. Metric hexagon head bolts (partially threaded, ISO 4014), nuts (ISO 4032) and washers (DIN 125) are used. Basic bolt calculations were done to check the feasibility of the bolt size choice (see Appendix 1), note that maximum average shear stress for the bolts was also calculated under maximum fatigue wind load. The maximum stress was relatively small; therefore, bolt fatigue calculation by damage summation is omitted.

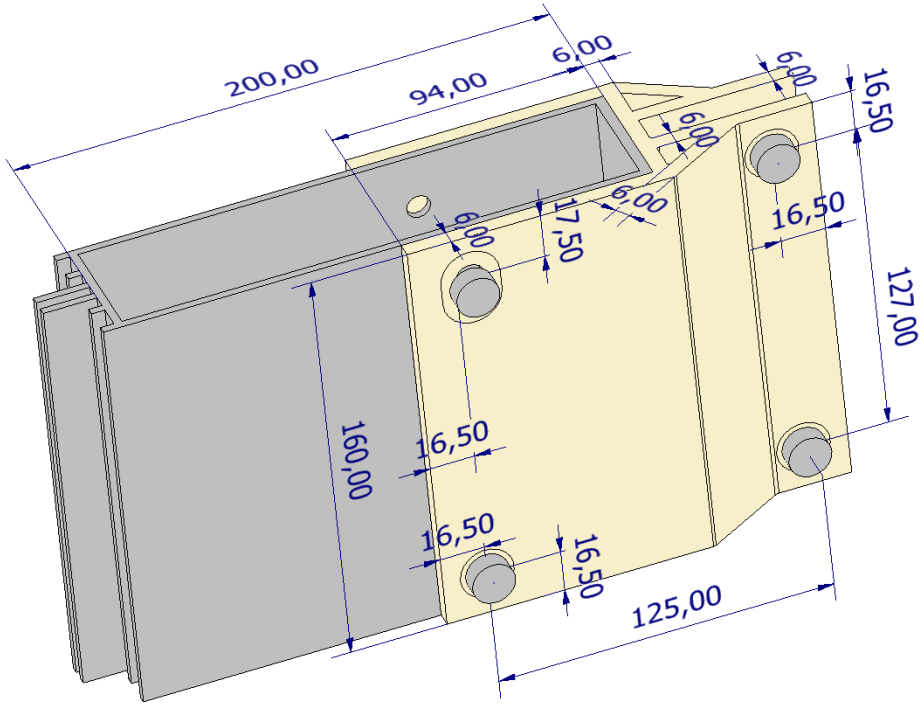

Figure 26 *Initial dimensions of large custom profile. Dimensions in mm. Note that symmetry is used in FEA; the geometry displayed here is split longitudinally.*

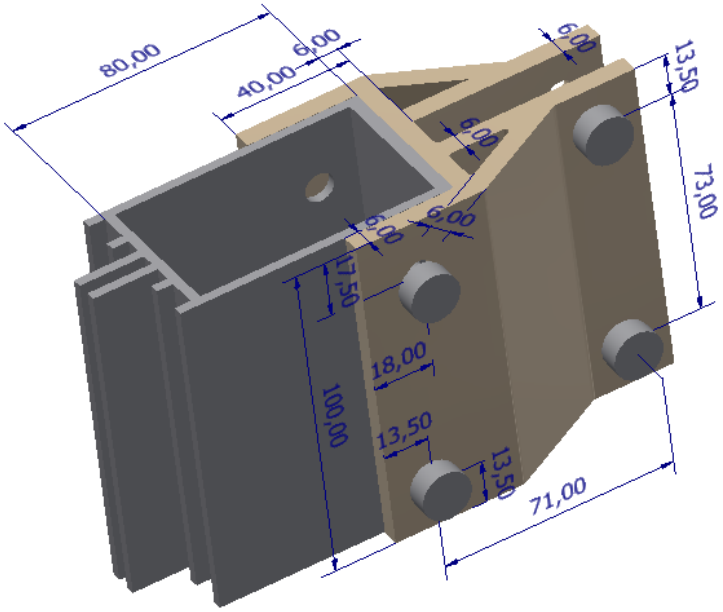

Figure 27 *Initial dimensions of the small custom profile. Dimensions in mm. Note that symmetry is used in FEA; the geometry displayed here is split longitudinally.*

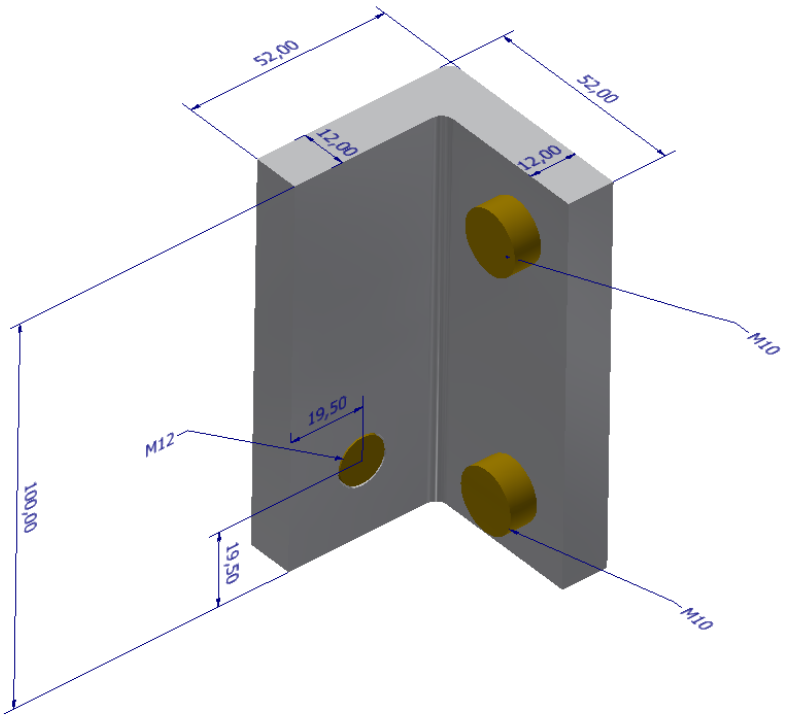

Figure 28 *Initial dimensions of the small L-profile*

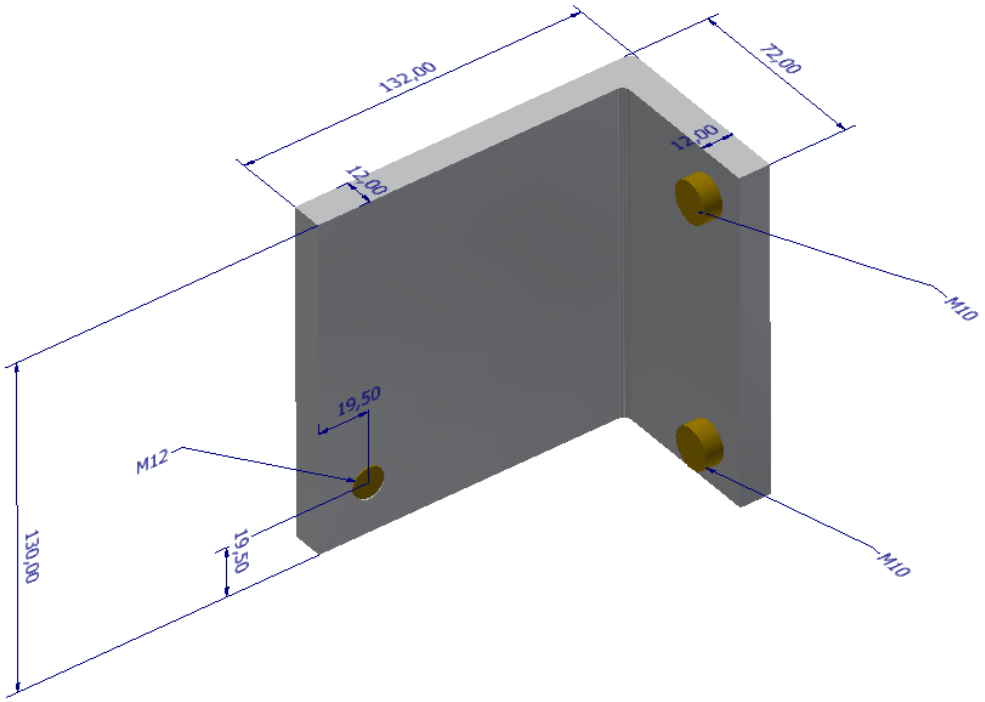

Figure 29 *Initial dimensions of the large L-profile*

The initial designs for the custom profiles and L-profiles (guesses) can be seen in Figures 26 , 27 and 28,29 respectively. Extrusion height set so that the moment arms between bolt groups are roughly the same. Wall thicknesses were all set according to the guessed front outstand thickness. Bolts are generally size M10; M12 is used for the front bolts of the L-profiles.

8 OPTIMIZATION

There is an immense amount of literature concerning the field of optimization. The goal is not to investigate the field, only the narrow application of two algorithms to the design of aluminium profiles; therefore, only a brief introduction of the algorithms used is presented. Two different optimization algorithms are applied to the parametrized finite element models; namely, the genetic (GA) and SORVI algorithms implemented in the ACT extension SORVI design booster (SORVI db).

The GA implemented in SORVI db is based on the algorithm provided in the global optimization toolbox of the proprietary software MATLAB. However, the implementation has been slightly augmented in SORVI Design Booster to allow the use of discrete variables [28]. Genetic algorithms are well-known algorithms that are based on nature; specifically, natural selection. A great deal of literature is available on the subject. For more information on genetic algorithms, the reader is referred to [29] Information on the genetic algorithm implementation in MATLAB version R2017a is available in [30].

The SORVI algorithm uses a surrogate-model based approach to optimization problems. The algorithm is based on the successive response surface method (SRSM). The idea behind this method is to successively create surrogate models (response surfaces) based on input variables and response values on subspaces of the design space (region of interest). The surrogate-models are created by fitting the data to polynomial basis functions via the method of least squares. The limits of the region of interest (ROI) are shifted for each successive optimization iteration based on the current optimal solution and a new region is explored. The motivation to use surrogate-modelling techniques is due to most engineering problems relying on computationally expensive calculations, which often only provide response values without gradients. By employing surrogate-model methods, it is possible to approximate gradients in the region near the solved response values and apply gradient based optimization methods. Therefore, the use of a surrogate-modelling techniques provides two immediate benefits; savings in calculation costs and the possibility to apply gradient based methods [28]. For further information on the method, the reader is referred to [31].

The total mass of the connection profile is chosen as the objective function to be minimized. The CAD geometry is fully parameterized. The design parameters include profile wall thicknesses, extrusion length and various other geometrical dimensions.

Multiple constraints are applied to the objective function. Briefly:

- Von Mises stress is limited (according to Eurocode 9 guidance)
- Maximum principle stress is limited at probe points (fatigue)
- Bolt shear limits (parameterized and based on Eurocode design equations)

The implementation of constraints and design parameters of the different models is further discussed in Section 9. The total evaluation count and results obtained by these algorithms are compared and the better overall design is chosen

The standard formulation for optimization of the custom profile designs is defined as

$$
\begin{aligned}
&\min f_{massC}(x_1, x_2, x_3, x_4, x_5, x_6, x_7) \\
&\text{s.t.} \\
&g_{VM}(x_1, x_2, x_3, x_4, x_5, x_6, x_7) - f_{eq,Rd} \le 0 \\
&g_{Fat1}(x_1, x_2, x_3, x_4, x_5, x_6, x_7) - f_{Fat15.2,Rd2} \le 0 \\
&g_{Fat2}(x_1, x_2, x_3, x_4, x_5, x_6, x_7) - f_{Fat15.2,Rd2} \le 0 \\
&g_{Fat3}(x_1, x_2, x_3, x_4, x_5, x_6, x_7) - f_{Fat15.2,Rd2} \le 0 \\
&g_{Fat4}(x_1, x_2, x_3, x_4, x_5, x_6, x_7) - f_{Fat15.2,Rd2} \le 0 \\
&g_{Fat5}(x_1, x_2, x_3, x_4, x_5, x_6, x_7) - f_{Fat15.2,Rd2} \le 0 \\
&g_{Fat6}(x_1, x_2, x_3, x_4, x_5, x_6, x_7) - f_{Fat15.2,Rd2} \le 0 \\
&g_{Fat7}(x_1, x_2, x_3, x_4, x_5, x_6, x_7) - f_{Fat15.2,Rd2} \le 0 \\
&g_{Fat8}(x_1, x_2, x_3, x_4, x_5, x_6, x_7) - f_{Fat15.2,Rd2} \le 0 \\
&g_{Fat9}(x_1, x_2, x_3, x_4, x_5, x_6, x_7) - f_{Fat1.4,Rd} \le 0 \\
&g_{Fat10}(x_1, x_2, x_3, x_4, x_5, x_6, x_7) - f_{Fat1.4,Rd} \le 0 \\
&g_{BoltUt1}(x_1, x_2, x_3, x_4, x_5, x_6, x_7) - 1 \le 0 \\
&g_{BoltUt2}(x_1, x_2, x_3, x_4, x_5, x_6, x_7) - 1 \le 0 \\
&g_{BoltUt3}(x_1, x_2, x_3, x_4, x_5, x_6, x_7) - 1 \le 0 \\
&x_{1min} \le x_1 \le x_{1\max} \text{ (Extrusion height)} \\
&x_{2min} \le x_2 \le x_{2\max} \text{ (Front leg thickness)} \\
&x_{3min} \le x_3 \le x_{3\max} \text{ (Triangle base length)} \\
&x_{4min} \le x_4 \le x_{4\max} \text{ (Triangle base thickness)} \\
&x_{5min} \le x_5 \le x_{5\max} \text{ (Hypotenuse thickness)} \\
&x_{6min} \le x_6 \le x_{6\max} \text{ (Throat wall thickness)} \\
&x_{7min} \le x_7 \le x_{7\max} \text{ (Rear leg thickness),}
\end{aligned}
$$

where the objective function f_{massC} is the total mass of the custom connection profile, g_{VM} is the von Mises stress in the profile, $g_{Fati}, i = 1...8$ the maximum principle stress at bolt hole probe points, $g_{Fati}, i = 9...10$ the maximum principle stress at material fatigue probe points and $g_{BoltUti}, i = 1...3$ the bolt UT-ratios. The variable definitions are listed alongside the variable bounds in brackets. The variable limits used can be seen in Table 19.

The standard formulation for optimization of the L-profile designs is as defined as

$$
\begin{aligned}
&\min f_{massL}(x_1, x_2, x_3, x_4) \\
&s.t. \\
&g_{VM}(x_1, x_2, x_3, x_4) - f_{eq,Rd} \le 0 \\
&g_{Fat1}(x_1, x_2, x_3, x_4) - f_{Fat15.2,Rd} \le 0 \\
&g_{Fat2}(x_1, x_2, x_3, x_4) - f_{Fat15.2,Rd} \le 0 \\
&g_{Fat3}(x_1, x_2, x_3, x_4) - f_{Fat1.4,Rd} \le 0 \\
&g_{Fat4}(x_1, x_2, x_3, x_4) - f_{Fat1.4,Rd} \le 0 \\
&g_{BoltUt1}(x_1, x_2, x_3, x_4) - 1 \le 0 \\
&g_{BoltUt2}(x_1, x_2, x_3, x_4) - 1 \le 0 \\
&g_{BoltUt3}(x_1, x_2, x_3, x_4) - 1 \le 0 \\
&x_{1min} \le x_1 \le x_{1\max} \text{ (Extrusion height)} \\
&x_{2min} \le x_2 \le x_{2\max} \text{ (Foot length)} \\
&x_{3min} \le x_3 \le x_{3\max} \text{ (Foot thickness)} \\
&x_{4min} \le x_4 \le x_{4\max} \text{ (Leg thickness),}
\end{aligned}
$$

where the objective function f_{massL} is the total mass of the L-profile, g_{VM} is the von Mises stress in the profile, $g_{Fati}, i = 1...2$ the maximum principle stress at bolt hole probe points, $g_{Fati}, i = 2...4$ the maximum principle stress at material fatigue probe points and $g_{BoltUti}, i = 1...3$ the bolt UT-ratios. The variable definitions are listed alongside the variable bounds in brackets. The variable limits used can be seen in Table 20. Both optimization problems are continuous. No discrete variables are used (such as bolt size).

9 CAD AND FEA MODELLING

A total of 8 CAD geometry models were created. The models are as follows:

- Light sized, self-weight + wind load, L-profile
- Light size, wind load, L-profile
- Heavy sized, self-weight + wind load, L-profile
- Heavy size, wind load, L-profile
- Light sized, self-weight + wind load, Custom profile
- Light size, wind load, Custom profile
- Heavy sized, self-weight + wind load, Custom profile
- Heavy size, wind load, Custom profile

The geometry dimensions and constraints were applied and fully parameterized in Autodesk Inventor Professional. The CAD geometry was then linked to Ansys via a direct associative interface. Using this method of modelling, all the mathematics involved in parameterizing and constraining the geometry can be separated from the FEA model. The CAD system acts like a black box which returns updated geometry to the FEA model when the imported parameters are changed in the FEA program. The direct interface provides ways of filtering unnecessary parameters with regards to FEA modelling, such as driven parameters. This is done by only importing parameters with a predefined prefix (prefix defined by user). Furthermore, parametric named selections and user defined coordinate systems are imported; this provides robust means of applying boundary conditions in FEA modelling to specific entities of imported geometry which change parametrically. The use of named selections and user defined coordinate systems insures that boundary conditions are not dropped when geometry is changed.

Design choices were made in choosing the specific key parameters to be imported and used in the search for a better design by optimization. The chosen parameters (variables) were mentioned in Section 8, where the standard formulations of the optimization problems were given. The key parameters for the custom profile models along with corresponding initial guesses and ranges can be seen in Table 19. Table 20 shows parameters, initial guesses and ranges for the L-profiles.

Table 19 *Input parameters and initial guesses for optimization of custom profiles.*

	Parameter	Initial [mm] (Light)	Range [mm] (Light)	Initial [mm] (Heavy)	Range [mm] (Heavy)
1.	Extrusion height	120	80-200	160	140-200
2.	Front leg thickness	6	3-10	6	3-10
3.	Triangle base length	30	10-30	30	10-30
4.	Triangle base thickness	6	3-10	6	3-10
5.	Hypotenuse thickness	6	3-10	6	3-10
6.	Throat wall thickness	6	3-10	6	3-10
7.	Rear leg thickness	6	3-10	6	3-10

Table 20 *Input parameters and initial guesses for optimization of L-profiles.*

	Parameter	Initial [mm] (Light)	Range [mm] (Light)	Initial [mm] (Heavy)	Range [mm] (Heavy)
1.	Extrusion height	100	80-200	130	100-200
2.	Foot length	40	40-100	60	40-100
3.	Foot thickness	12	5-15	12	5-15
4.	Leg thickness	12	5-15	12	5-15

Sorvi db modifies the input parameters and the FEA model acts as a black box which calculates and returns results as output parameters, based on given input parameters and boundary conditions. After calculations are done, the results must be checked to determine design feasibility; in other words, check if the design fulfils the requirements specified in Section 6. The output parameters along with their uses in Sorvi db (in brackets) are:

1. Total weight (minimize),
2. Maximum nominal principle stress at front bolt hole (constraint).
3. Maximum nominal principle stress at rear bolt hole (constraint).
4. Maximum nominal principle stress at triangle transition (constraint).
5. Maximum von mises stress (constraint).
6. Force reactions at bolt holes (constraint).

Both L- and custom profile models use the same output parameter types. Von Mises stress was read from predefined surface regions that omitted high stress areas around the bolt holes. This was done by splitting the surfaces with 20 mm diameter circles around bolt holes (see Figure 30). The bolt UT-ratio checks and edge distance requirements ensure that these regions can resist the applied load. Bolts are modelled monolithically; only basic dimensions are considered, and excess detail is omitted.

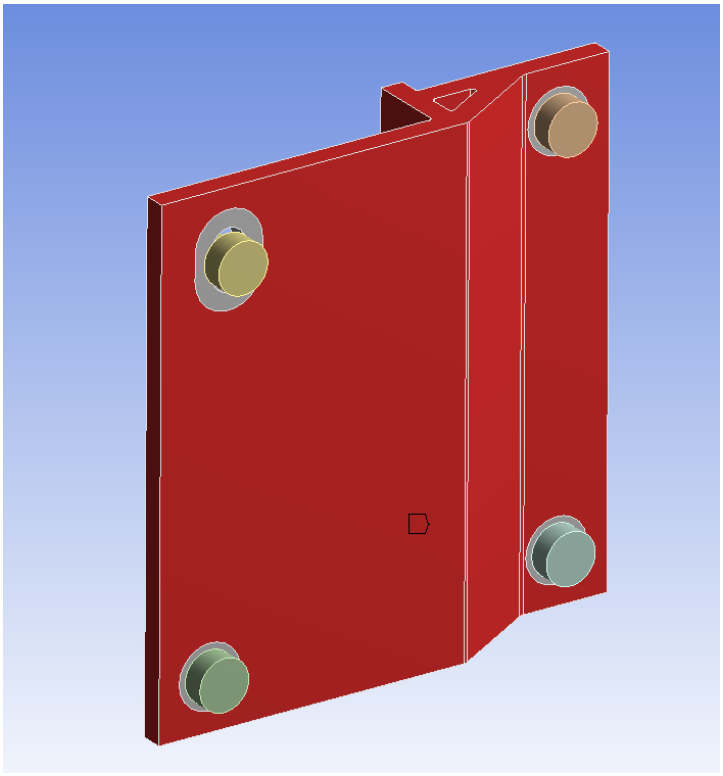

Figure 30 *Von Mises stress regions, note omitted areas around bolts.*

The probe points for maximum principle stresses are modelled using named user defined coordinate systems (UCS) placed 5 mm away from points of interest in the CAD program; this way the probe points follow the parametric changes of the geometry. Ansys supports the use of Python 2.6 expressions in output parameter definitions. This is particularly convenient, as Python expressions can be used to evaluate the current UT-ratios of bolts according to EC9 requirements and only the UT-ratios need to be passed to Sorvi db. The probe points along with parameter definitions are shown in Figures 31 and 32. Note the fatigue stress probes labels (PXX). These are referred to in result plots shown in Appendix 2.

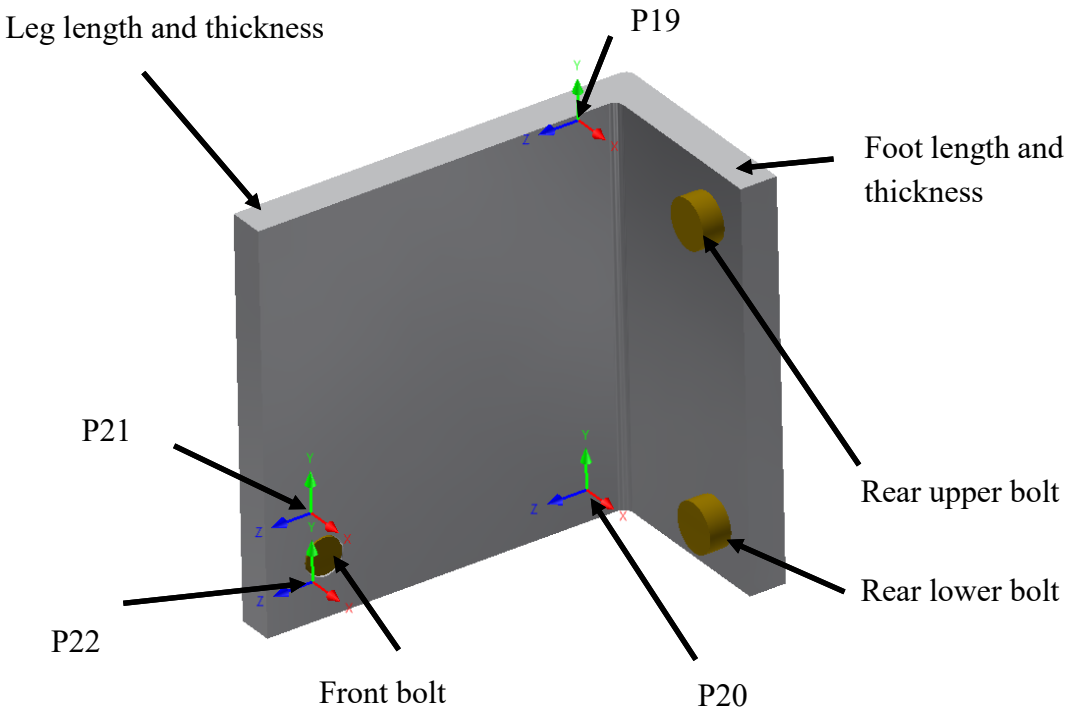

Figure 31 *Parameter names and fatigue probe points for L-profiles.*

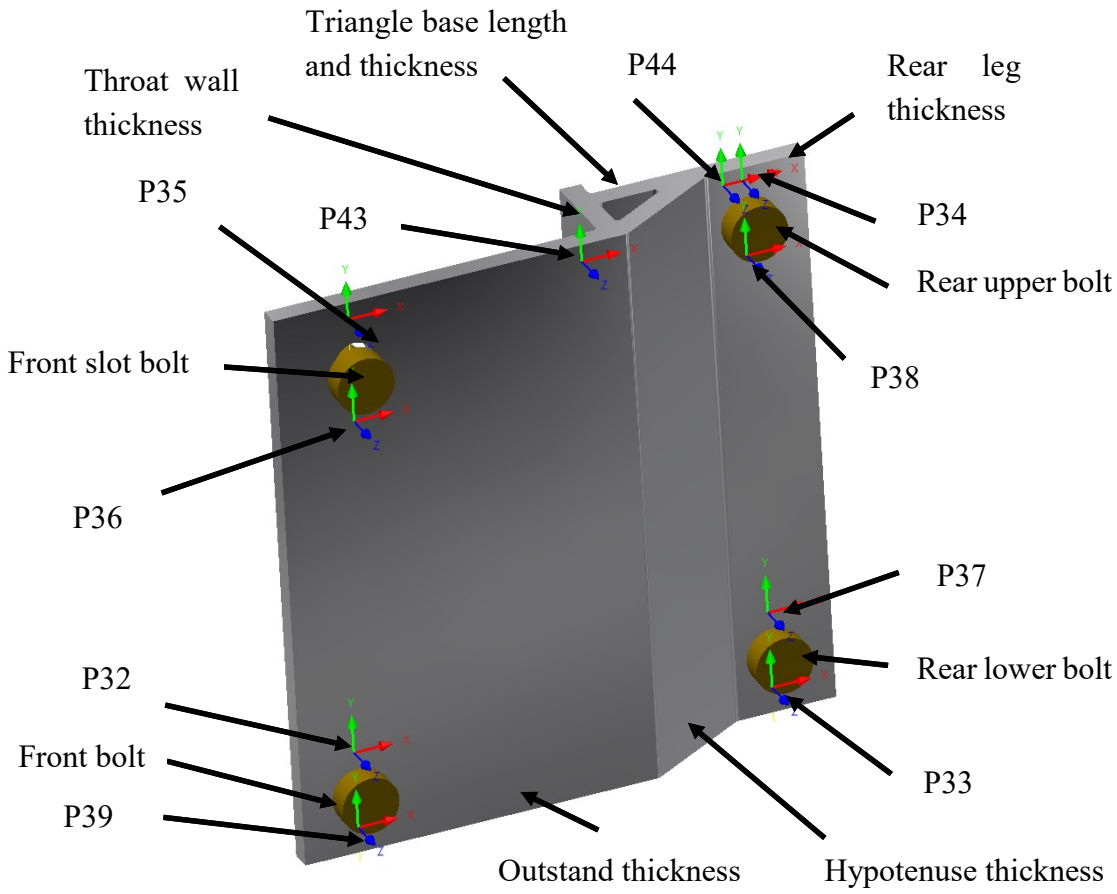

Figure 32 *Parameter names and fatigue probe points for custom profiles.*

To save on tool and manufacturing costs, the main profile shape is kept the same for the two different connection types of each connection profile size; in other words, the optimized self-weight + wind load profile shape is also used for wind load only connection type. Only profile bolt hole types and placement are changed. To achieve this, the profile optimization is primarily done on the self-weight + wind load profiles. The loads are much larger in these cases, as self-weight causes significant bending moments which result in larger stresses in the profile walls when compared to loading by wind alone.

Only governing load cases are checked to minimize calculation costs. The largest mullion profiles designed to be accommodated by each custom profile are used for load distribution; this ensures eccentricity (neutral axis of mullion) is considered. The 200 mm mullion is used for the large and the 100 mm mullion is used for the small custom profile analyses. Mullion side wall thickness is 3 mm in all cases as contact difficulties arise with smaller thickness (2 mm). This slightly overestimates mullion stiffness; however, in these cases the effect is minimal and mullion stiffness is not critical in determining internal load distribution. The entire loading (wind + self-weight) was applied to one face (top face) of the mullion, which could be the reality if the connection is situated as a lower end support. This simulates the worst-case scenario and causes the largest stresses at the top of the profile. Loads were applied directly to the front bolt faces for the L-profiles; only shear is used to carry the load and no prying forces occur as the mullion base is not placed directly into contact with the load bearing structure. Figures 33 and 34 show the project schematics for the custom and L-profile cases respectively. The schematics show the load cases covered. Note that the amount of load cases for the L-profiles is larger. This is due to investigation of compressive wind loading which was deemed to be non-governing in the custom profile cases due to alternative load paths (throat wall); furthermore, self-weight could be advantageous in reducing wind stress; therefore, wind load alone needed to be checked too.

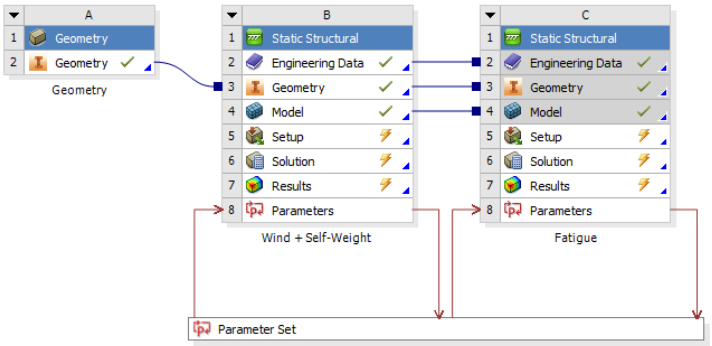

Figure 33 *Project schematic for custom profiles.*

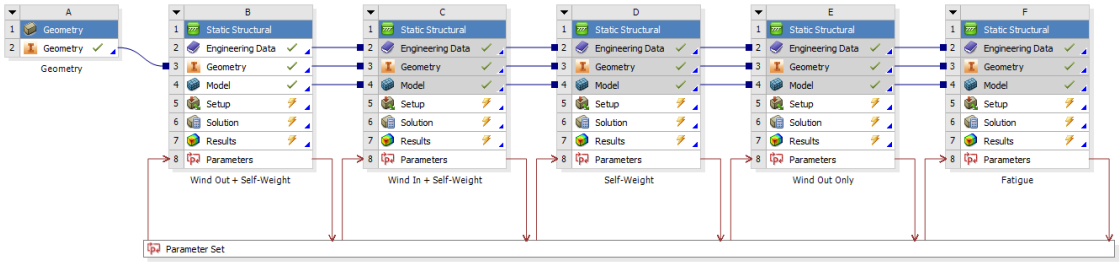

Figure 34 *Project schematic for L-profiles.*

Quadratic tetrahedral elements were used in all models. The element type was chosen to remedy meshing difficulties which often arise (and did) when geometry is changed. It would be possible to mesh using hexahedral meshing and precise mesh controls; however, tetrahedral meshes require considerably less pre-processing time in this regard. Element sizing was parameterized and set to as half of the minimum wall thickness present in the profile at each evaluation. This ensured that the mesh was of satisfactory quality and that geometry could be meshed regardless of the current geometry under consideration. The results of each run were checked by refining the mesh (h-method) and using quadratic hexahedral elements after the optimization process was finished. The results did not differ significantly (stiffness, stress levels) after mesh refinement; thus, the results were considered acceptable and not dependent on the mesh. An example of meshes used in the optimization process can be seen in Figure 35.

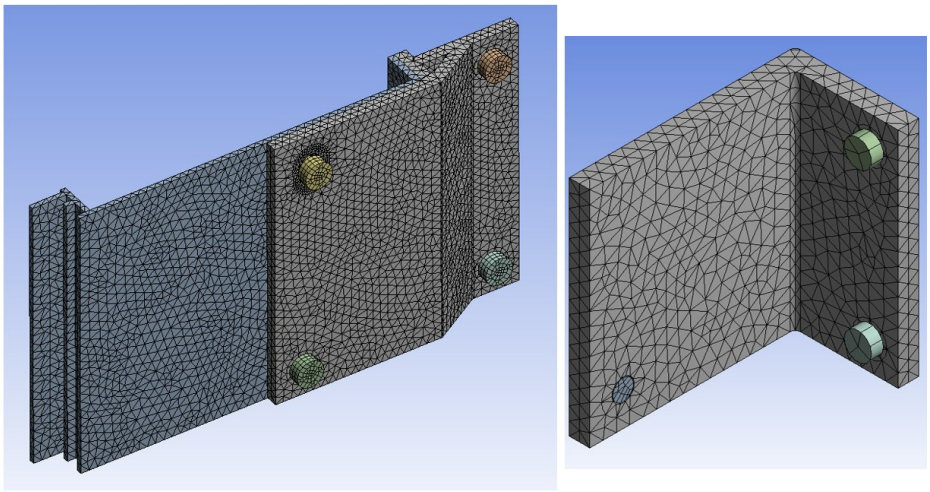

Figure 35 *Meshed geometry. Note refinement around slotted hole to ensure contact. Bolts and mullion profile are relatively uninteresting, only used to transfer loads.*

The material model used in the optimization process was linear elastic for both bolts and aluminium alloy. A Young's modulus of 70 GPa was used for aluminium, while 200 GPa was used for the steel bolts. Both material models use a Poisson ratio of 0.3. EC9 provides a great deal of alternative material models of different aluminium alloy types for use in non-linear analysis, including the well-known Ramberg Osgood model. A detailed presentation of the different models is available in [32]. Figure 36 shows the material

models for EN-AW 6082-T6 alloy. The bilinear isotropic hardening model (conservatively modified to $f_o = 227$ MPa design yield strength) is used in the non-linear analyses presented (GMNA and GMNIA).

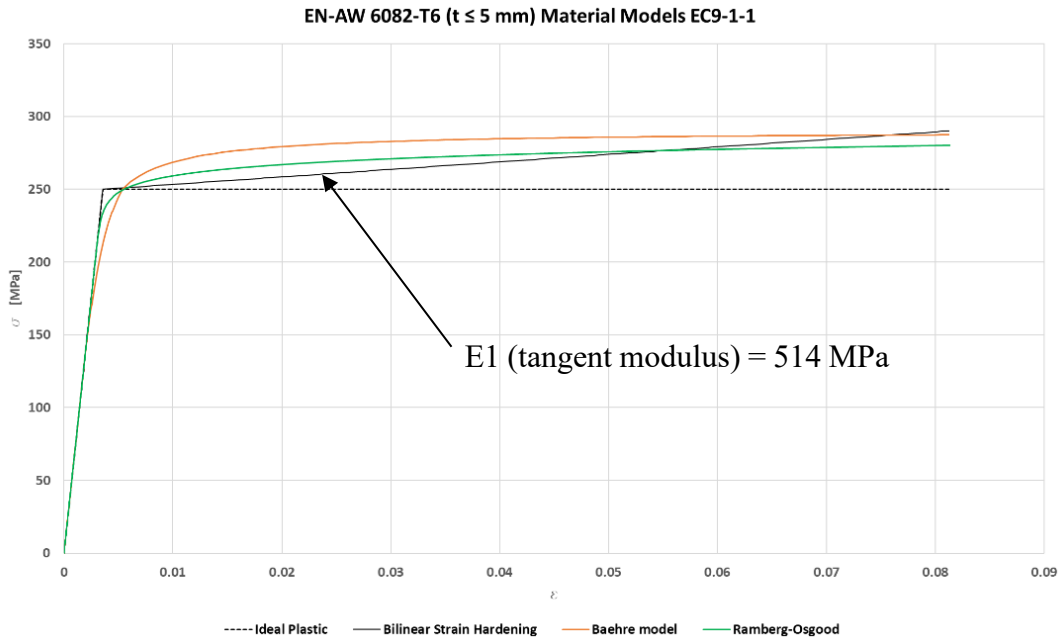

Figure 36 *Material models according to EC9-1-1. E1 is the bilinear tangent modulus. Note that the models do not take material safety factors into account ($f_o = 250$ MPa).*

Contacts and applied boundary conditions applied to the models can be seen in Figures 37 and 38.

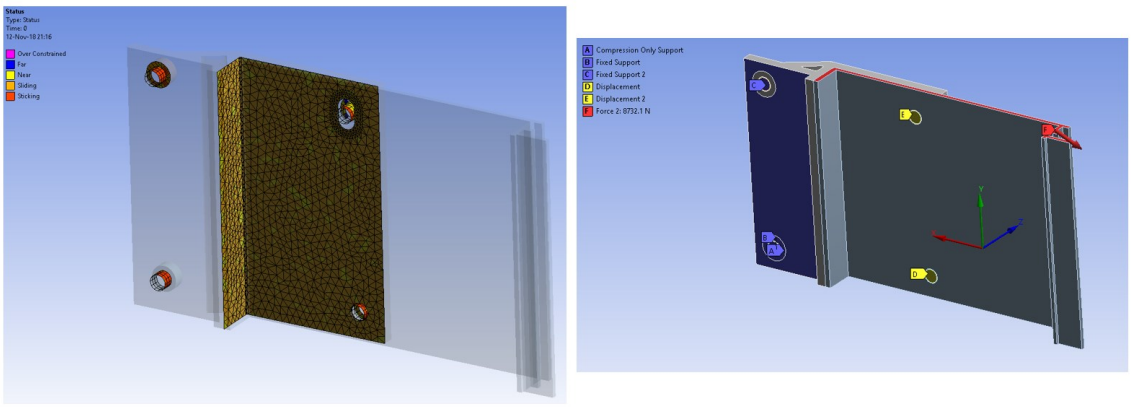

Figure 37 *Custom profile contact regions and initial status (left) and boundary conditions (right). Symmetry boundary conditions were also set to split regions.*

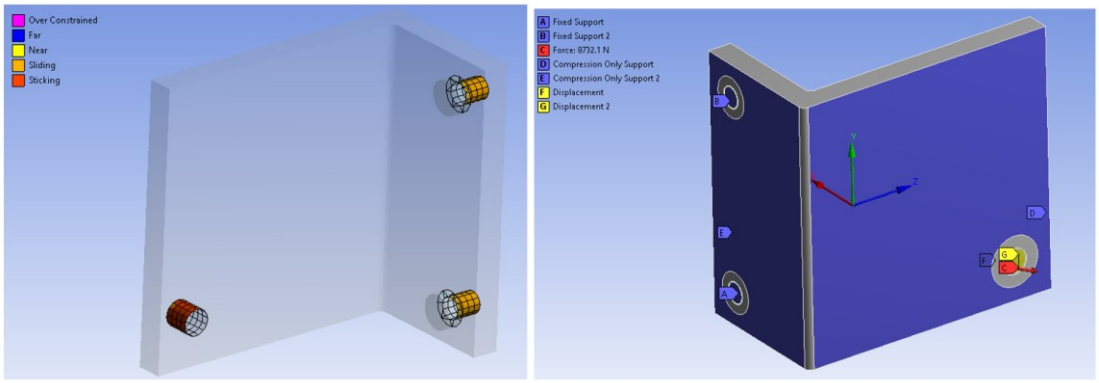

Figure 38 *L-profile contact regions and initial status (left) and boundary conditions (right). Symmetry boundary conditions were also set to split regions.*

Table 21 *Contacts used in custom profile analyses. Note, contact names in camelCase (used for easy reading in Ansys Workbench contact tree).*

Contact Type and Bodies
Rough - rearTopShank To upperRearBoltHole
Rough - frontBoltShank To frontBoltHole
Rough - rearBottomBoltShank To rearLowerBoltHole
Rough - frontBoltShank To mullionBoltHole
Frictionless - outstandMullion To mullionOutstand
Frictionless - throatWall To mullionRear
Frictionless - frontBoltBase To outstand
Frictionless - rearBottomBoltHeadBase To rearLeg
Frictionless - RearTopBoltHeadBase To rearLeg
Frictionless - slotBoltShank To frontBoltSlot
Frictionless - frontBoltBase To outstand
Rough - slotBoltShank To mullionSlotBoltHole

Table 22 *Contacts used in L-profile analyses. Note, contact names in camelCase (used for easy reading in Ansys Workbench contact tree).*

Contact Type and Bodies
Rough - frontBoltShank To frontBoltHole
Frictionless - rearBoltLowerShank To rearLowerBoltHole
Frictionless - rearBoltUpperShank To rearTopBoltHole
Frictionless - rearBoltLowerBase To lowerBoltBasePlate
Frictionless - rearBoltUpperBase To upperBoltBasePlate

The type of contact used (rough, frictionless), was chosen to conservatively estimate the forces transferred to the bolts contacts are listed in Table 21 and 22. The augmented Lagrange contact formulation with asymmetric contact behaviour is used in all contacts. Contact reaction forces used in bolt UT-ratio calculations were read from the contact elements. The stiffness of the contacts was updated with each iteration

10 RESULTS AND FINAL DESIGNS

The results of the optimization runs are presented in Appendix 2. The results are presented in the following order for each run:

1. Objective history
2. Iteration history (if SORVI algorithm)
3. Wall thicknesses
4. Lengths
5. Von Mises Stress
6. Bolt UT-Ratios (2 plots for L-profiles)
7. Stress Probes (maximum principle stress, 2 plots for custom profiles)

The caption below each figure provides information of the data depicted. Discussion of the results takes place in Section 11. Final design FEA results and stability are checked in sections 10.1 and 10.2. A summary of the results of optimization can be seen in Tables 23 and 24. Note the relevant section numbers listed alongside results point to the profile in question.

Table 23 *Summary of custom profile results.*

		Initial Variables							
Section	Algorithm	Rear leg thickness	Extrusion h	Outstand thickness	Triangle base length	Throat wall thickness	Triangle base thickness	Hypotenuse thickness	Mass [kg]
Large Custom	SORVI	6	160	6	30	6	6	6	0.557
Large Custom	SORVI ADAP.	6	160	6	30	6	6	6	0.557
Large Custom	SORVI ADAP.	7	160	7	30	7	7	7	0.644
Small Custom	SORVI	6	100	6	30	6	6	6	0.246
Small Custom	GA	6	100	6	30	6	6	6	0.246

		Best Variables								
Section	Algorithm	Rear leg thickness	Extrusion h	Outstand thickness	Triangle base length	Throat wall thickness	Triangle base thickness	Hypotenuse thickness	Mass [kg]	Mass % Savings
Large Custom	SORVI	5.9	140.0	5.6	30.0	4.9	6.2	4.9	0.449	19%
Large Custom	SORVI ADAP.	6.7	140.0	5.4	26.0	4.6	5.8	5.0	0.443	21%
Large Custom	SORVI ADAP.	6.8	140.0	5.4	21.3	5.3	5.5	5.4	0.444	31%
Small Custom	SORVI	6.1	80.0	5.0	24.0	4.8	5.8	4.8	0.167	32%
Small Custom	GA	5.1	81.3	5.2	27.8	4.9	5.3	4.8	0.168	32%

Table 24 *Summary of L-profile results.*

		Initial Variables				
Section	**Algorithm**	**Foot Length**	**Foot Thickness**	**Leg Thickness**	**Extrusion h**	**Mass [kg]**
Small L	Sorvi	40	12	12	100	0.295
Large L	Sorvi	60	12	12	130	0.819

		Best Variables				
Section	**Algorithm**	**Foot Length**	**Foot Thickness**	**Leg Thickness**	**Extrusion h**	**Mass [kg]**
Small L	Sorvi	40.0	6.6	7.0	80.0	0.125
Large L	Sorvi	43.7	9.9	8.7	100.0	0.427

The chosen designs for the custom profiles are highlighted in Table 23. The choice was made on overall savings and wall thickness consistency; large differences in wall thicknesses are not desired. The relative difference between results is small.

10.1 Linear and GMNA Results for Final Designs

The final design results were checked for mesh dependency; furthermore, a materially and geometrically non-linear analysis (large displacements) was performed for each model. The largest results were read from the analyses. Table 25 and 26 show the results summary of the custom and L-profiles respectively. Figures 40 to 43 show von Mises stress plots (GMNA) for each model.

Table 25 *Custom profile result summary.*

Model	Type	Mesh	Element Size [mm]	Max Displacement [mm]	Max Eqv. Stress [Mpa]	Shear Top Bolt Front [kN]	Shear Top Bolt Rear [kN]	Shear Bottom Bolt Front [kN]	Shear Bottom Bolt Rear [kN]
Custom Small	Linear	Original (Tetra)	3.2	0.2	214.4	7952	10983	2700	6123
	Linear	Ref1 (Hexa)	3	0.3	227.4	7946	10981	2675	6123
	GMNA	Ref2 (Hexa)	2	0.9	225.5	8255	10849	2355	6168
Custom Large	Linear	Original (Tetra)	3.2	0.3	220.8	10384	14338	3492	6302
	Linear	Ref1 (Hexa)	3	0.3	237.8	10371	14336	3487	6302
	GMNA	Ref2 (Hexa)	2	0.7	230.0	10293	14418	3561	6330

Table 26 *L-Profile result summary.*

						Bolt forces from Wind Out+Self-Weight				
Model	Type	Mesh	Element Size [mm]	Max Displacement [mm]	Max Eqv. Stress [Mpa]	Shear Bolt Front [kN] (Applied)	Shear Top Bolt Rear [kN]	Shear Bottom Bolt Rear [kN]	Tension Bottom Bolt Rear [kN]	Tension Top Bolt Rear [kN]
L-Small	Linear	Original (Tetra)	4.4	0.4	225.1	5483	1125	1980	4685	2344
	Linear	Ref1 (Hexa)	3	0.5	236 (Approx.)	5483	1232	1646	4783	2510
	GMNA	Ref2 (Hexa)	2	0.5	224.6	5483	1145	1765	4934	2516
L-Large	Linear	Original (Tetra)	5.8	1.080	198.3	8732	2835	1411	3925	8728
	Linear	Ref1 (Hexa)	3	1.0	237.0	8732	2530	1501	4309	9482
	GMNA	Ref2 (Hexa)	2	0.8	226.6	8732	2423	1672	5020	10055

The non-linear analyses initially displayed peculiar results; von Mises stresses above yield limit were plotted in postprocessing, although no plastic deformation was present in these elements. The reason for this is how stresses are calculated and plotted in ANSYS. Stresses are calculated at Gaussian integration points and extrapolated to the nodes. To rectify this, an APDL command snippet is used (see Figure 39).

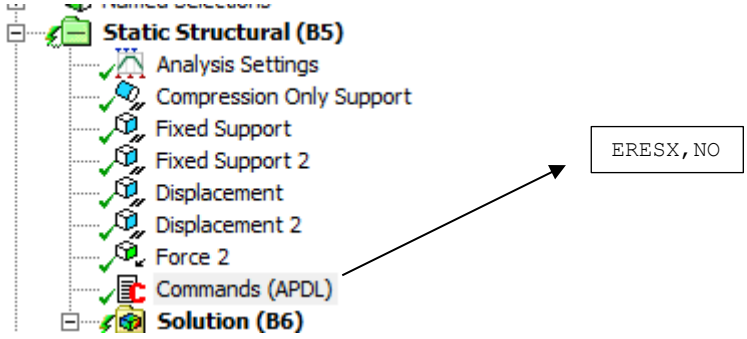

Figure 39 *APDL command snippet.*

This command prevents integration result extrapolation to the nodes; integration point results are copied to the nodes instead [33]. Another method to rectify this would be to use a finer mesh in these regions; however, this was considered unnecessarily expensive (computationally) as the mesh was already relatively refined. Furthermore, the irrational stresses were only present at single nodes intermittently.

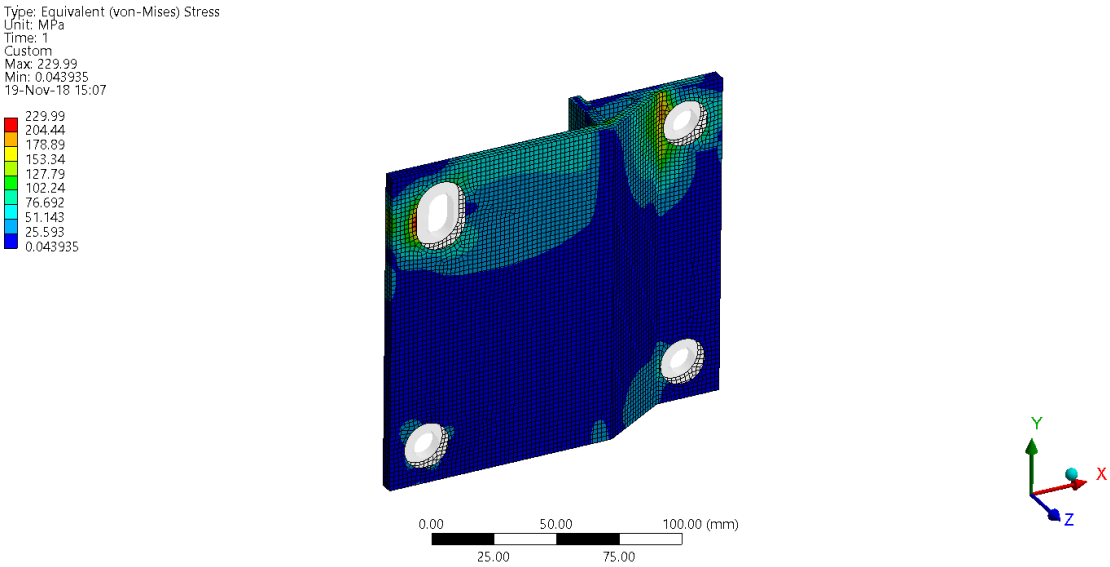

Figure 40 *GMNA von Mises Stress, Large Custom Profile.*

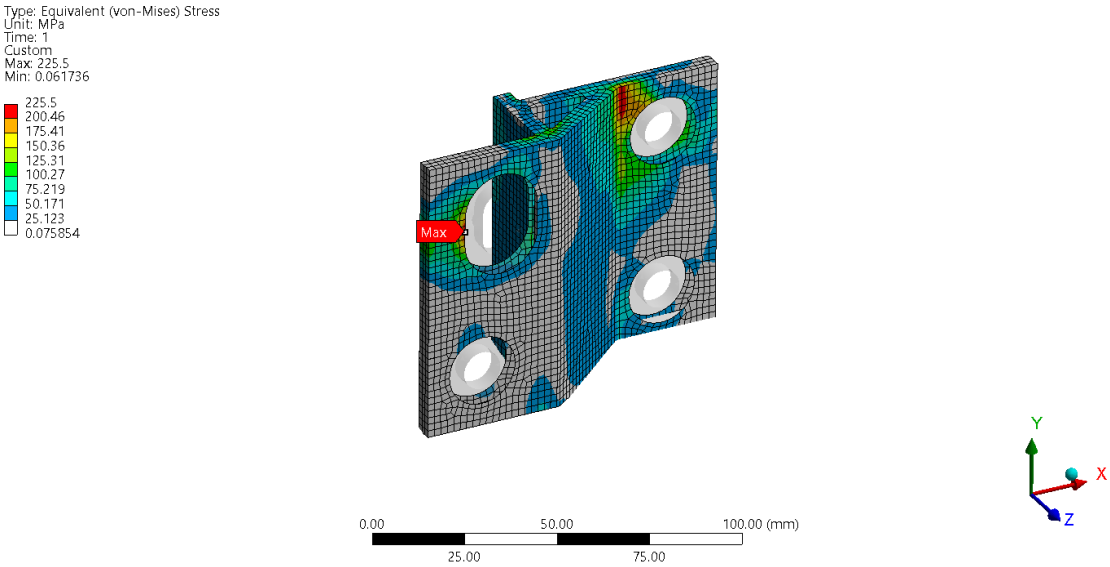

Figure 41 *GMNA von Mises Stress, Small Custom Profile*

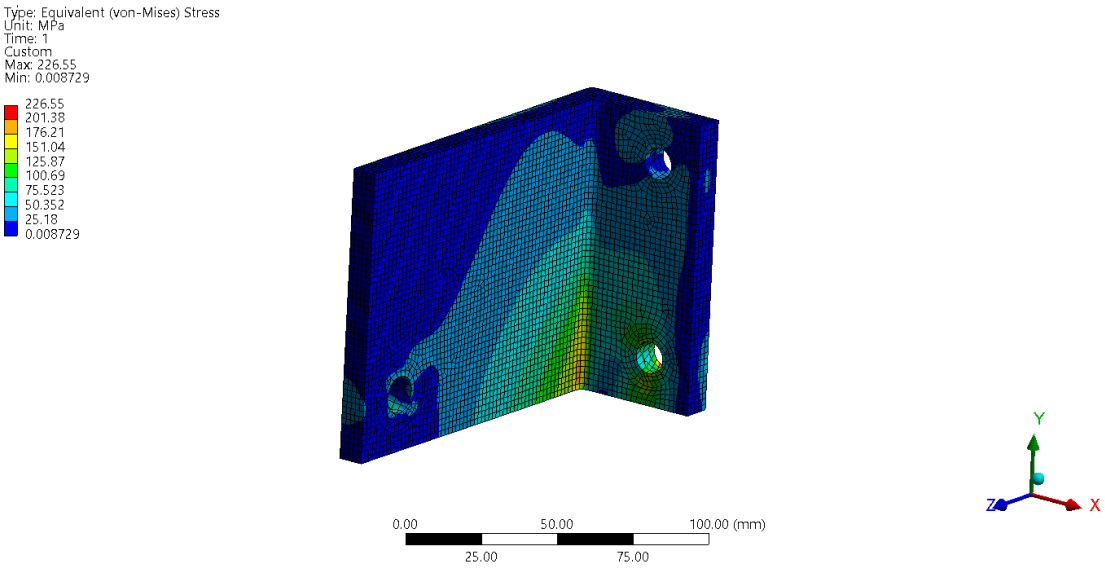

Figure 42 *GMNA von Mises Stress, Large L-Profile*

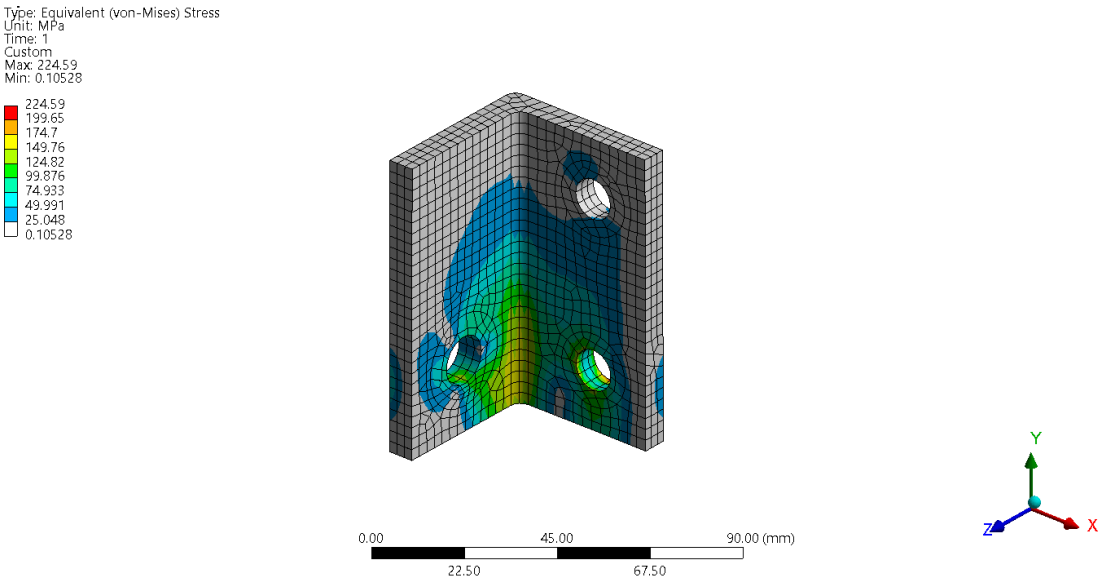

Figure 43 *GMNA von Mises Stress, Small L-Profile*

Only a small amount of plastic deformation was present in the GMNA analyses. The plastic strain was localized around the bolt holes (all models). This is to be expected as bolt holes cause stress concentration; however, this is irrelevant, as EC9-1-1 the bolt calculations ensure resistance.

10.2 GMNIA Results

GMNIA analyses were done to ensure local buckling resistance of profile designs with relatively large distance/thickness ratios of plates in compression. Table 8.2 of EC9-1-1 does mention checking of local buckling between bolts in bolt groups. The check need not be done if

$$\frac{p_1}{t} \leq 9\epsilon \ , \tag{10.1}$$

where p_1 is the distance between bolts in direction of compression, t is material thickness and ϵ is defined as

$$\epsilon \quad \sqrt{\frac{\text{MPa}}{f_0}} \ . \tag{10.2}$$

This could be applied by assuming sufficient stiffness at the base outstand parts; however, the limit of 9ϵ is obviously broken in both cases.

The large L-Profile carries compression loads of wind and self-weight in the plate section. The large custom profile only carries self-weight (shear buckling); wind loads are transferred via a secondary load path when the mullion compresses against the throat of the connection profile. This was also noted in fatigue calculations; the stress ratio for custom profile front bolt holes is $f_{Fat15.2,Rd2} = 110$ MPa, not $f_{Fat15.2,Rd} = 55$ MPa which was used for L-profiles.

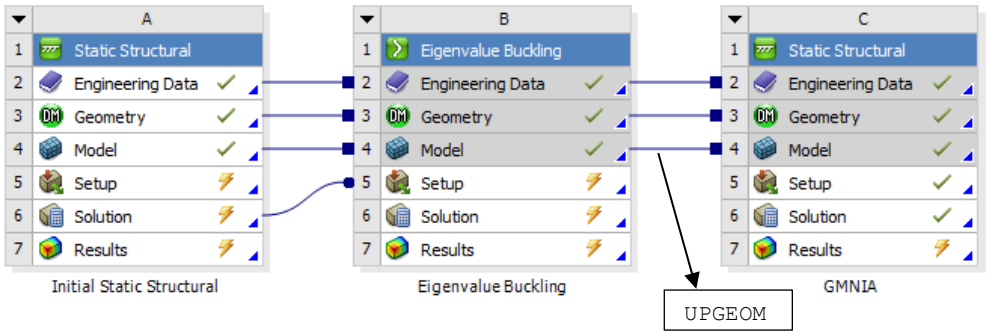

Figure 44 *Basic schematic for GMNIA analysis. The lowest eigenvalue shape is used as an initial imperfection (amplitude scaled to L/200).*

Figure 44 shows the basic schematic for GMNIA.

The relevant design loads which cause the largest compressive stresses were applied and a linear buckling analysis was carried out. The lowest eigenmode shape of each model (see Figures 47 and 48) were then used as imperfections for subsequent GMNI -analyses ("UPGEOM" APDL -command). Imperfection amplitude was scaled to 3 mm for both models according to the provisions of Table G.4 in [22]. The bilinear isotropic hardening material model presented earlier (see Figure 36) is used.

The boundary conditions of both modes were simplified in a conservative manner; the mullion in the custom profile model and the compression only boundary condition representing the mullion wall in the L-profile model were omitted. This choice results in longer buckling lengths for both models and overall conservative results, without the need to estimate mullion stiffness effects which can vary significantly. Bolts were also left out in both models and replaced by fixed connections (at rear) and direct load application (front); only the plate stress state is of interest here and Saint-Venant's principle applies. A loading of 200 % the design load was applied over 15 substeps in the GMNI -analyses. In many cases displacement control would be the preferred method for GMNI -analysis [34]; however, stability issues, singular stiffness matrices and convergence problems were not expected, and the analyses were done only to prove ductile failure mode. Figures 45 and 46 show the boundary conditions and loads applied in the GMNI -analyses.

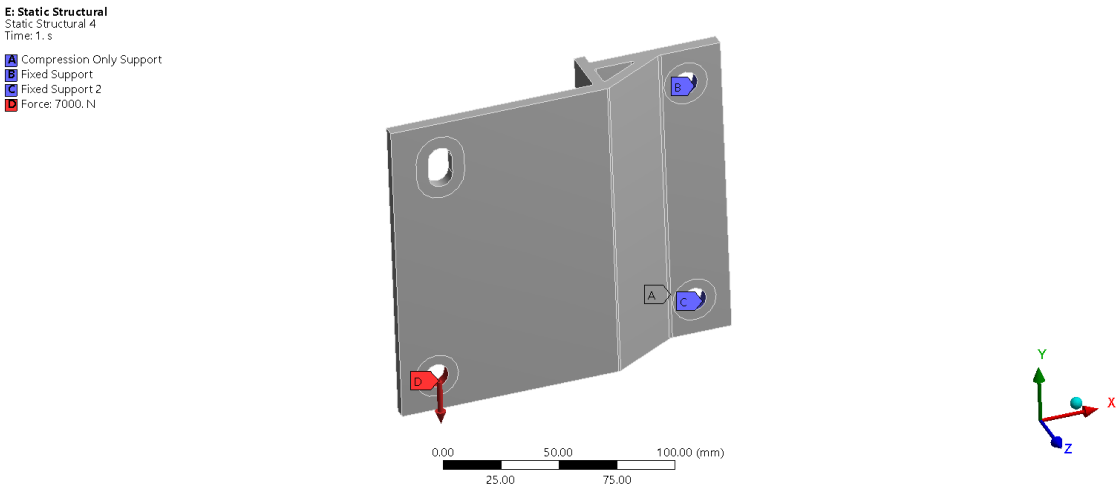

Figure 45 *Simplified boundary conditions for large custom profile. Only plate stability and stress state are of concern. Note that only self-weight is applied (shear buckling check); wind loads have an alternate compressional load path; through the throat of the profile.*

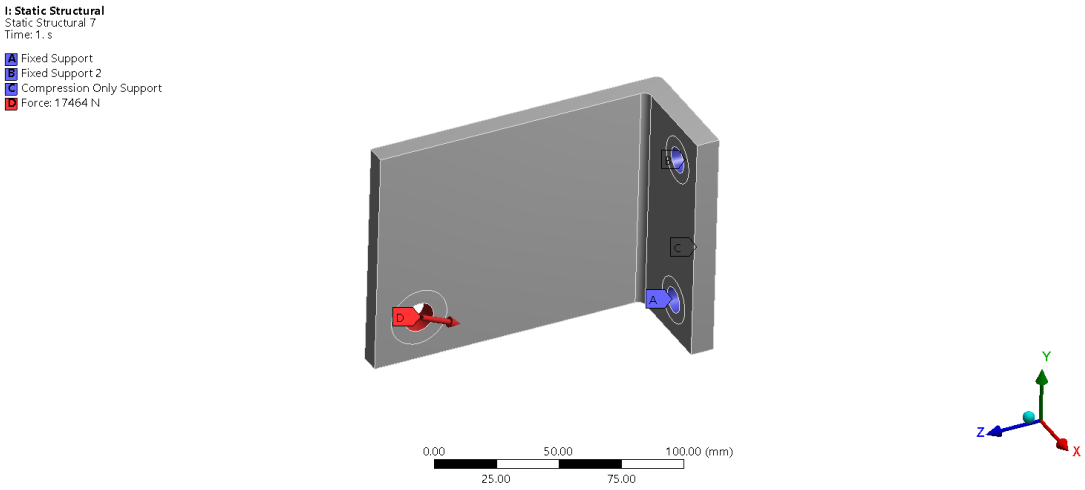

Figure 46 *Simplified boundary conditions of large L-profile. Only plate stability and stress state are of concern. Governing compressional load case: self-weight and wind load (compression).*

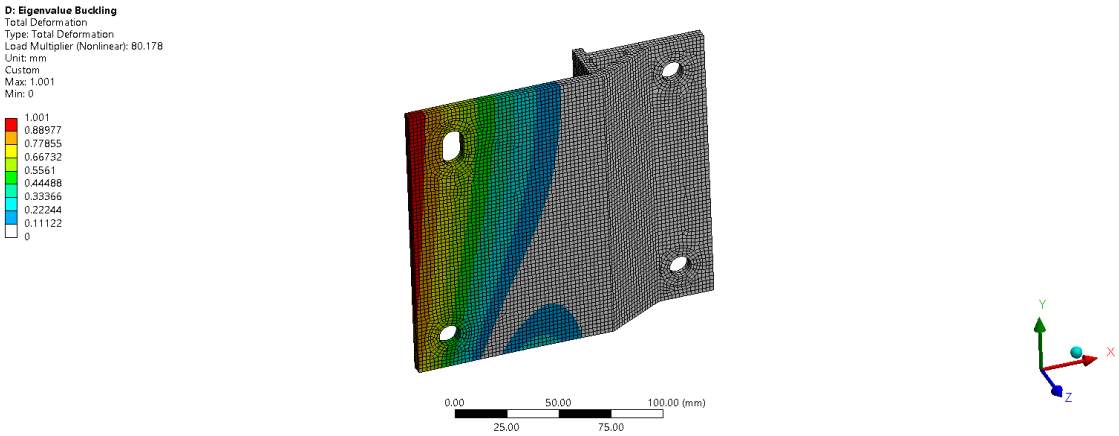

Figure 47 *Lowest eigenmode (local buckling mode) used as imperfection for large custom profile. Amplitude scaled to 3 mm. Load multiplier 80.*

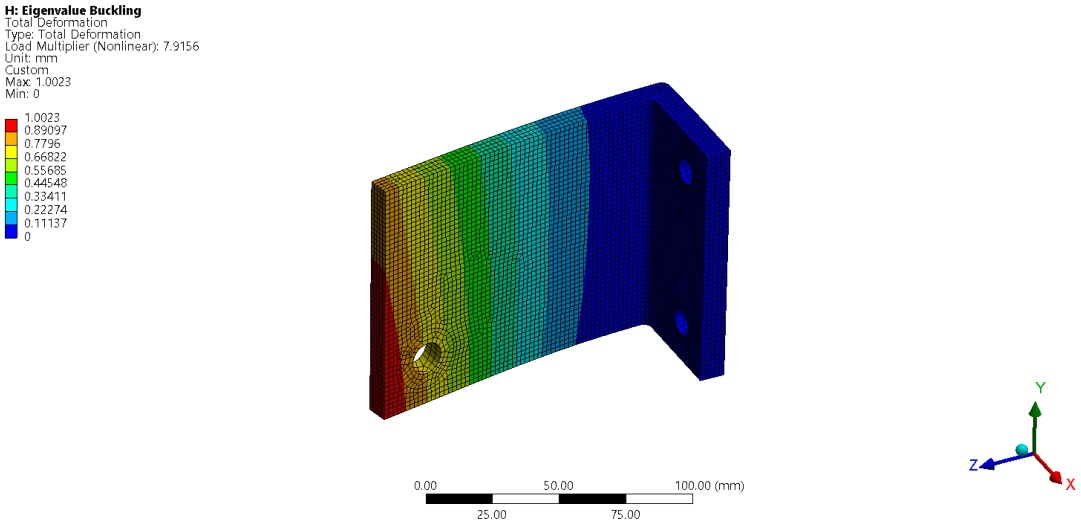

Figure 48 *Lowest eigenmode (sway mode) used as imperfection for large L-profile. Amplitude scaled to 3 mm. Load multiplier 7.9.*

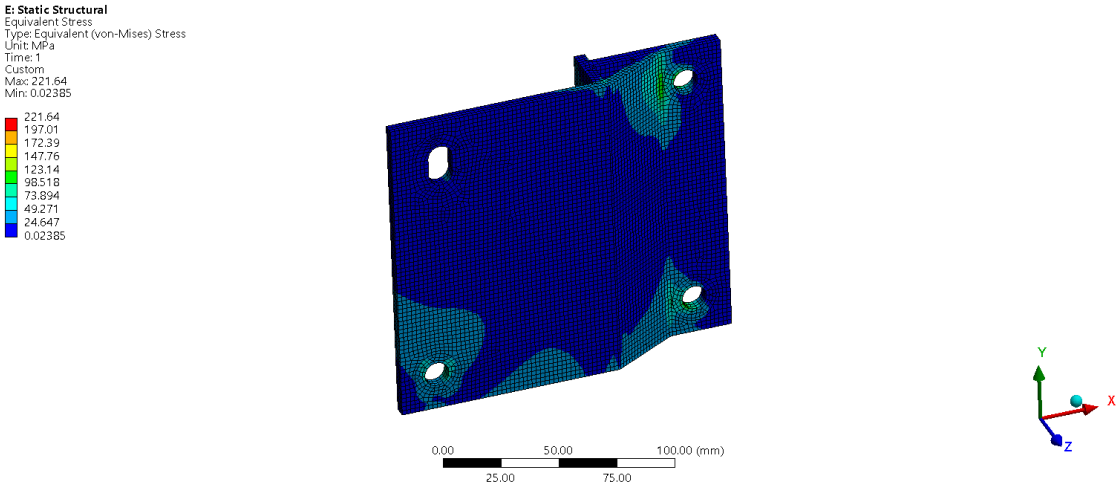

Figure 49 *Stresses in large custom profile material at 200 % load level. Note plastification soon to initiate around rear upper bolt hole.*

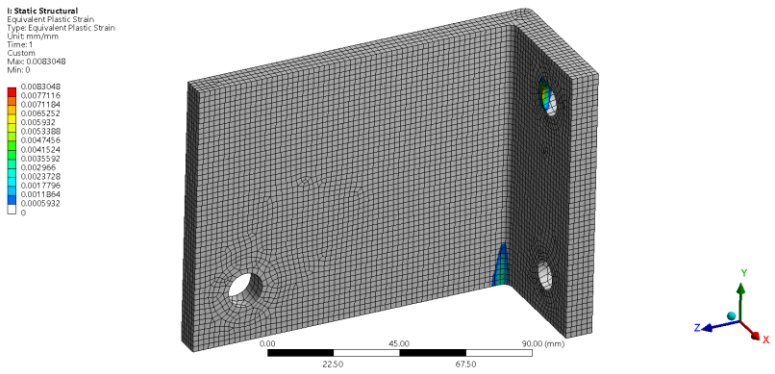

Figure 50 *Plastification present in material of large L-profile at 200 % design load.*

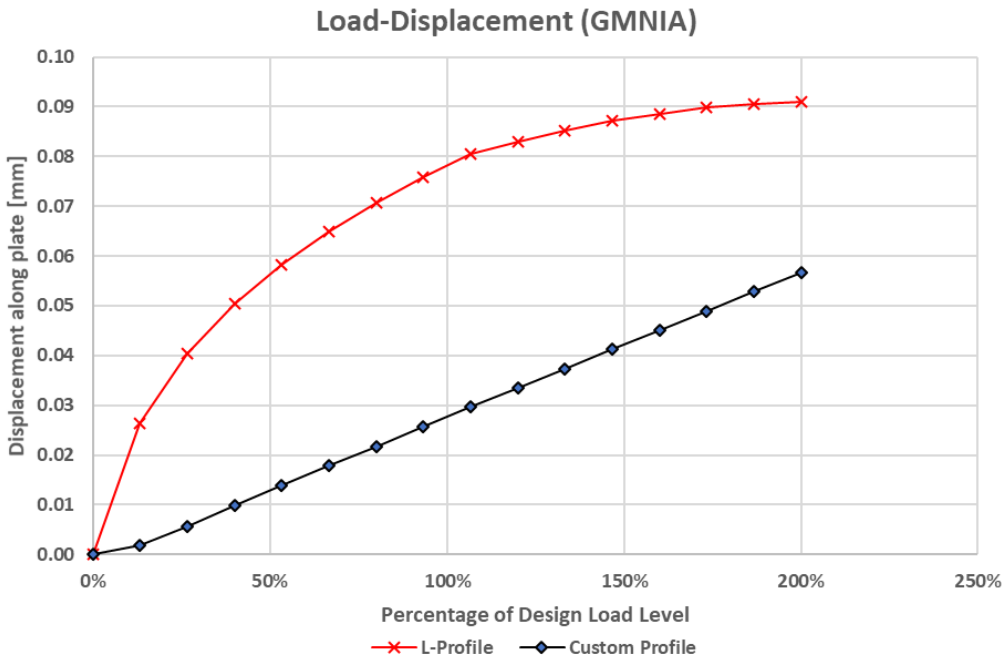

Figure 51 *Load-Displacement curves for front bolt holes. Note that the L-profile sway mode and plastification causes non-linearity; furthermore, note relatively small displacements.*

Figure 51 shows load-displacement results of the analyses. The displacements were from the loaded bolt hole faces along the direction of the plate. The resulting displacements are relatively small, and the overall behaviour of the connections was ductile (see Figures 49 and 50). The largest total (absolute value) displacement for the L-profile was 1.42 mm at the outermost edge of the plate and 0.2 mm for the large custom profile. The GMNIA results show that stability problems are not present in the designs.

10.3 Final Designs

Figures 53 to 56 portray the final designs of each connection type. Bolt placement is modified for the small custom wind-only connections. This is necessary; a long bolt slot is needed, and it would not be possible otherwise as two slotted bolts can't fit.

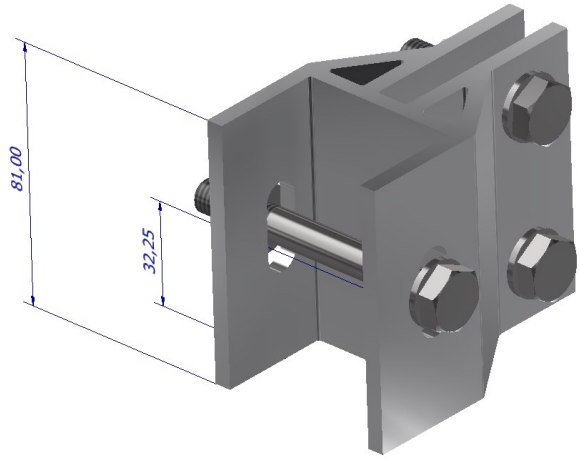

Figure 52 *Bolt placement for small custom profile (wind load only).*

This modification limits the amount of wind load capacity due to prying forces. With prying forces considered, (approximate max value of 2.5x wind load with single bolt at edge of slot) the resistance of the single bolt M10 bolt connection is limited to 6 kN for mullion profiles with 2 mm wall thicknesses and 9 kN for profiles with 3 mm wall thicknesses (see Appendix 1; specifically, M10 5mm Outstand Thickness (Shear Only)).

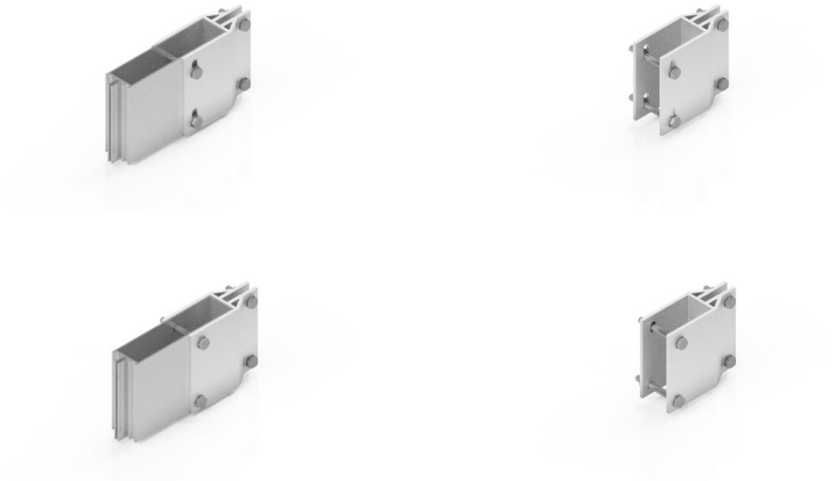

Figure 53 *Rendered images of final large custom profile designs. The top of the figure depicts the slotted (wind) profile with and without 200mm mullion and the bottom depicts the self-weight profile.*

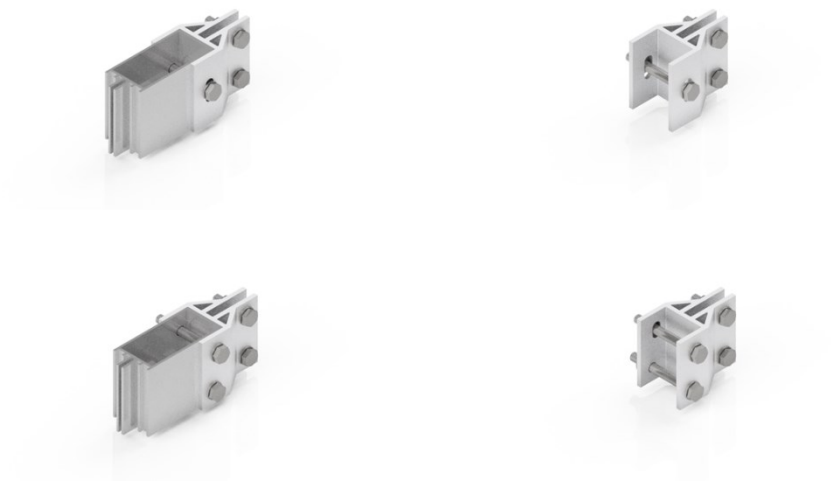

Figure 54 *Rendered images of final small custom profile designs. The top of the figure depicts the slotted (wind) profile with and without 100mm mullion and the bottom depicts the self-weight profile.*

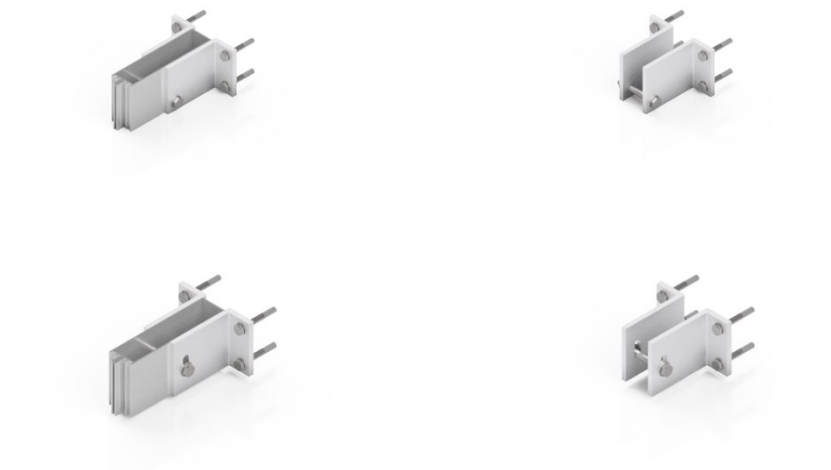

Figure 55 *Rendered images of final large L-profile designs. The bottom of the figure depicts the slotted (wind) profile with and without 200mm mullion and the top depicts the self-weight profile.*

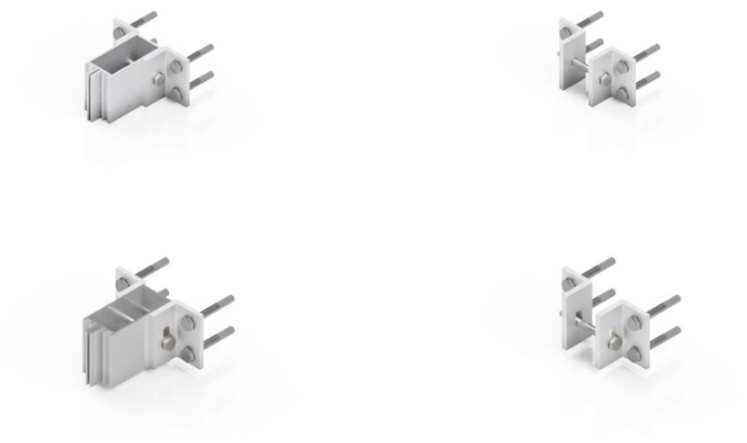

Figure 56 *Rendered images of final small L-profile designs. The bottom of the figure depicts the slotted (wind) profile with and without 100mm mullion and the top depicts the self-weight profile.*

The connections can resist the loads used to design them; in other words, if the force reactions encountered during curtain wall design are smaller than the design loads specified in Section 5.5 (except for modified small custom profile for wind load only), the connection UT-ratio is under 100 % and resistance is sufficient. The largest total deflection of the larger connections is approximately 1 mm under full load; however, the models are ideal and fit up tolerances are not considered. The smallest L-profile connection exhibited approximately 0.5 mm of total deflection under load. The CAD drawings and pictures for manufacturing the connections are available in Appendix 3. Note that prying forces are not considered in the L-profile designs as the mullion is assumed to be installed with a gap between it and the load bearing structure. In addition, mullion resistance must be considered separately (as mentioned earlier).

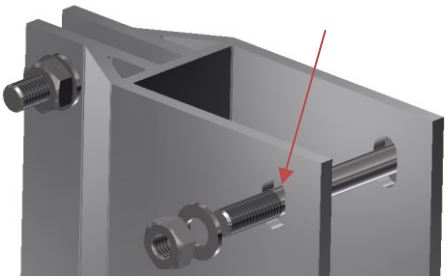

Figure 57 *Bolt length, threaded portion not in shear plane.*

M10 or M12 (see Appendix 3) grade 8.8 (DIN 931) bolts must be used in all cases with lengths long enough that threaded parts are not situated in shear planes (see Figure 57). This rule applies to all bolts. Washers (DIN 125-1) and nuts (DIN 934) are used. Care must be taken to ensure that bolts stay tight under dynamic loading; crushing of threads after tightening or other methods should be used.

11 CONCLUSIONS

A total of 8 different connection types were developed (4 original custom designs) and the application of modern optimization and analysis techniques to extruded aluminium alloy profile design was investigated. The designs fulfil Eurocode and product standard requirements; however, some limitations in adjustability and thermal expansion are present due to slotted bolt provisions of Eurocode 9 and the choice to not use pretensioned bolts in the designs. Further development of the connections is possible via testing and statistical analysis according to the requirements of Annex D of EC0, but this is beyond the scope of this work.

In all cases, the limiting factor was the strength of the profile material; fatigue was not limiting. Furthermore, the designs are based on materially and geometrically linear finite element analysis which typically overestimates stresses (upper bound with regards to stiffness), thus underestimating capacity in this case. Taking into account material yielding and strength hardening may have given higher load capacity; however, non-linear analysis in conjunction with optimization procedures would be cost prohibitive with regards to calculation time, and conservative designs were desired.

The use of modern analysis and design techniques provided great benefits to the design process. The methods provided a way to analyse a large range of different designs which would have otherwise not been considered; furthermore, it was possible to reuse models with little modification due to the use of parametric modelling techniques. This greatly reduced the amount of manual labour required. Instead of creating separate models from scratch for each connection size, a few parameters could be changed, and the next model was ready for use. The models can also be archived for future use, if other sizes or revisions are desired.

During the optimization process it was apparent that the choice of parameter design ranges greatly affects the end results. In addition, it was also noticed that most of the weight savings were made from limiting the extrusion length; the wall thicknesses had a relatively small, although noticeable effect. This effect can be seen in all the objective function histories presented in Appendix 2; the slope of the objective function history is steep at first, but then the angle suddenly becomes shallow. Further examination of the bolt UT-ratio and parameter histories show that this is indeed the case. This caused the optimization algorithms to quickly minimize the extrusion length to the minimum boundary set and thicken the profile walls. If the extrusion length ranges were not chosen carefully (particularly the lower boundary), the results would have relatively thick wall thicknesses that would cause significant manufacturing difficulties. To remedy this, wall thicknesses could have also been limited, but in this case limiting a single parameter (extrusion

length) was enough. Wall thickness parameters and extrusion length parameter boundaries could not be chosen independently of each other.

The SORVI algorithm proved to be the most efficient; approximately 3-4 times more evaluations were needed to obtain a comparable result for the light custom profile using the genetic algorithm compared to SORVI. Due to this, the genetic algorithm was abandoned for all other design cases as the resulting calculation times would have been impractical for larger models (days vs. hours).

Mass savings were achieved; however, the relative amount of savings made was clearly dependent on initial guess. This is demonstrated in Appendix 2 (3. Large Custom Profile, SORVI Algor. (Adaptive, 7mm)), where 7 mm wall thicknesses were chosen with this purpose in mind. This resulted in a total mass saving of approximately 30 %, while 6 mm wall thicknesses only provided 20% (see Section 2). There are clearly benefits to be had in both cases; however, it appears that a substantial portion is lost if the design and static behaviour (internal force distribution) is relatively simple to understand and decent educated guesses can be made.

The total amount of financial impact realized by the optimization of the connection profiles will undoubtably be relatively insignificant, as the amount of connections sold annually is expected to remain relatively small. Approximately 10 connection profiles can be made from a single extruded meter for any size of connection chosen. Assuming a price of approximately 2 € / kg aluminium, the amount of savings per extruded meter is around 1-2 €; however, the knowledge obtained in this work is also applicable to other profiles where noteworthy financial savings can be made, such as in the case of profiles extruded for the highly competitive customer profile market (thousands of meters annually). The amount of savings to be had by applying the methods used in this thesis are therefore promising. Figure 58 shows an example of one of these profiles where future application is expected (rear underrun protective device profile).

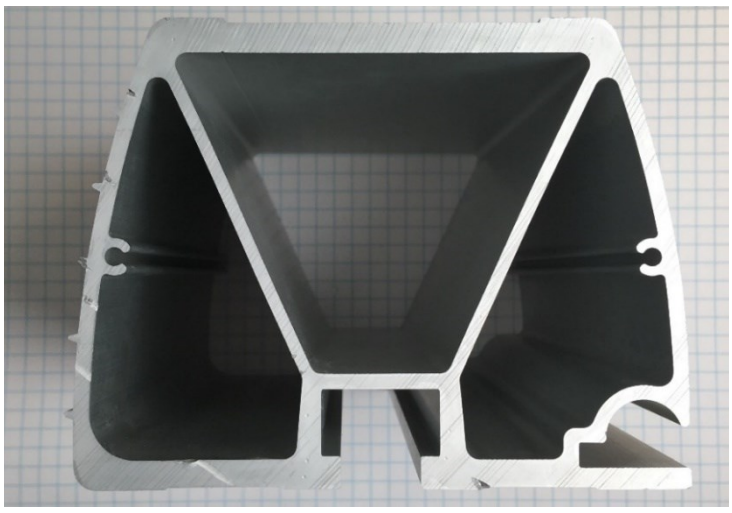

Figure 58 *Rear underrun protective device profile.*

Although there are obviously benefits, there are also limitations to the adoption and application of the methods used in this work. The process requires a substantial amount of CAD, FEA, mechanics and normative knowledge along with a large amount of decision making. This complication may be alleviated by future software development and tool integration. Furthermore, software licensing and hardware expenses can be considerable. The hunt for a better design requires expected benefits to be weighed against the cost and effort of the pursuit.

REFERENCES

[1] SFS-EN 13830:2003, Curtain Walling. Product Standard, Finnish Standards Association, Helsinki, 2003.

[2] SFS-EN 13830:2015, Curtain Walling. Product Standard, Finnish Standards Association, Helsinki, 2015.

[3] P50L/P50LE Facade System Brochure, Purso Oy, 2018.

[4] A.M. Memari, Architectural Engineering Institute. Committee on Curtain Wall Systems, Curtain Wall Systems: A Primer, American Society of Civil Engineers, 2013.

[5] HALFEN HCW Curtain Wall Technical Product Information, HCW-14.1 US, 2014.

[6] PEC Fixing Solutions Technical Product Information and Product Range, 2016.

[7] Levolux TRINITI Bracket Brochure , 2010.

[8] SFS-EN 1991-1-1 + AC, Eurocode 1: Actions on structures. Part 1-1: General actions. Densities, self-weight, imposed loads for buildings, Finnish Standards Association, Helsinki, 2002.

[9] (RAL) Guideline for installation of windows and external pedestrian doors, IFT Institut für Fenstertechnik e.V., Rosenheim, 2016, 251 p.

[10] SFS-EN 1991-1-4 + A1 + AC, Eurocode 1: Actions on structures. Part 1-4: General actions. Wind actions, Finnish Standards Association, Helsinki, 2011.

[11] Kansallinen liite standardiin SFS-EN 1991-1-4: Rakenteiden kuormat.
Osa 1-4: Yleiset kuormat. Tuulikuormat, Ympäristöministeriö, Helsinki, 2016.

[12] RIL 205-1-2017, Suomen Rakennusinsinöörien Liitto RIL ry, Helsinki, 2017.

[13] W.C. Young, R.G. Budynas, A.M. Sadegh, R.J. Roark, Roark's formulas for stress and strain, 8. ed. McGraw-Hill, New York, 2012, 1054 p.

[14] J. Wheaton, Successful Designs for Curtain Wall Attachment, Modern Steel Construction, Vol. 3, 2001.

[15] J. Chakrabarty, Theory of plasticity, 3. ed. Elsevier Butterworth-Heineman, Amsterdam, 2006.

[16] SFS-EN 1999-1-1:en, Eurocode 9. Design of aluminium structures, Finnish Standards Association, Helsinki, 2007.

[17] SFS-EN 1999-1-3, Eurocode 9: Design of aluminium structures – Part 1-3: Structures susceptible to fatigue, Finnish Standards Association, Helsinki, 2007.

[18] F.M. Mazzolani, Aluminium alloy structures, 2. ed. CRC Press, London, 1995.

[19] N. Cook, Designers' Guide to EN 1991-1-4 Eurocode 1: Actions on structures, general actions part 1-4. Wind actions, Thomas Telford Publishing, London, 2007.

[20] M. Donà, M. Overend, Fatigue Performance of a Connection for GRC Cladding Panels, Proceedings of the 8th International Conference on Advanced Composites in Construction (ACIC 2017), 5-7.9.2017, Sheffield, pp. 253-259.

[21] Kansallinen liite standardiin SFS-EN 1999-1-3 Osa 1-3: Väsymiselle alttiit rakenteet, Ympäristöministeriö, Helsinki, 2018.

[22] SFS-EN 1090-3, Execution of steel structures and aluminium structures. Part 3: Technical requirements for aluminium structures, Finnish Standards Association, Helsinki, 2008.

[23] SFS-EN 1090-2 + A1, Suomen standardoimisliitto, Helsinki, 2012.

[24] Purso Profile Design Handbook, 2014.

[25] SFS-EN 13670, Execution of concrete structures, Finnish Standards Association, Helsinki, 2010.

[26] SFS 5978, Execution of timber structures. Rules for load-bearing structures of buildings, Finnish Standards Association, Helsinki, 2014.

[27] SFS-EN 1990 + A1 + AC, Eurocode. Basis of structural design, Finnish Standards Association, Helsinki, 2006.

[28] SORVI Design Booster User Manual, 1.1 ed., 2018.

[29] D.E. Goldberg, Genetic algorithms in search, optimization, and machine learning, Reprinted with corr., 12. print. Addison-Wesley, Reading, Mass., 1994.

[30] MATLAB documentation, R2017a., 2017.

[31] S. Pajunen, P. Laakkonen, Surrogate-model based method and software for practical design optimization problems, Rakenteiden Mekaniikka (Journal of Structural Mechanics), Vol. 49, 2016, pp. 100-118.

[32] J. Fillion, Finite Element Modelling of Aluminium End Plate Connections Under Biaxial Bending -- Plastic Mechanisms and Weld Failure, Bachelor’s Thesis, Tampere University of Technology, 2017.

[33] ANSYS, Release 19.1, Mechanical APDL Theory Reference, Ansys,Inc., SAS IP Inc., 2018.

[34] R.d. Borst, Non-linear Finite Element Analysis of Solids and Structures, 2nd. ed. Wiley, Chichester, 2012.

APPENDIX 1: BOLT RESISTANCE CALCULATIONS

1. M10, 5mm Outstand Thickness (Shear Only)

Edge Distances and Spacing

Bolt (rear/front lower):

$d_{0.Rear} := 11 \text{ mm}$

$e_{1.Rear} := 2 \cdot d_{0.Rear} = 22.00 \text{ mm}$

$e_{2.Rear} := 1.5 \cdot d_{0.Rear} = 16.50 \text{ mm}$

Slotted Bolt (front):

$d_{0.Slot} := 11 \text{ mm}$

$d := 10 \text{ mm}$

$e_{3.Slot} := 1.5 \cdot (d + 1 \text{ mm}) = 16.50 \text{ mm}$

$e_{4.Slot} := d + 1 \text{ mm} = 11.00 \text{ mm}$

$e_{1.Slot} := e_{3.Slot} + \frac{d}{2} = 21.50 \text{ mm}$

$e_{2.Slot} := e_{4.Slot} + \frac{d}{2} = 16.00 \text{ mm}$

$l_{maxShortSlot} := 1.5 \cdot (d + 1 \text{ mm}) = 16.50 \text{ mm}$

$l_{maxLongSlot} := 2.5 \cdot (d + 1 \text{ mm}) = 27.50 \text{ mm}$

Partial Safety Factors:

$\gamma_{M2} := 1.25$

Shear Bolt shank (gross section, unthreaded portion):

$A_s := \pi \cdot \left(\frac{d}{2}\right)^2 = 78.54 \text{ mm}^2$

$\alpha_v := 0.6$

$f_{ub} := 800 \text{ MPa}$

$F_{vRd} := \frac{\alpha_v \cdot f_{ub} \cdot A_s}{\gamma_{M2}} = 30.16 \text{ kN}$

Bearing Capacity (Connection Profile):

Bolt (rear/front lower):

$f_u := 290 \text{ MPa}$

$t := 5 \text{ mm}$

$\alpha_d := \frac{e_{1.Rear}}{3 \cdot d_{0.Rear}} = 0.67$

$\alpha_b := min\left(\frac{f_{ub}}{f_u}, \alpha_d, 1\right) = 0.65$

$k_1 := min\left(2.8 \cdot \frac{e_{2.Rear}}{d_{0.Rear}} - 1, 2.5\right) = 2.50$

$F_{bRd.RProfile} := \frac{k_1 \cdot 1 \cdot f_u \cdot d_{0.Rear} \cdot t}{\gamma_{M2}} = 31.90 \text{ kN}$

Slotted Bolt (front):

$f_u := 290 \text{ MPa}$ **EN-AW 6082-T6**

$t := 5 \text{ mm}$

$\alpha_d := \frac{e_{1.Slot}}{3 \cdot d_{0.Slot}} = 0.65$

$\alpha_b := min\left(\frac{f_{ub}}{f_u}, \alpha_d, 0.66\right) = 0.65$

$k_1 := min\left(2.8 \cdot \frac{e_{2.Slot}}{d_{0.Slot}} - 1, 2.5\right) = 2.50$

$F_{bRd.SShortProfile} := \frac{k_1 \cdot 0.8 \cdot \alpha_b \cdot f_u \cdot d_{0.Slot} \cdot t}{\gamma_{M2}} = 16.63 \text{ kN}$

$F_{bRd.SLongProfile} := \frac{k_1 \cdot \alpha_b \cdot 0.65 \cdot f_u \cdot d_{0.Slot} \cdot t}{\gamma_{M2}} = 13.51 \text{ kN}$

Bearing Capacity (Mullion Profile):

Both Bolts (front, mullion holes not slotted, edge distances assumed):

$f_u := 175\ \text{MPa}$ **EN-AW 6063-T5**

$t := 2\ \text{mm}$

$\alpha_d := \frac{e_{1.Rear}}{3 \cdot d_{0.Rear}} = 0.67$

$\alpha_b := min\left(\frac{f_{ub}}{f_u}, \alpha_d, 1\right) = 0.67$

$k_1 := min\left(2.8 \cdot \frac{e_{2.Rear}}{d_{0.Rear}} - 1, 2.5\right) = 2.50$

$F_{bRd.RMullion2mm} := \frac{k_1 \cdot 1 \cdot f_u \cdot d_{0.Rear} \cdot t}{\gamma_{M2}} = 7.70\ \text{kN}$

$t := 3\ \text{mm}$

$F_{bRd.RMullion3mm} := \frac{k_1 \cdot 1 \cdot f_u \cdot d_{0.Rear} \cdot t}{\gamma_{M2}} = 11.55\ \text{kN}$

Total Shear Resistances:

$F_{vDtot} := 2 \cdot min\left(F_{bRd.RProfile}, F_{vRd}\right) = 60.32\ \text{kN}$	Bolt to connection profile.
$F_{vDtot.SlotShort} := 2 \cdot min\left(F_{bRd.SShortProfile}, F_{vRd}\right) = 33.25\ \text{kN}$	Slotted bolt (short) to connection profile.
$F_{vDtot.SlotLong} := 2 \cdot min\left(F_{bRd.SLongProfile}, F_{vRd}\right) = 27.02\ \text{kN}$	Slotted bolt (long) to connection profile.
$F_{vDtot} := 2 \cdot min\left(F_{bRd.RMullion2mm}, F_{vRd}\right) = 15.40\ \text{kN}$	Bolt to 2 mm wall of mullion
$F_{vDtot} := 2 \cdot min\left(F_{bRd.RMullion3mm}, F_{vRd}\right) = 23.10\ \text{kN}$	Bolt to 3 mm wall of mullion

$R_{kWindMax} := 9\ \text{kN}$

$\tau_{AvgMaxWind} := \frac{R_{kWindMax}}{2 \cdot A_s} = 57.3\ \text{MPa}$ Maximum average shear (from fatigue load only).

2. M12, 5 mm Outstand Thickness (Shear Only)

Edge Distances and Spacing

Bolt (rear/front lower):

$d_{0.Rear} := 13\ \text{mm}$

$e_{1.Rear} := 2 \cdot d_{0.Rear} = 26.00\ \text{mm}$

$e_{2.Rear} := 1.5 \cdot d_{0.Rear} = 19.50\ \text{mm}$

Slotted Bolt (front):

$d_{0.Slot} := 13\ \text{mm}$

$d := 12\ \text{mm}$

$e_{3.Slot} := 1.5 \cdot (d + 1\ \text{mm}) = 19.50\ \text{mm}$

$e_{4.Slot} := d + 1\ \text{mm} = 13.00\ \text{mm}$

$e_{1.Slot} := e_{3.Slot} + \frac{d}{2} = 25.50\ \text{mm}$

$e_{2.Slot} := e_{4.Slot} + \frac{d}{2} = 19.00\ \text{mm}$

Partial Safety Factors:

$\gamma_{M2} := 1.25$

$l_{maxShortSlot} := 1.5 \cdot (d + 1\ \text{mm}) = 19.50\ \text{mm}$

$l_{maxLongSlot} := 2.5 \cdot (d + 1\ \text{mm}) = 32.50\ \text{mm}$

Shear Bolt shank (gross section, unthreaded portion):

$A_s := \pi \cdot \left(\frac{d}{2}\right)^2 = 113.10\ \text{mm}^2$

$\alpha_v := 0.6$

$f_{ub} := 800\ \text{MPa}$

$F_{vRd} := \frac{\alpha_v \cdot f_{ub} \cdot A_s}{\gamma_{M2}} = 43.43\ \text{kN}$

Bearing Capacity (Connection Profile):

Bolt (rear/front lower):

$f_u := 290\ \text{MPa}$

$t := 5\ \text{mm}$

$\alpha_d := \frac{e_{1.Rear}}{3 \cdot d_{0.Rear}} = 0.67$

$\alpha_b := min\left(\frac{f_{ub}}{f_u}, \alpha_d, 1\right) = 0.65$

$k_1 := min\left(2.8 \cdot \frac{e_{2.Rear}}{d_{0.Rear}} - 1, 2.5\right) = 2.50$

$F_{bRd.RProfile} := \frac{k_1 \cdot 1 \cdot f_u \cdot d_{0.Rear} \cdot t}{\gamma_{M2}} = 37.70\ \text{kN}$

Slotted Bolt (front):

$f_u := 290\ \text{MPa}$ **EN-AW 6082-T6**

$t := 5\ \text{mm}$

$\alpha_d := \frac{e_{1.Slot}}{3 \cdot d_{0.Slot}} = 0.65$

$\alpha_b := min\left(\frac{f_{ub}}{f_u}, \alpha_d, 0.66\right) = 0.65$

$k_1 := min\left(2.8 \cdot \frac{e_{2.Slot}}{d_{0.Slot}} - 1, 2.5\right) = 2.50$

$F_{bRd.SShortProfile} := \frac{k_1 \cdot 0.8 \cdot \alpha_b \cdot f_u \cdot d_{0.Slot} \cdot t}{\gamma_{M2}} = 19.72\ \text{kN}$

$F_{bRd.SLongProfile} := \frac{k_1 \cdot \alpha_b \cdot 0.65 \cdot f_u \cdot d_{0.Slot} \cdot t}{\gamma_{M2}} = 16.02\ \text{kN}$

Bearing Capacity (Mullion Profile):

Both Bolts (front, mullion holes not slotted, edge distances assumed):

$f_u := 175\ \text{MPa}$ **EN-AW 6063-T5**

$t := 2\ \text{mm}$

$\alpha_d := \frac{e_{1.Rear}}{3 \cdot d_{0.Rear}} = 0.67$

$\alpha_b := min\left(\frac{f_{ub}}{f_u}, \alpha_d, 1\right) = 0.67$

$k_1 := min\left(2.8 \cdot \frac{e_{2.Rear}}{d_{0.Rear}} - 1, 2.5\right) = 2.50$

$F_{bRd.RMullion2mm} := \frac{k_1 \cdot 1 \cdot f_u \cdot d_{0.Rear} \cdot t}{\gamma_{M2}} = 9.10\ \text{kN}$

$t := 3\ \text{mm}$

$F_{bRd.RMullion3mm} := \frac{k_1 \cdot 1 \cdot f_u \cdot d_{0.Rear} \cdot t}{\gamma_{M2}} = 13.65\ \text{kN}$

Total Shear Resistances:

$F_{vDtot} := 2 \cdot min\left(F_{bRd.RProfile}, F_{vRd}\right) = 75.40\ \text{kN}$ Bolt to connection profile.

$F_{vDtot.SlotShort} := 2 \cdot min\left(F_{bRd.SShortProfile}, F_{vRd}\right) = 39.44\ \text{kN}$ Slotted bolt (short) to connection profile.

$F_{vDtot.SlotLong} := 2 \cdot min\left(F_{bRd.SLongProfile}, F_{vRd}\right) = 32.05\ \text{kN}$ Slotted bolt (long) to connection profile.

$F_{vDtot} := 2 \cdot min\left(F_{bRd.RMullion2mm}, F_{vRd}\right) = 18.20\ \text{kN}$ Bolt to 2 mm wall of mullion

$F_{vDtot} := 2 \cdot min\left(F_{bRd.RMullion3mm}, F_{vRd}\right) = 27.30\ \text{kN}$ Bolt to 3 mm wall of mullion

$R_{kWindMax} := 9\ \text{kN}$

$\tau_{AvgMaxWind} := \frac{R_{kWindMax}}{2 \cdot A_s} = 39.79\ \text{MPa}$ Maximum average shear (from fatigue load only).

3. M10, 6 mm Thickness (Shear + Tension)

Edge Distances and Spacing

Bolt (rear/front lower):

$d_{0.Rear} := 11\ \text{mm}$

$e_{1.Rear} := 2 \cdot d_{0.Rear} = 22.00\ \text{mm}$

$e_{2.Rear} := 1.5 \cdot d_{0.Rear} = 16.50\ \text{mm}$

Slotted Bolt (front):

$d_{0.Slot} := 11\ \text{mm}$

$d := 10\ \text{mm}$

$e_{3.Slot} := 1.5 \cdot (d + 1\ \text{mm}) = 16.50\ \text{mm}$

$e_{4.Slot} := d + 1\ \text{mm} = 11.00\ \text{mm}$

$e_{1.Slot} := e_{3.Slot} + \frac{d}{2} = 21.50\ \text{mm}$

$e_{2.Slot} := e_{4.Slot} + \frac{d}{2} = 16.00\ \text{mm}$

Partial Safety Factors:

$\gamma_{M2} := 1.25$

$l_{maxShortSlot} := 1.5 \cdot (d + 1\ \text{mm}) = 16.50\ \text{mm}$

$l_{maxLongSlot} := 2.5 \cdot (d + 1\ \text{mm}) = 27.50\ \text{mm}$

Shear Bolt shank (gross section, unthreaded portion):

$A_s := \pi \cdot \left(\frac{d}{2}\right)^2 = 78.54\ \text{mm}^2$

$\alpha_v := 0.6$

$f_{ub} := 800\ \text{MPa}$

$F_{vRd} := \frac{\alpha_v \cdot f_{ub} \cdot A_s}{\gamma_{M2}} = 30.16\ \text{kN}$

Bearing Capacity (Connection Profile):

Bolt (rear/front lower):

$f_u := 290\ \text{MPa}$

$t := 6\ \text{mm}$

$\alpha_d := \frac{e_{1.Rear}}{3 \cdot d_{0.Rear}} = 0.67$

$\alpha_b := min\left(\frac{f_{ub}}{f_u}, \alpha_d, 1\right) = 0.65$

$k_1 := min\left(2.8 \cdot \frac{e_{2.Rear}}{d_{0.Rear}} - 1, 2.5\right) = 2.50$

$F_{bRd.RProfile} := \frac{k_1 \cdot \alpha_b \cdot f_u \cdot d_{0.Rear} \cdot t}{\gamma_{M2}} = 24.94\ \text{kN}$

Slotted Bolt (front):

$f_u := 290\ \text{MPa}$ **6068-T6**

$t := 6\ \text{mm}$

$\alpha_d := \frac{e_{1.Slot}}{3 \cdot d_{0.Slot}} = 0.65$

$\alpha_b := min\left(\frac{f_{ub}}{f_u}, \alpha_d, 0.66\right) = 0.65$

$k_1 := min\left(2.8 \cdot \frac{e_{2.Slot}}{d_{0.Slot}} - 1, 2.5\right) = 2.50$

$F_{bRd.SShortProfile} := \frac{k_1 \cdot \alpha_b \cdot 0.8 \cdot f_u \cdot d_{0.Slot} \cdot t}{\gamma_{M2}} = 19.95\ \text{kN}$

$F_{bRd.SLongProfile} := \frac{k_1 \cdot \alpha_b \cdot 0.65 \cdot f_u \cdot d_{0.Slot} \cdot t}{\gamma_{M2}} = 16.21\ \text{kN}$

Bearing Capacity (Mullion Profile):

Both Bolts (front, mullion holes not slotted, edge distances assumed):

$f_u := 175\ \text{MPa}$ **6063-T5**

$t := 2\ \text{mm}$

$\alpha_d := \frac{e_{1.Rear}}{3 \cdot d_{0.Rear}} = 0.67$

$\alpha_b := min\left(\frac{f_{ub}}{f_u}, \alpha_d, 1\right) = 0.67$

$k_1 := min\left(2.8 \cdot \frac{e_{2.Rear}}{d_{0.Rear}} - 1, 2.5\right) = 2.50$

$F_{bRd.RMullion2mm} := \frac{k_1 \cdot 1 \cdot f_u \cdot d_{0.Rear} \cdot t}{\gamma_{M2}} = 7.70\ \text{kN}$

$t := 3\ \text{mm}$

$F_{bRd.RMullion3mm} := \frac{k_1 \cdot 1 \cdot f_u \cdot d_{0.Rear} \cdot t}{\gamma_{M2}} = 11.55\ \text{kN}$

Total Shear Resistances:

$F_{vDtot} := 2 \cdot min\left(F_{bRd.RProfile}, F_{vRd}\right) = 49.88\ \text{kN}$ Bolt to connection profile.

$F_{vDtot.SlotShort} := 2 \cdot min\left(F_{bRd.SShortProfile}, F_{vRd}\right) = 39.90\ \text{kN}$ Slotted bolt (short) to connection profile.

$F_{vDtot.SlotShort} := 2 \cdot min\left(F_{bRd.SLongProfile}, F_{vRd}\right) = 32.42\ \text{kN}$ Slotted bolt (long) to connection profile.

$F_{vDtot} := 2 \cdot min\left(F_{bRd.RMullion2mm}, F_{vRd}\right) = 15.40\ \text{kN}$ Bolt to 2 mm wall of mullion

$F_{vDtot} := 2 \cdot min\left(F_{bRd.RMullion3mm}, F_{vRd}\right) = 23.10\ \text{kN}$ Bolt to 3 mm wall of mullion

$R_{kWindMax} := 9\ \text{kN}$

$\tau_{AvgMaxWind} := \frac{R_{kWindMax}}{2 \cdot A_s} = 57.3\ \text{MPa}$ Maximum average shear (from fatigue load only).

Tension

$k_2 := 0.9$

$A_s := 58\ \text{mm}^2$ Tensile Stress Area M10

$F_{tRd} := \frac{k_2 \cdot f_{ub} \cdot A_s}{\gamma_{M2}} = 33.41\ \text{kN}$

Combined shear and tension

$F_{vEdEstimate} := 5\ \text{kN}$

$F_{tEdEstimate} := 15\ \text{kN}$

$\frac{F_{vEdEstimate}}{F_{vRd}} + \frac{F_{tEdEstimate}}{1.4 \cdot F_{tRd}} = 0.49$

Note. Single shear plane, FvRd taken as bolt shank shear resistance.

Punching

$d_m := 16\ \text{mm}$

$f_u := 290\ \text{MPa}$

$t_p := 6\ \text{mm}$

$B_{pRd} := \frac{0.6 \cdot \pi \cdot d_m \cdot t_p \cdot f_u}{\gamma_{M2}} = 41.98\ \text{kN}$

APPENDIX 2: OPTIMIZATION RUN RESULTS

1. Large Custom Profile, SORVI Algorithm

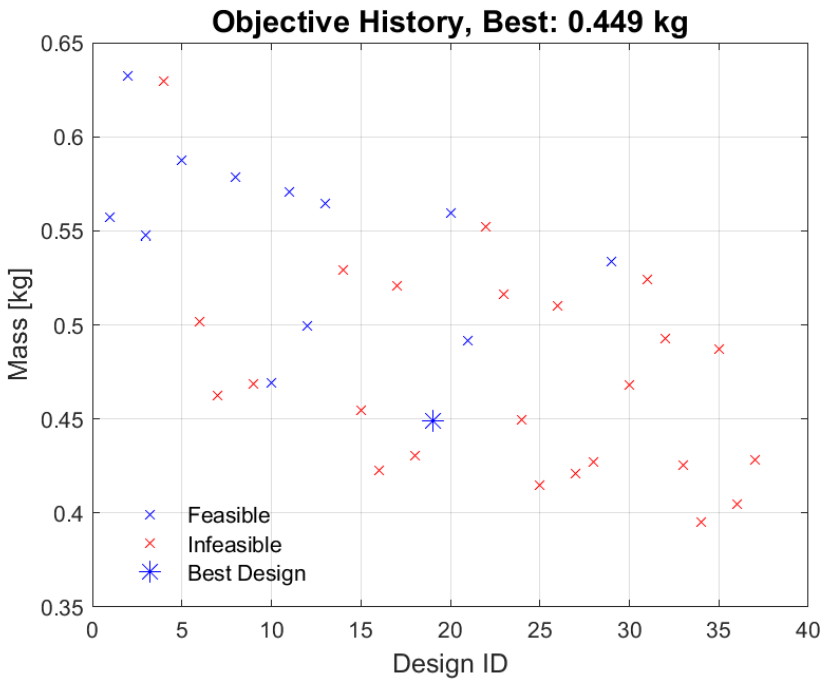

Figure 1 *Objective function design point history.*

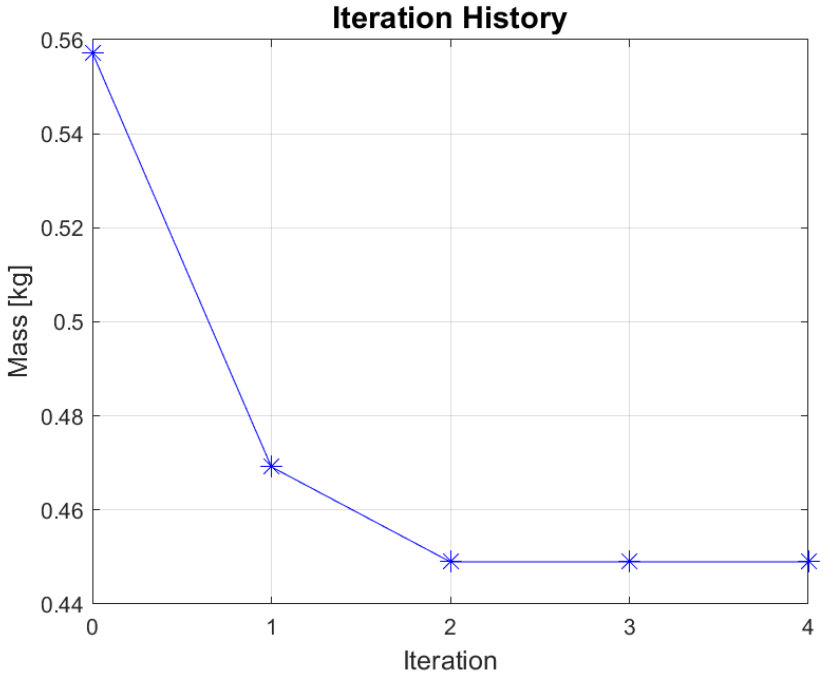

Figure 2 *Objective function iteration history.*

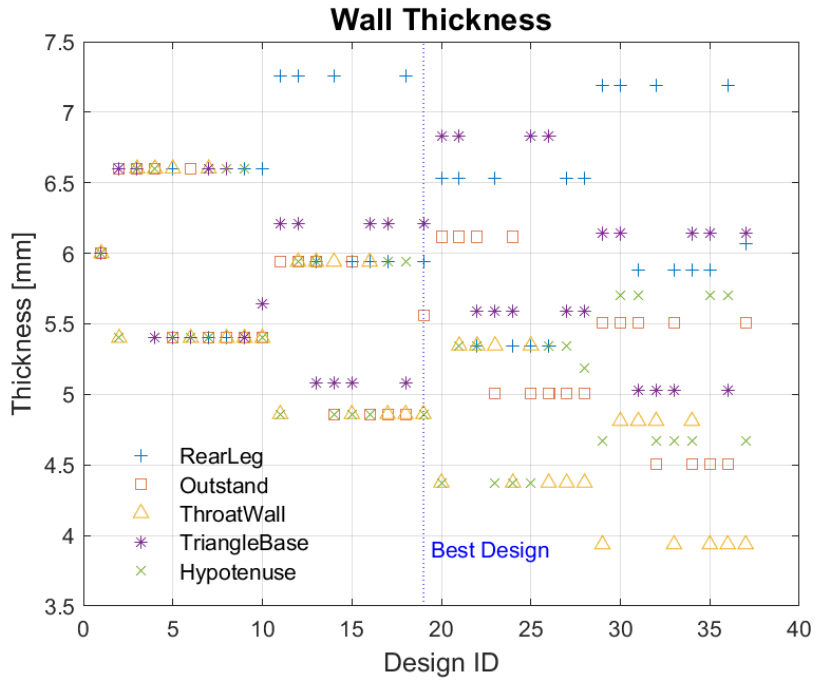

Figure 3 *Wall thickness parameter values of each design point.*

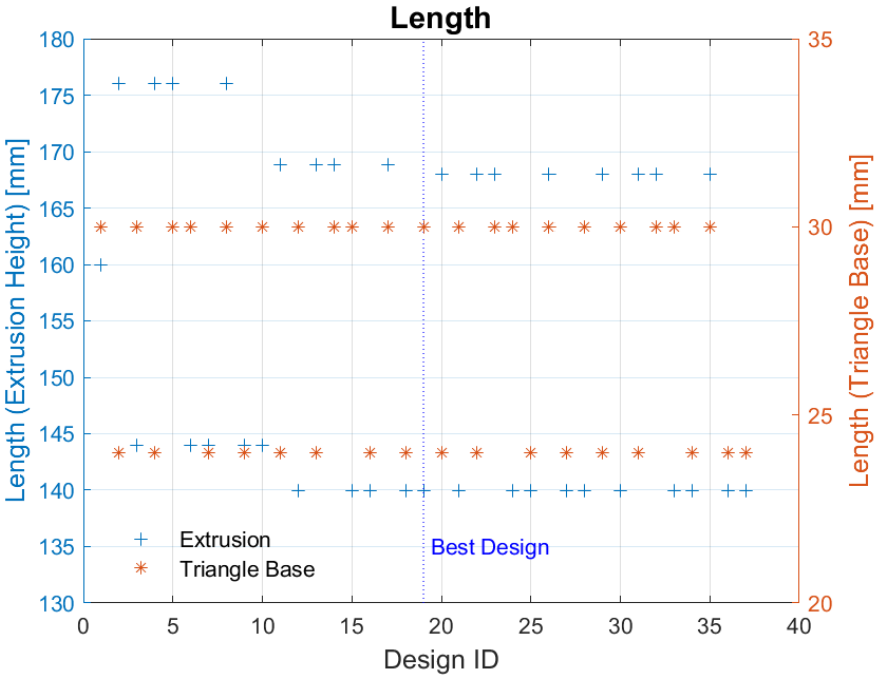

Figure 4 *Length parameter values of each design point.*

Figure 5 *Max von Mises stress result of each design point.*

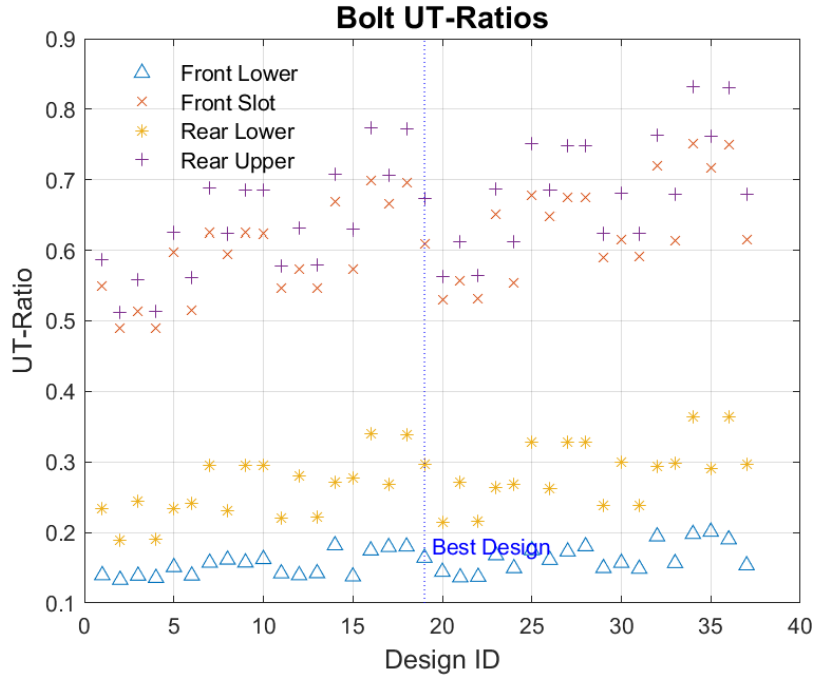

Figure 6 *Bolt UT-Ratios of each design point.*

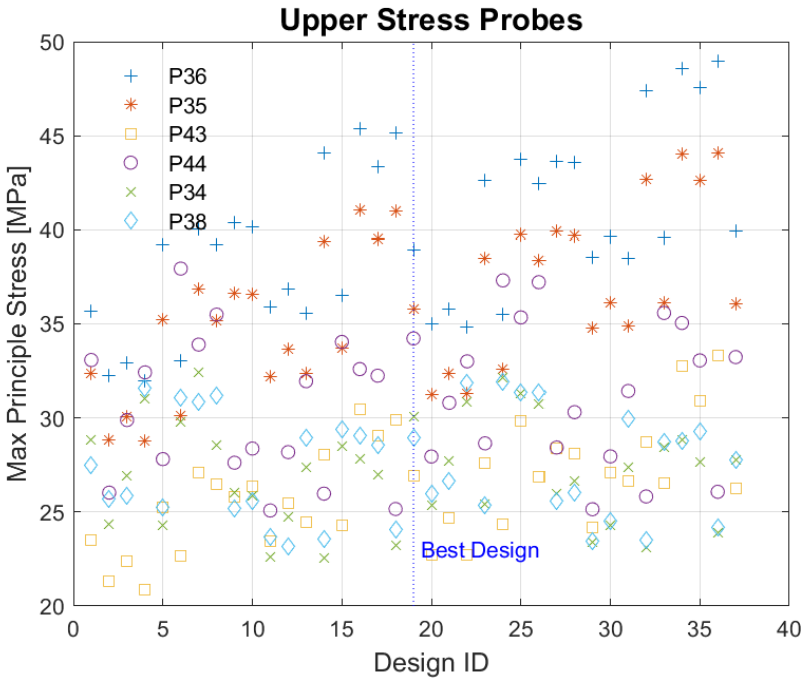

Figure 7 *Principle stress values at upper probe points for each design point.*

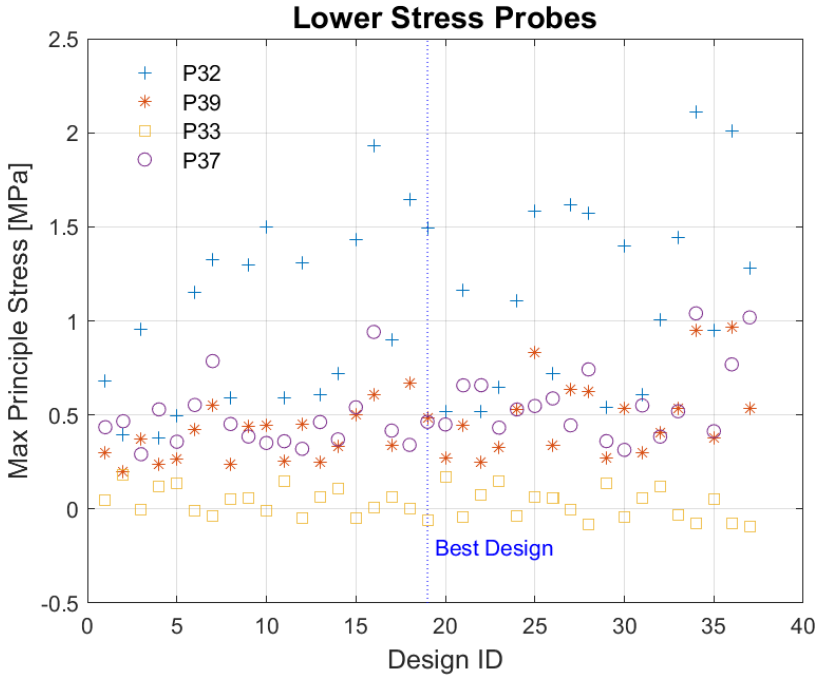

Figure 8 *Principle stress values at lower probe points for each design point.*

2. Large Custom Profile, SORVI Algorithm (Adaptive)

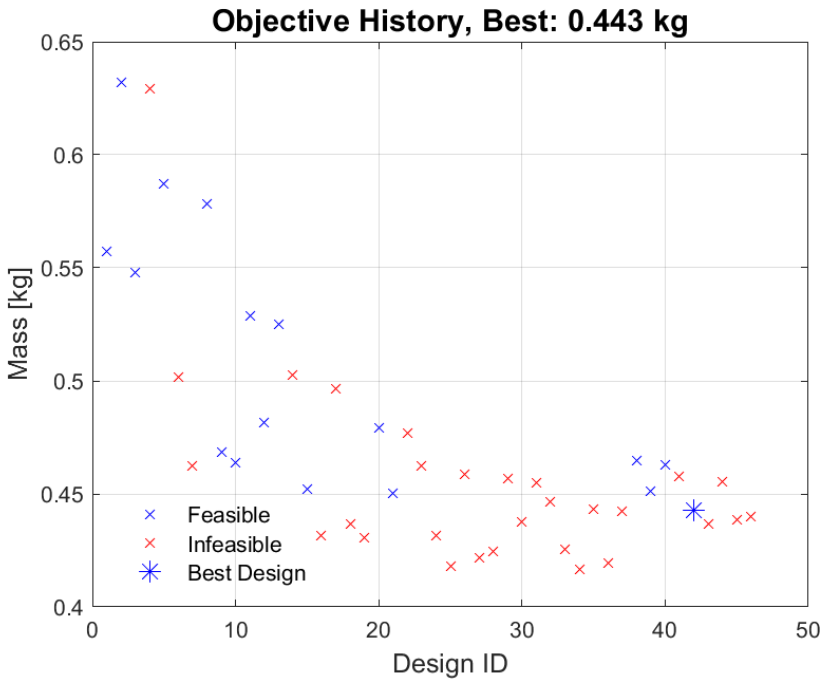

Figure 9 *Objective function design point history.*

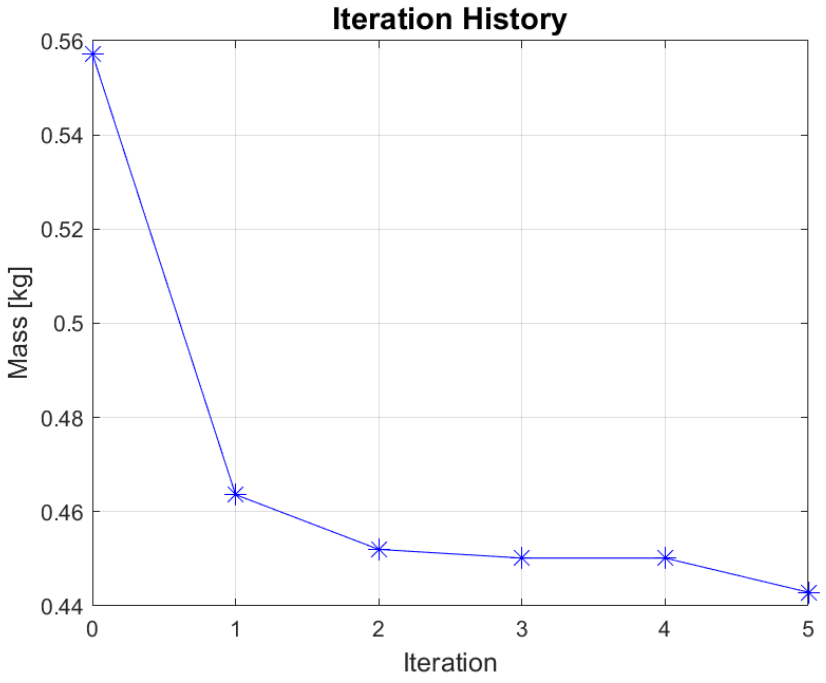

Figure 10 *Objective function iteration history.*

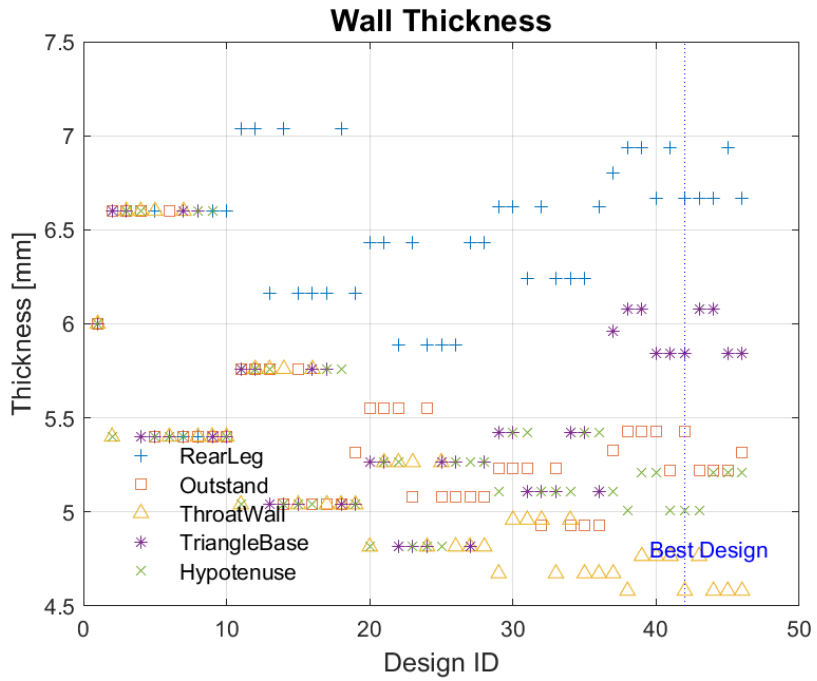

Figure 11 *Wall thickness parameter values of each design point.*

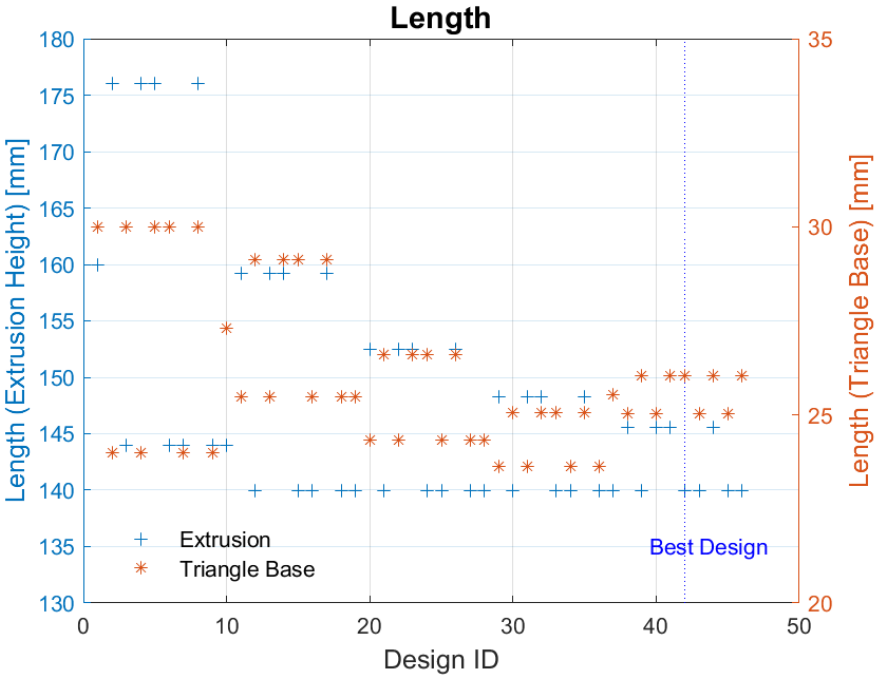

Figure 12 *Length parameter values of each design point.*

Figure 13 *Max von Mises stress result of each design point.*

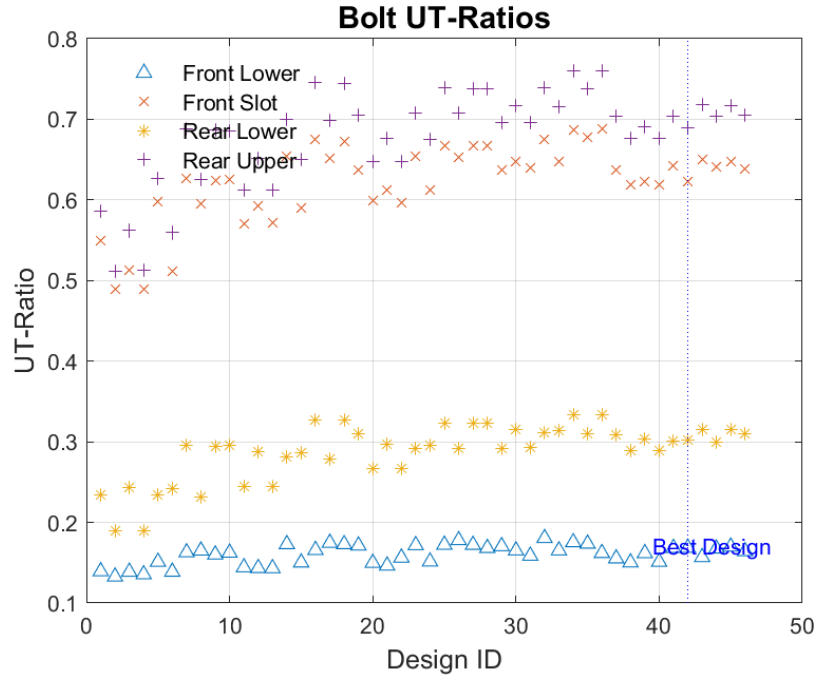

Figure 14 *Bolt UT-Ratios of each design point.*

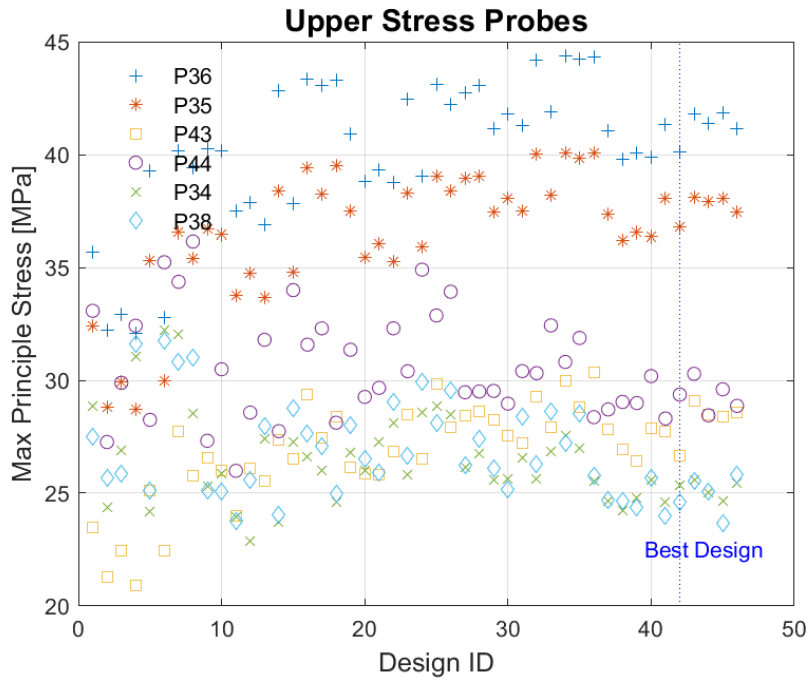

Figure 15 *Principle stress values at upper probe points for each design point.*

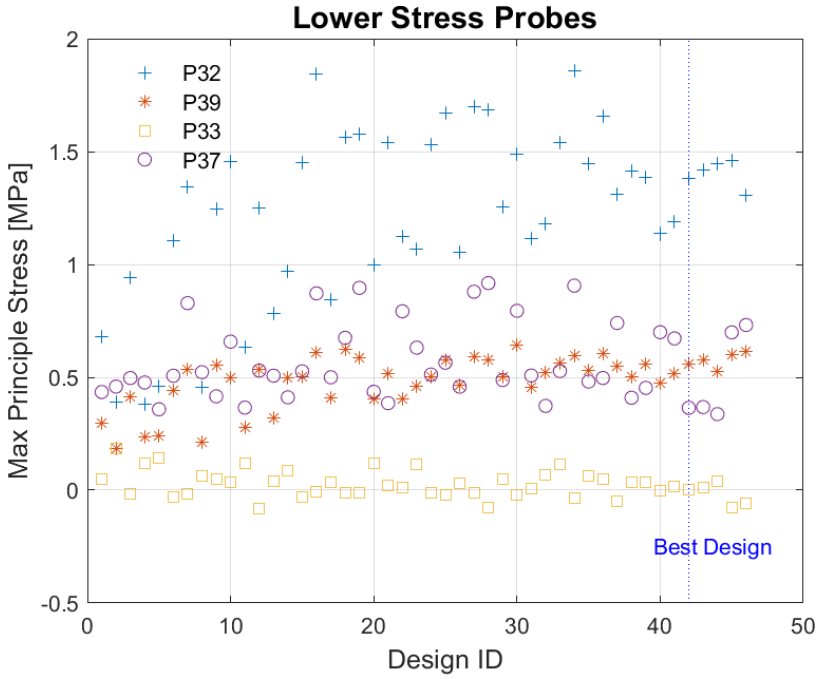

Figure 16 *Principle stress values at lower probe points for each design point.*

3. Large Custom Profile, SORVI Algor. (Adaptive, 7mm)

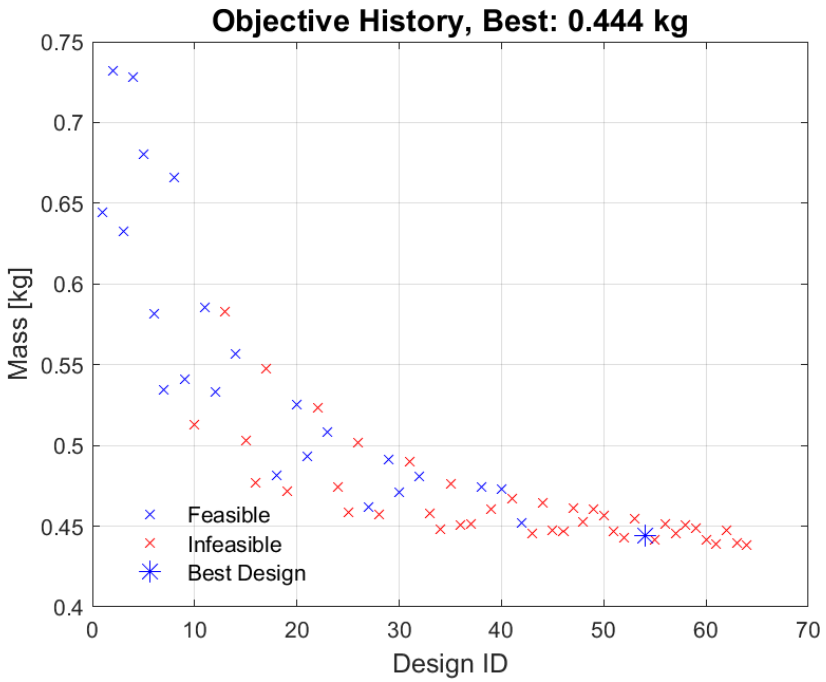

Figure 17 *Objective function design point history.*

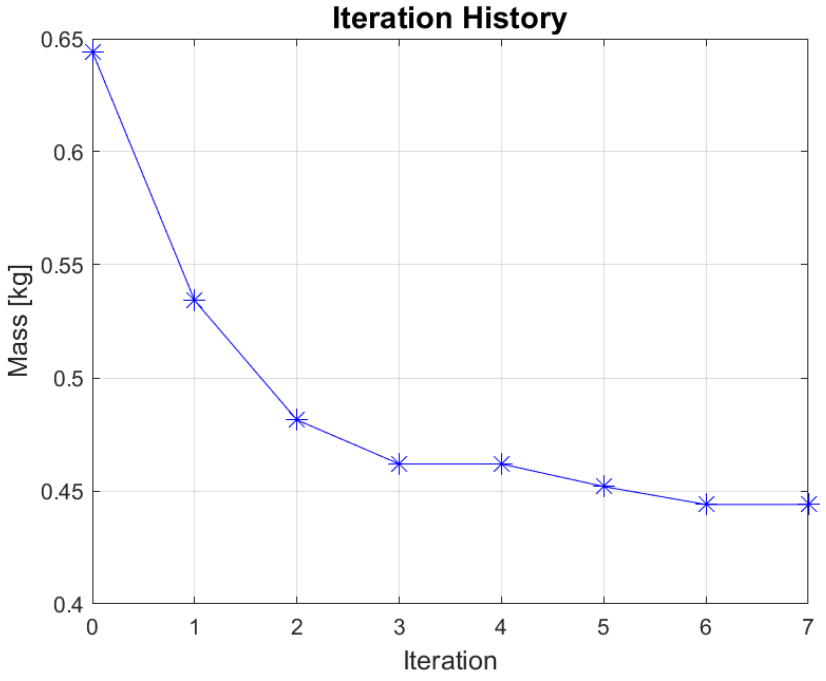

Figure 18 *Objective function iteration history.*

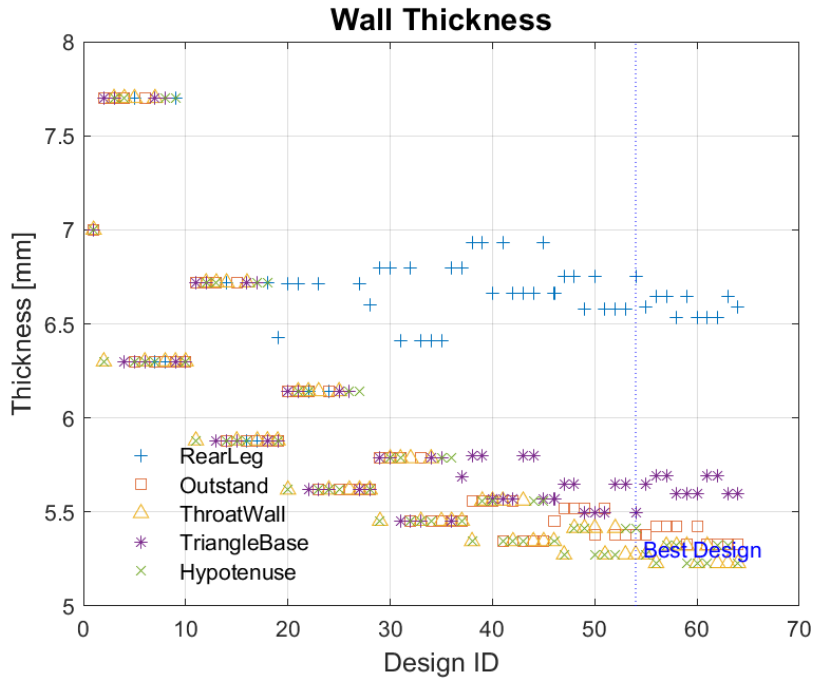

Figure 19 *Wall thickness parameter values of each design point.*

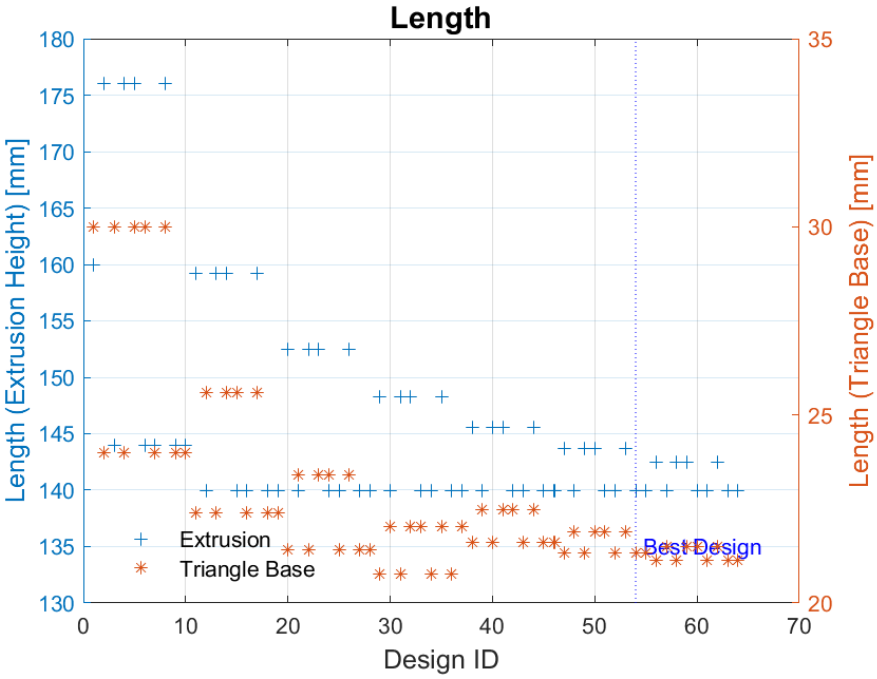

Figure 20 *Length parameter values of each design point.*

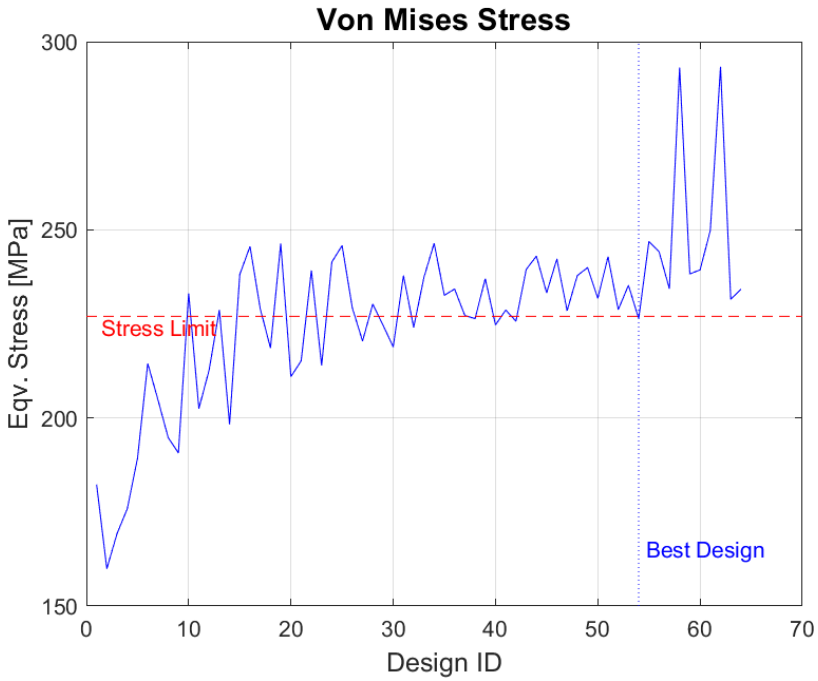

Figure 21 *Max von Mises stress result of each design point.*

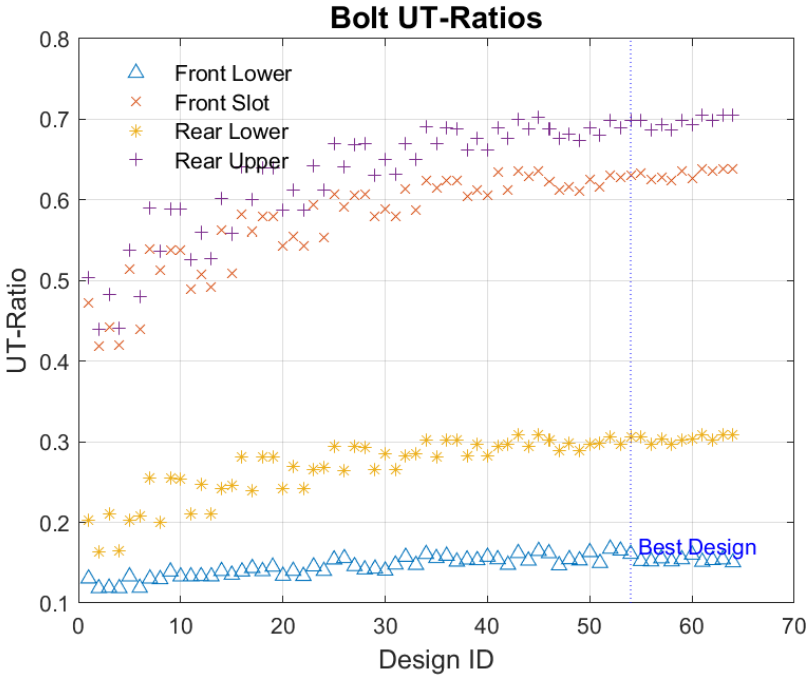

Figure 22 *Bolt UT-Ratios of each design point.*

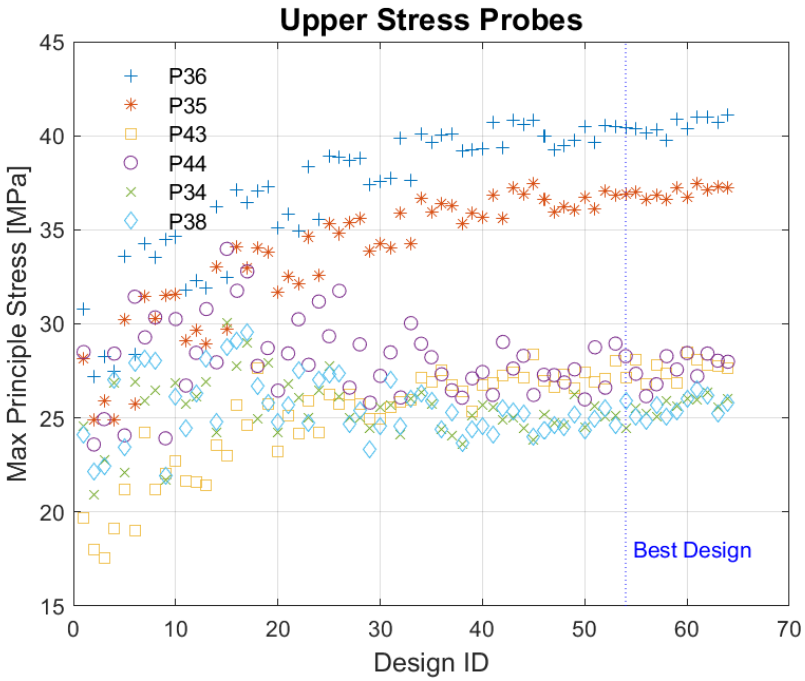

Figure 23 *Principle stress values at upper probe points for each design point.*

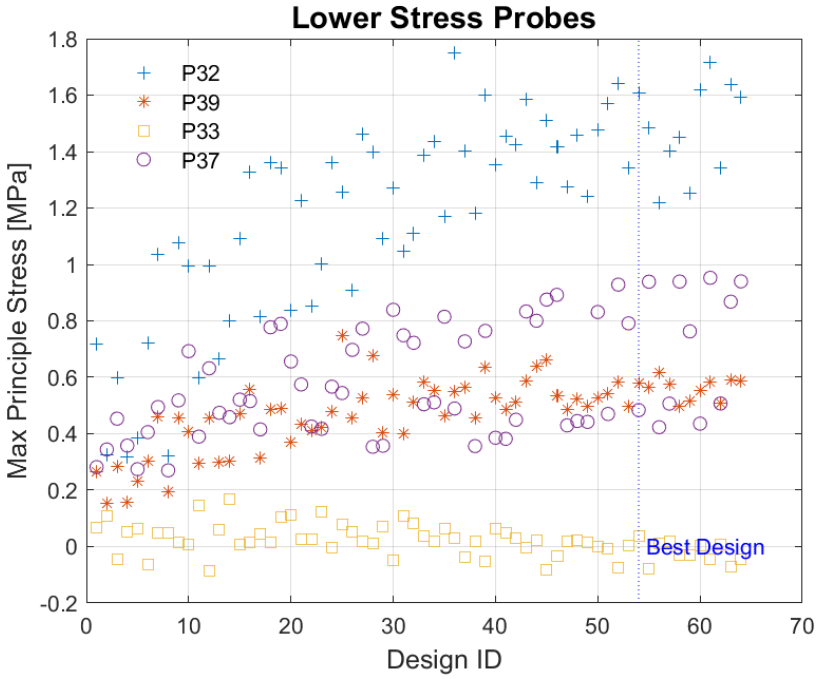

Figure 24 *Principle stress values at lower probe points for each design point.*

4. Small Custom Profile, SORVI Algorithm

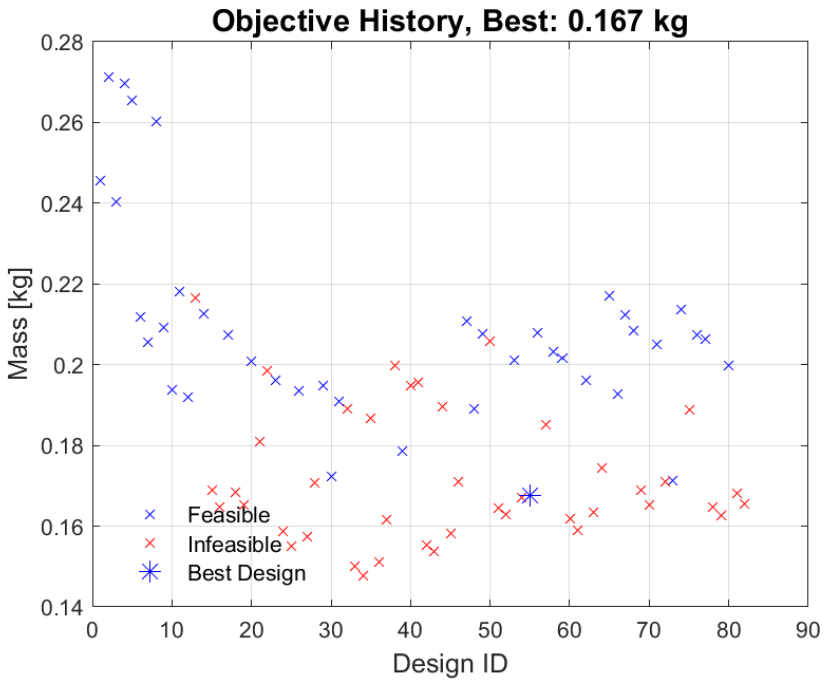

Figure 25 *Objective function design point history.*

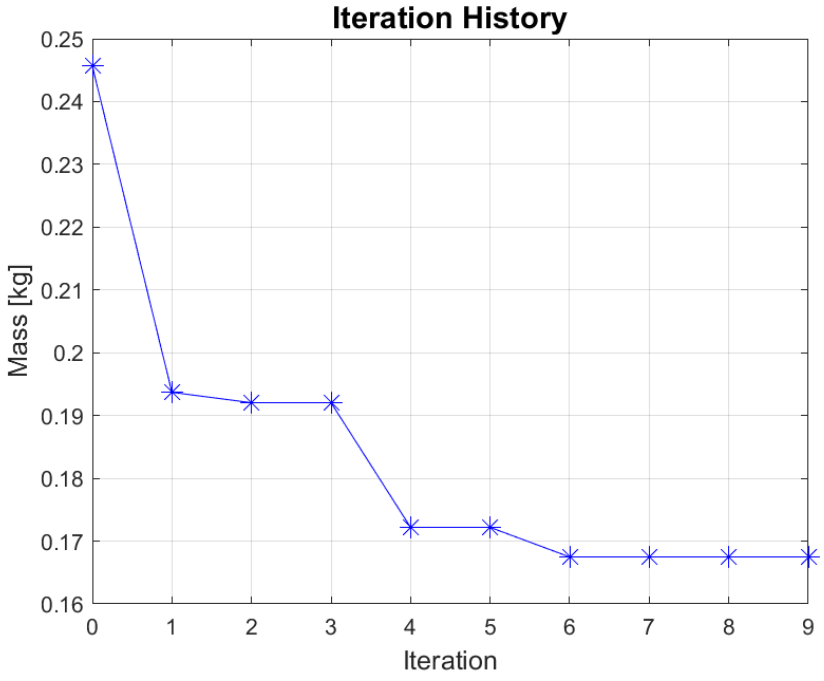

Figure 26 *Objective function iteration history.*

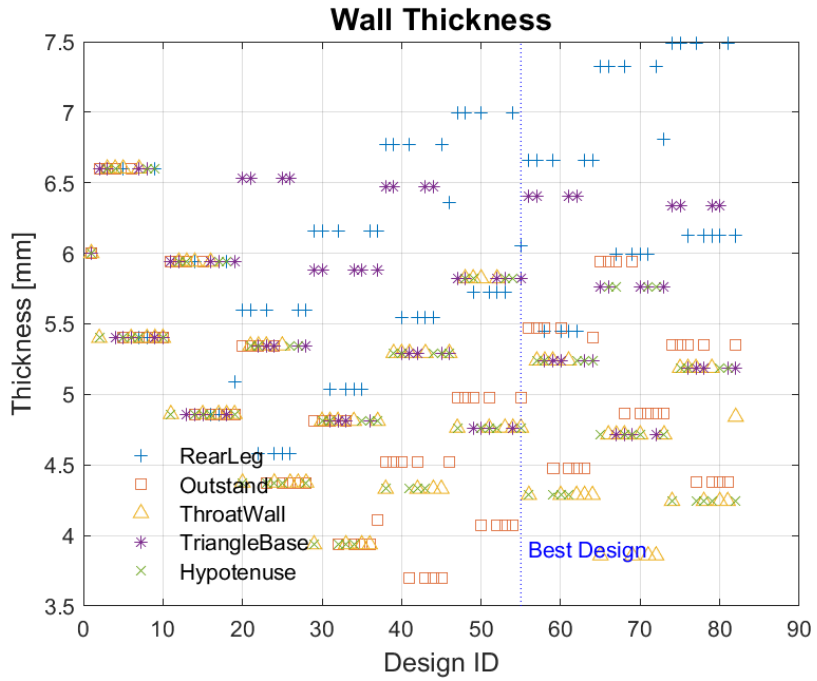

Figure 27 *Wall thickness parameter values of each design point.*

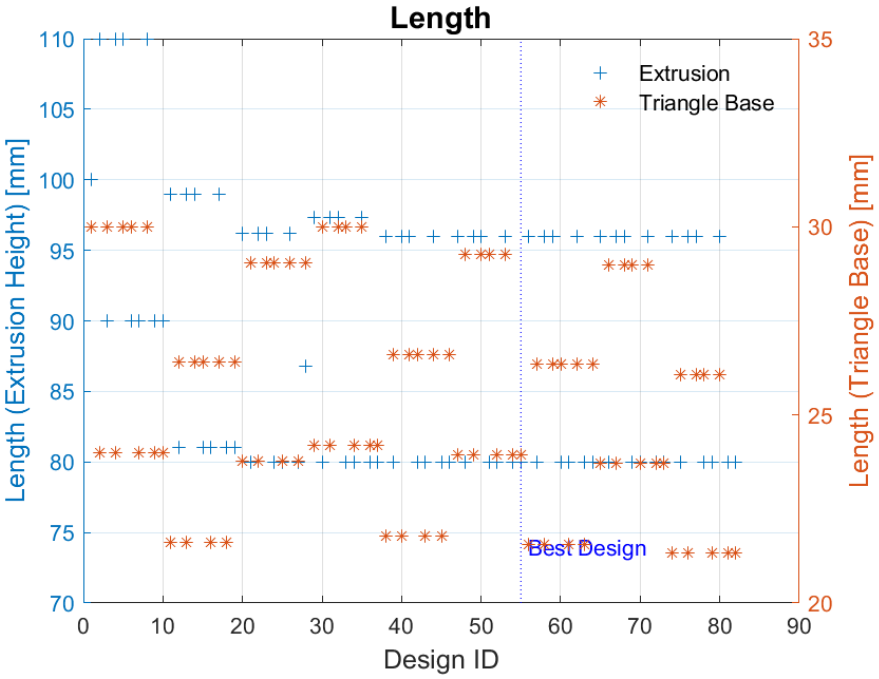

Figure 28 *Length parameter values of each design point.*

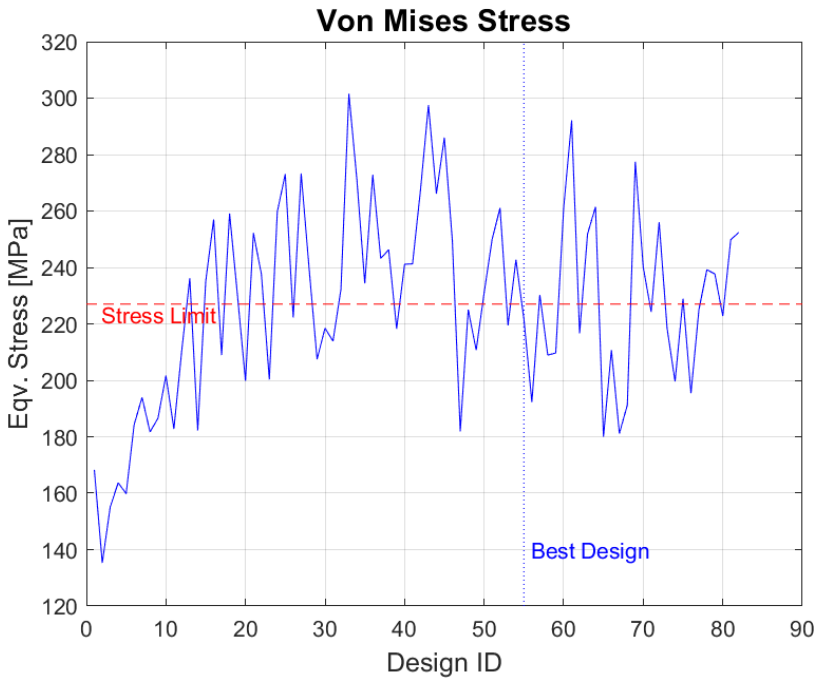

Figure 29 *Max von Mises stress result of each design point.*

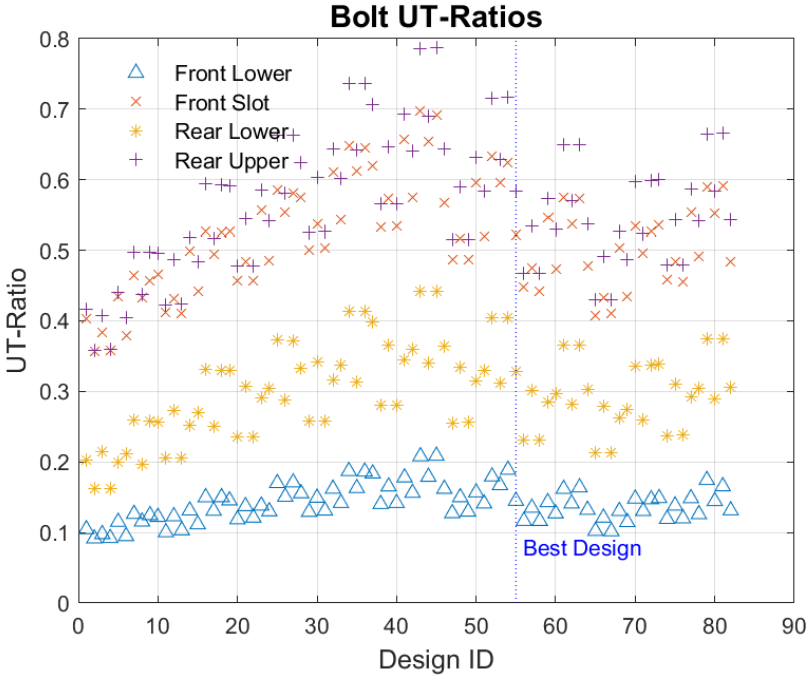

Figure 30 *Bolt UT-Ratios of each design point.*

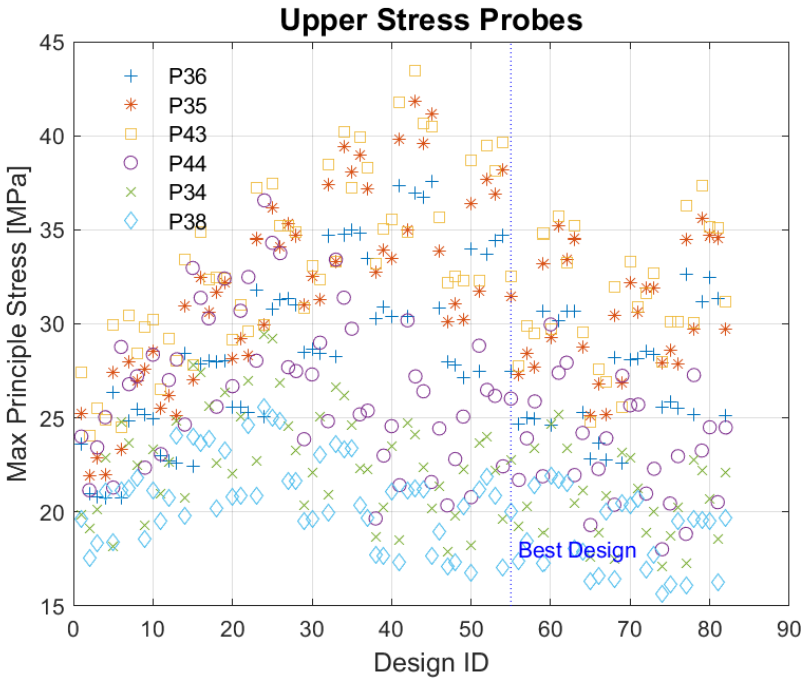

Figure 31 *Principle stress values at upper probe points for each design point.*

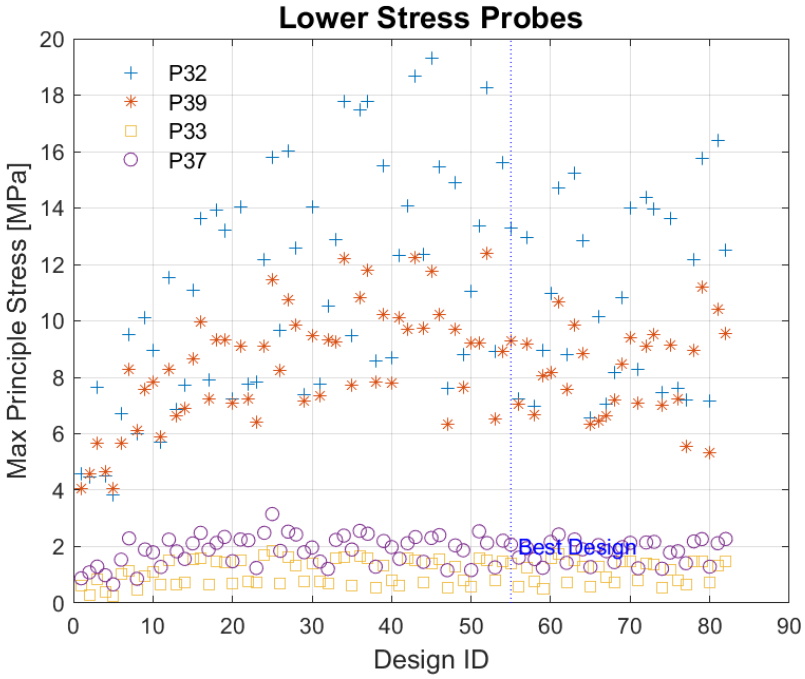

Figure 32 *Principle stress values at lower probe points for each design point.*

5. Small Custom Profile, Genetic Algorithm

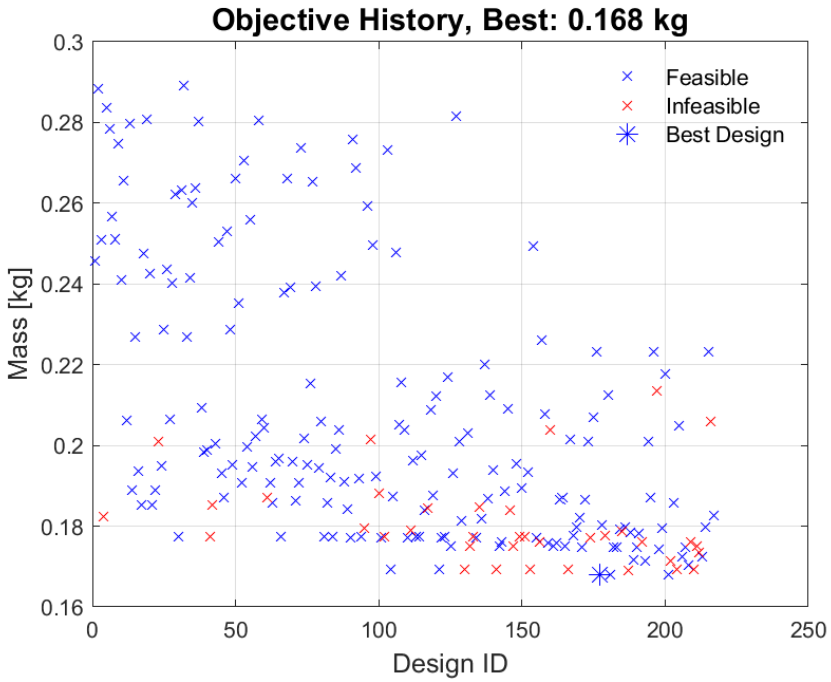

Figure 33 *Objective function design point history (20 % initial range).*

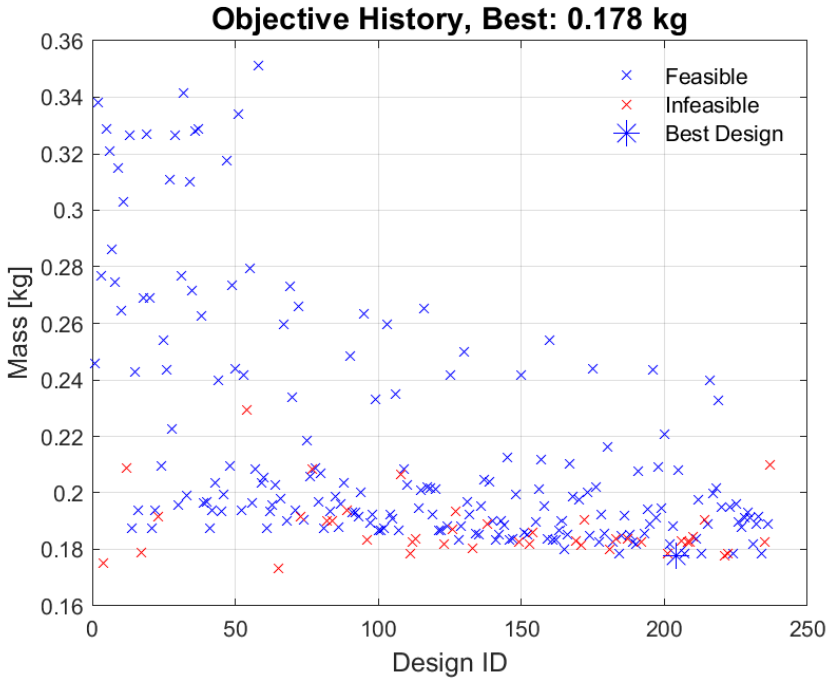

Figure 34 *Objective function design point history (run with 30% initial range, not related to the rest of the results presented here. Just to show convergence to approximately same solution, regardless of initial population and randomness).*

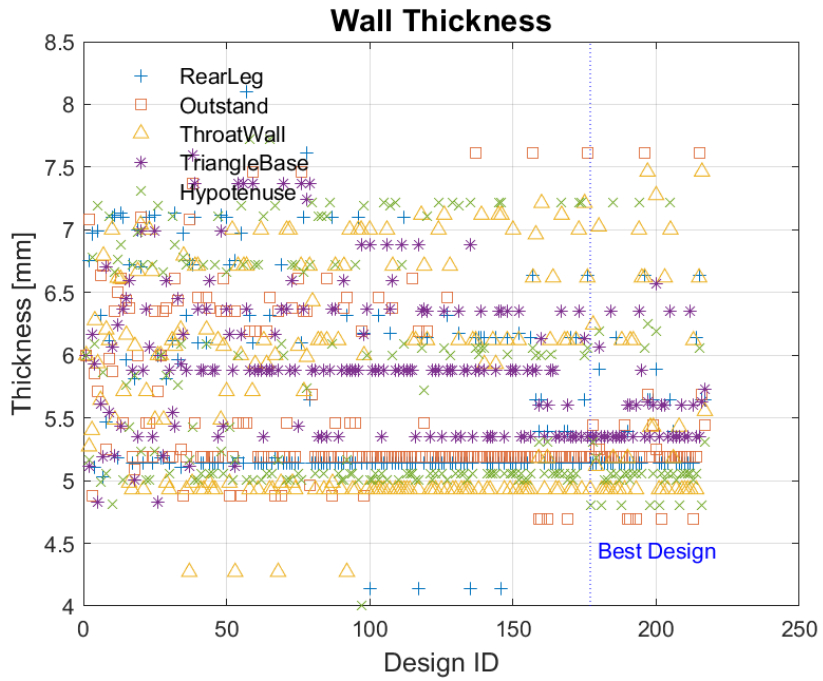

Figure 35 *Wall thickness parameter values of each design point.*

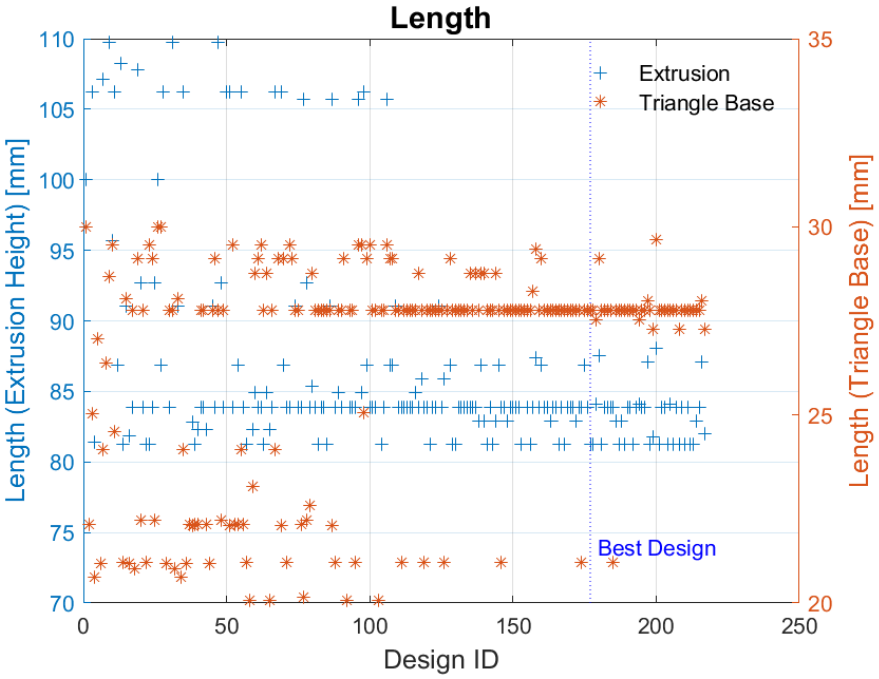

Figure 36 *Length parameter values of each design point.*

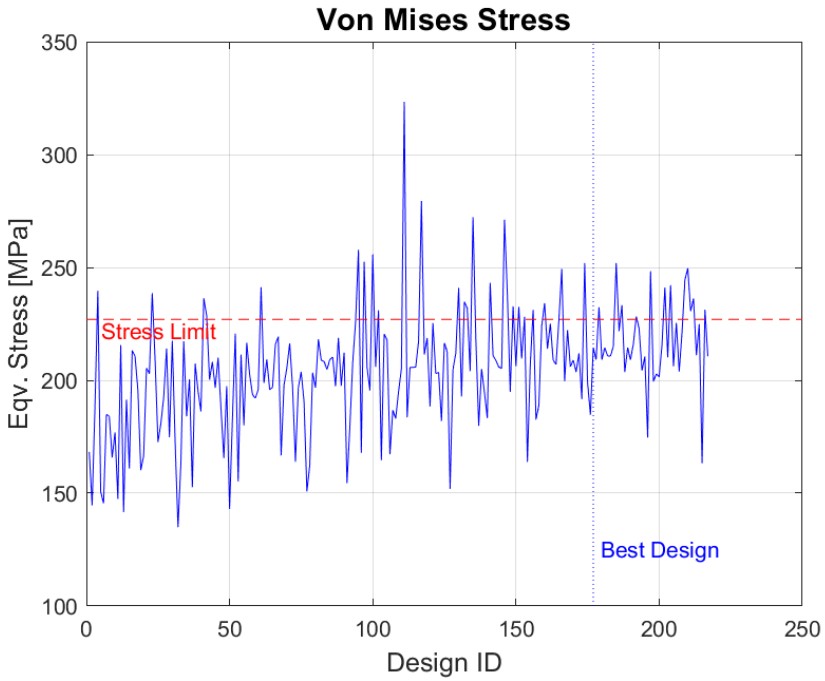

Figure 37 *Max von Mises stress result of each design point.*

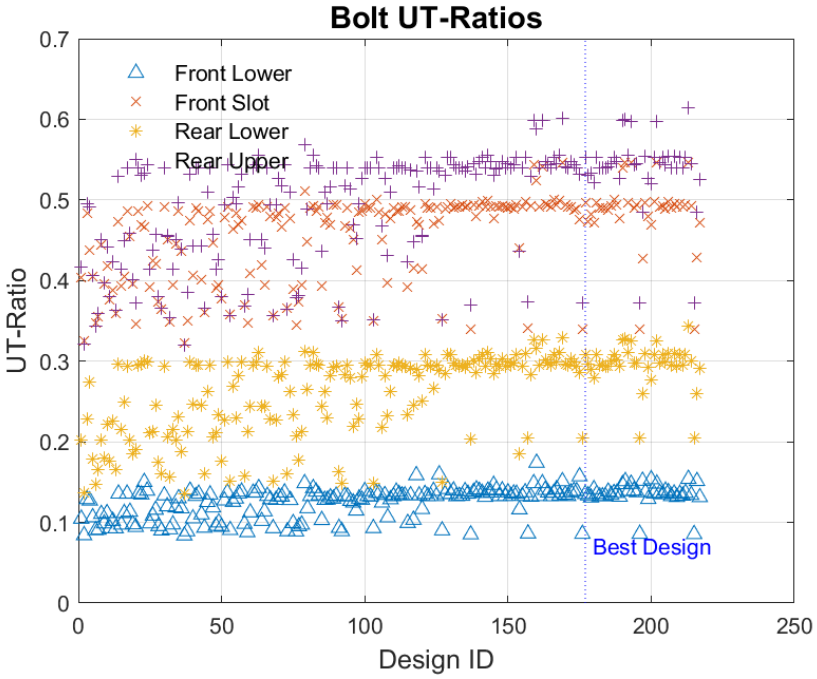

Figure 38 *Bolt UT-Ratios of each design point.*

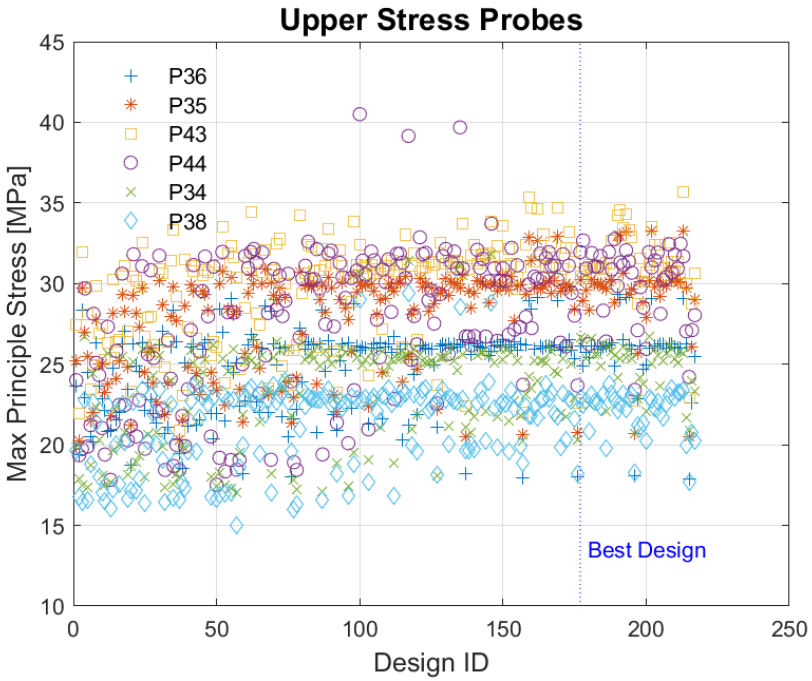

Figure 39 *Principle stress values at upper probe points for each design point.*

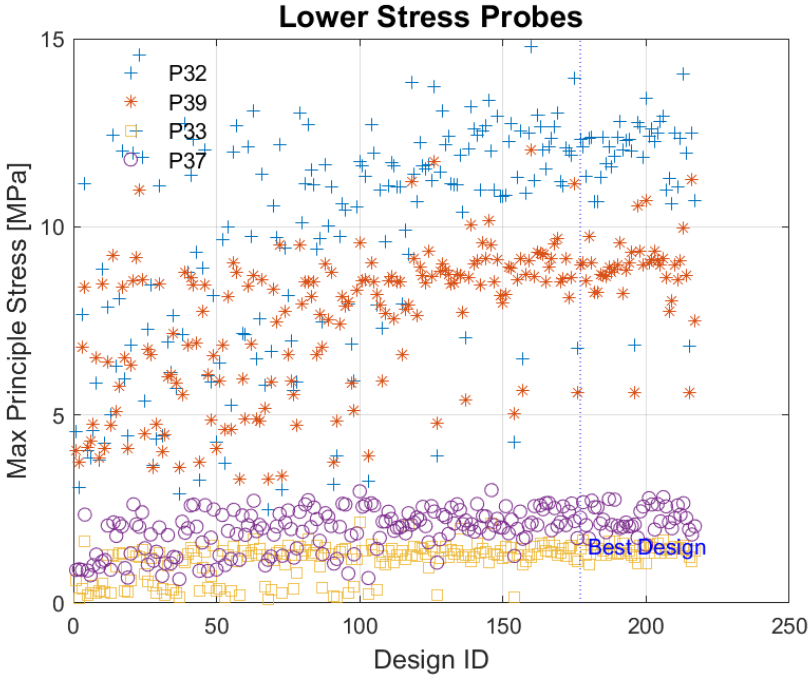

Figure 40 *Principle stress values at lower probe points for each design point.*

6. Small L-Profile SORVI Algorithm

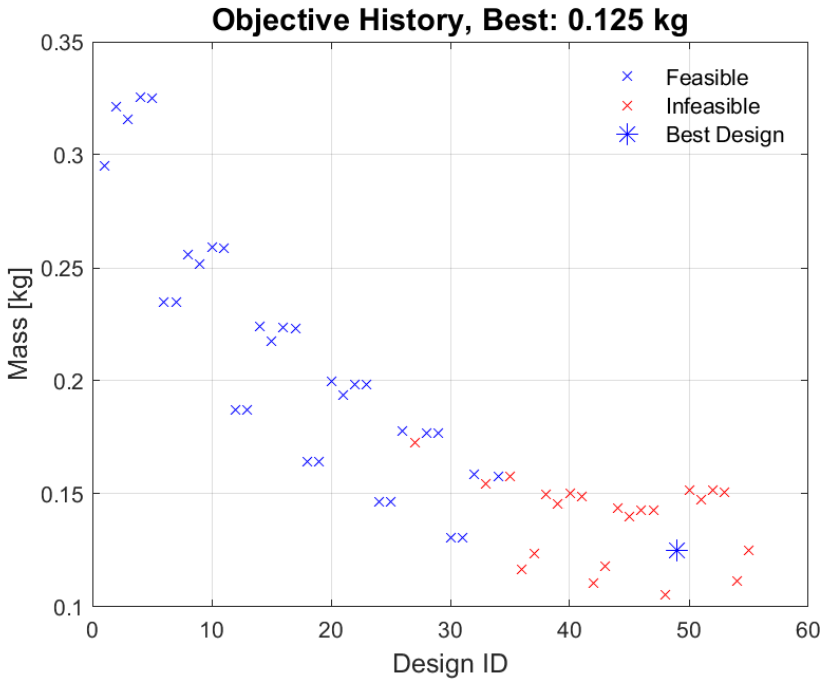

Figure 41 *Objective function design point history.*

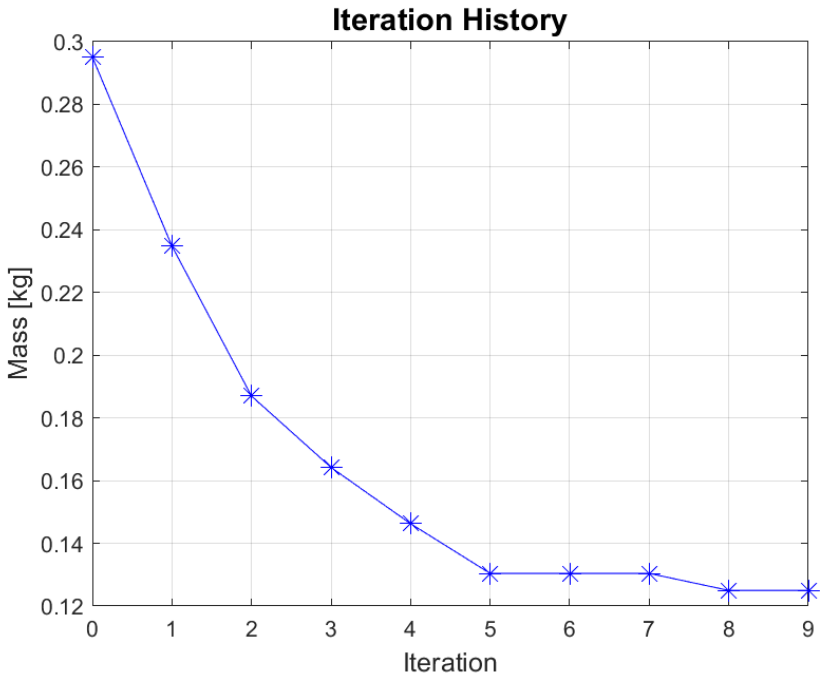

Figure 42 *Objective function iteration history.*

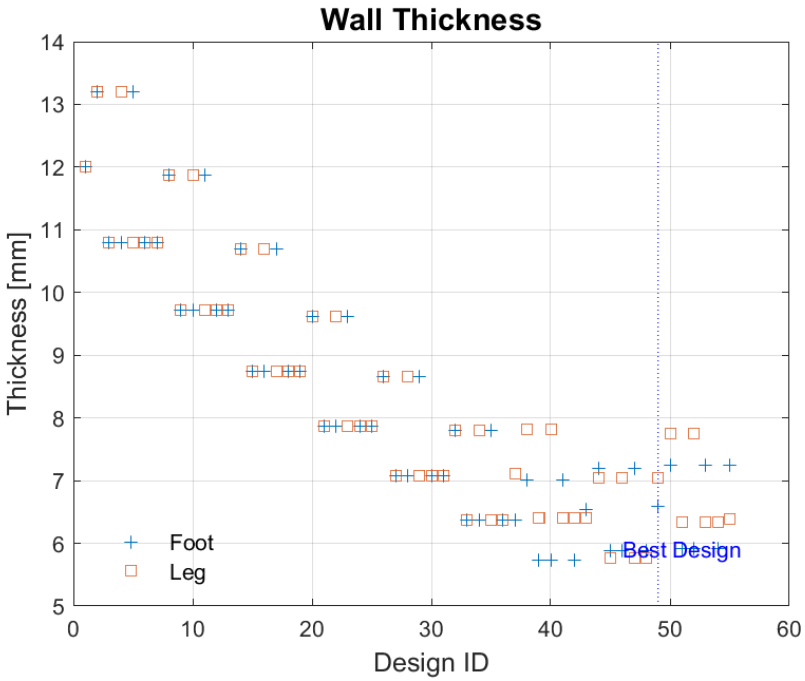

Figure 43 *Wall thickness parameter values of each design point.*

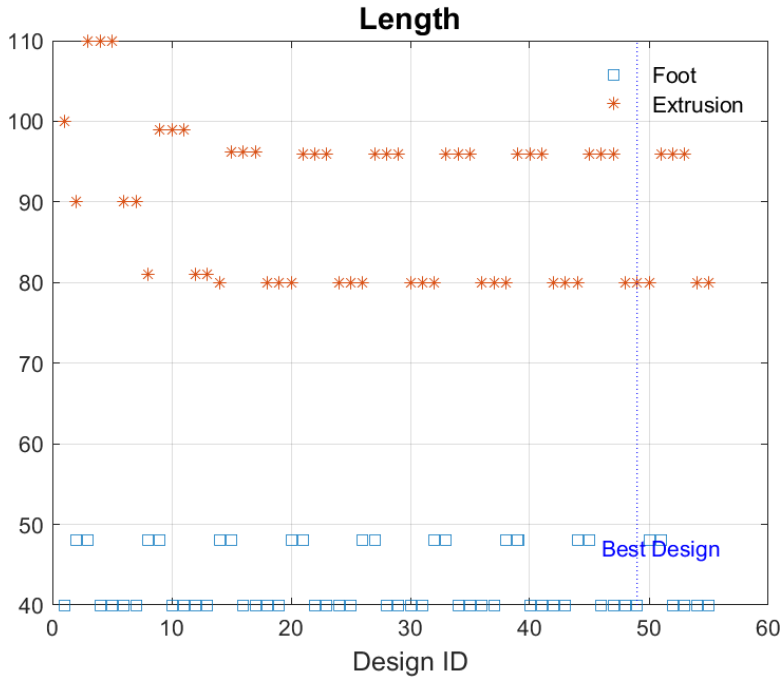

Figure 44 *Length parameter values of each design point.*

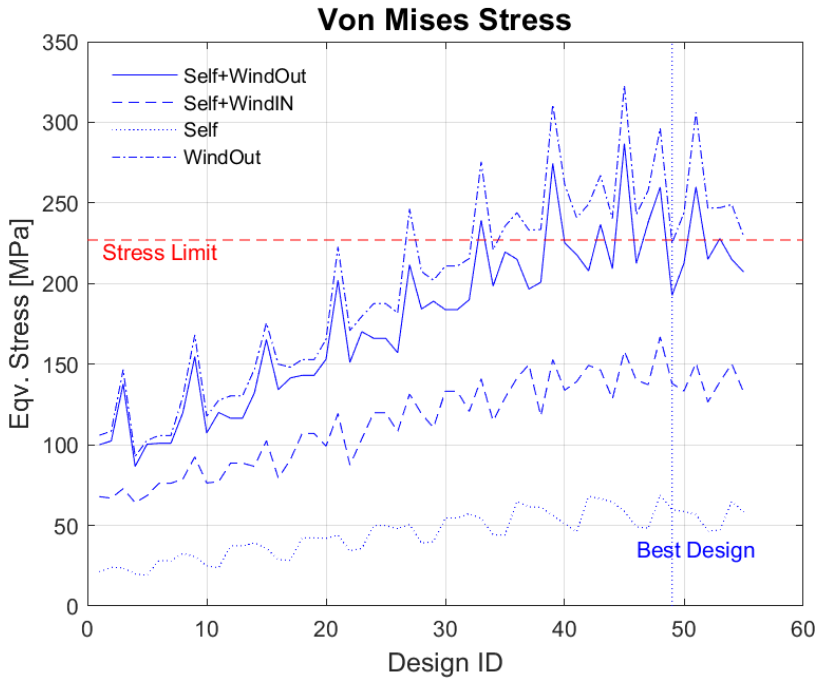

Figure 45 *Max von Mises stress result of each design point*

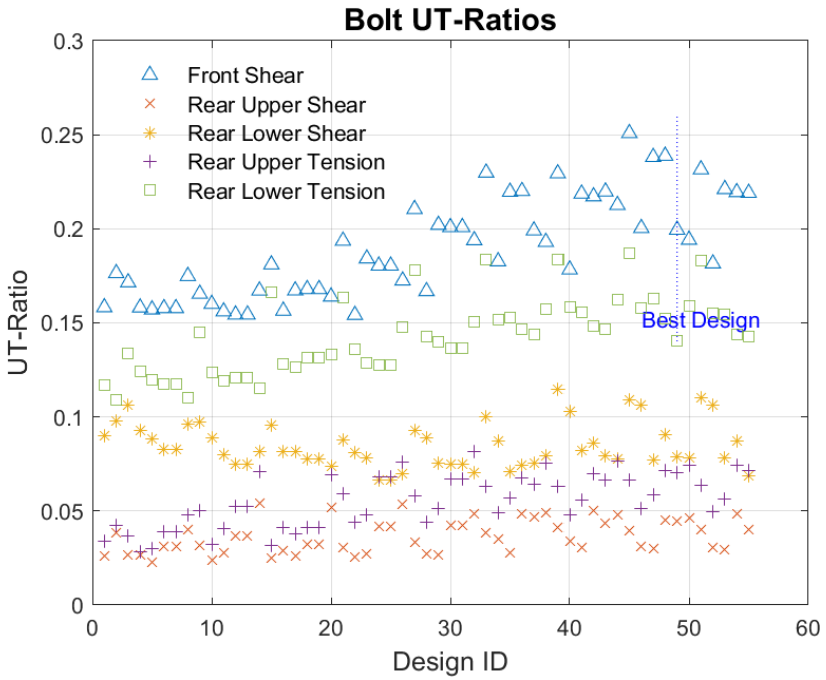

Figure 46 *Bolt UT-Ratios of each design point.*

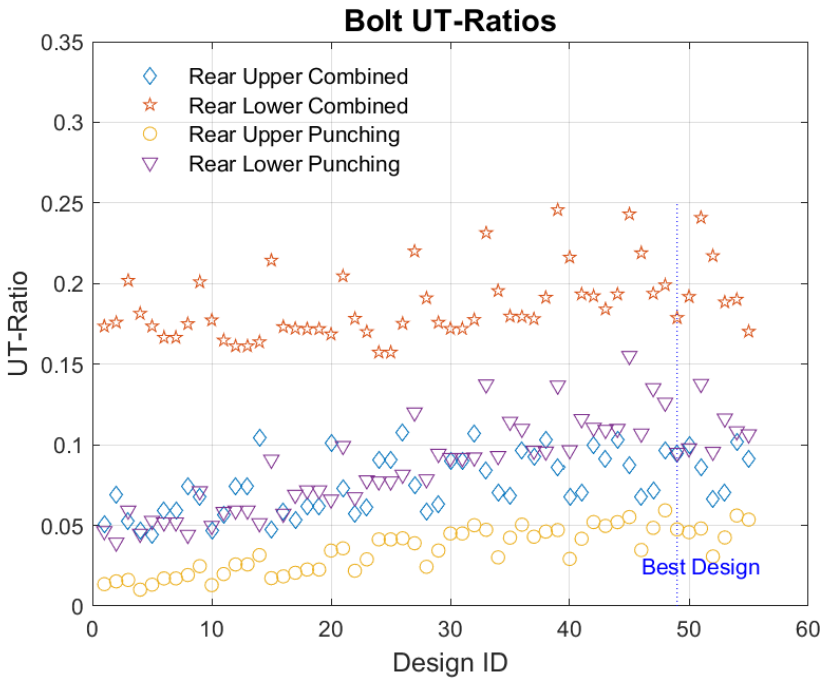

Figure 47 *Bolt UT-Ratios of each design point.*

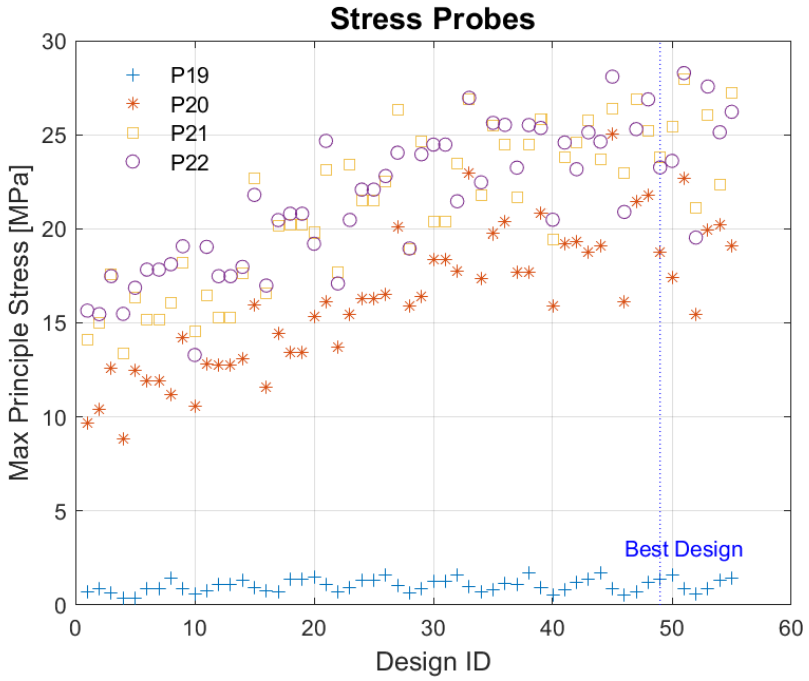

Figure 48 *Principle stress values at probe points for each design point.*

7. Large L-Profile SORVI Algorithm

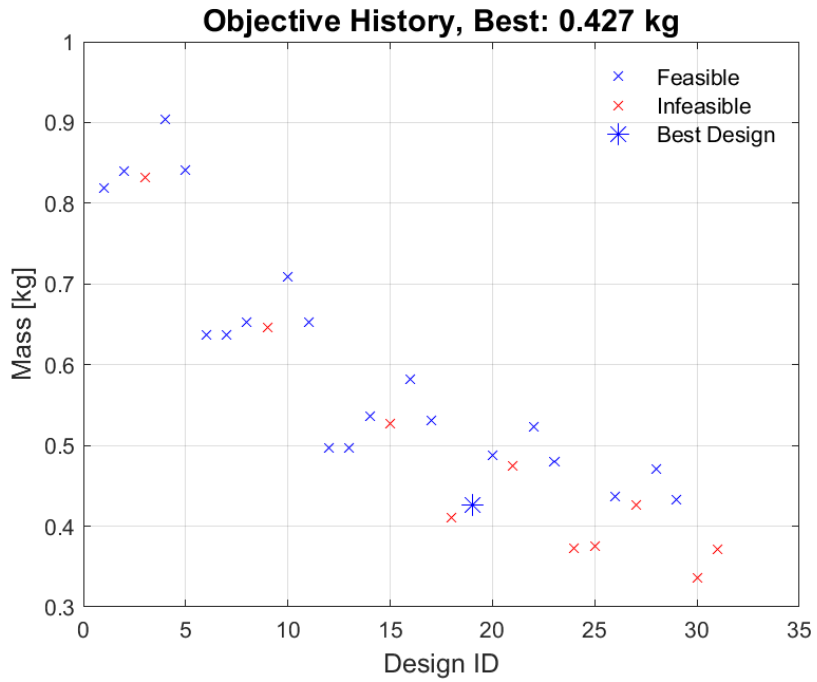

Figure 49 *Objective function design point history.*

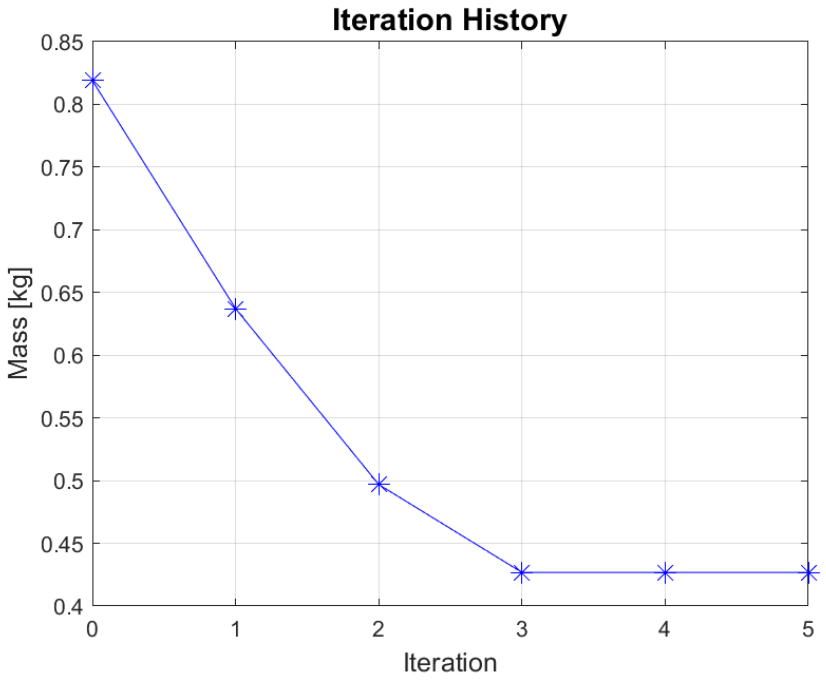

Figure 50 *Objective function iteration history.*

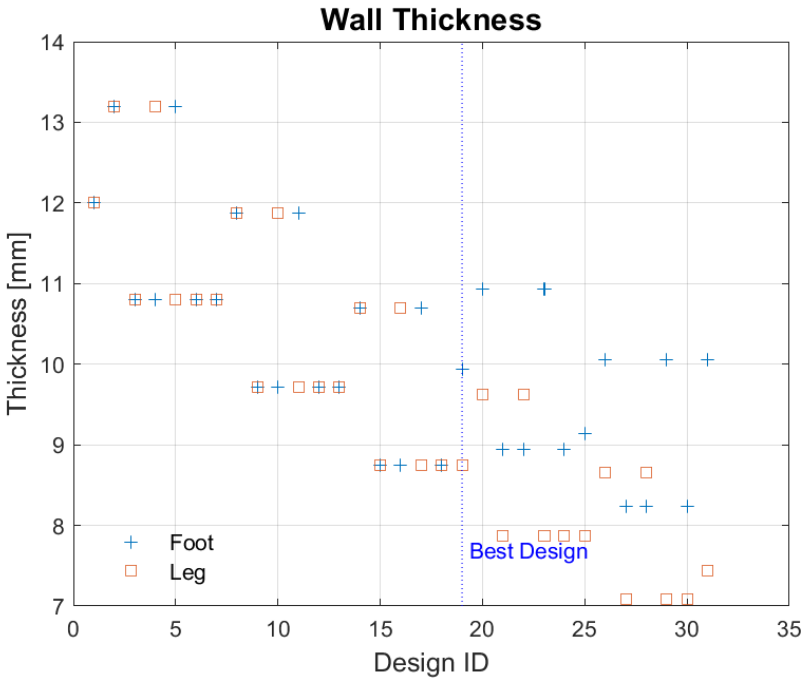

Figure 51 *Wall thickness parameter values of each design point.*

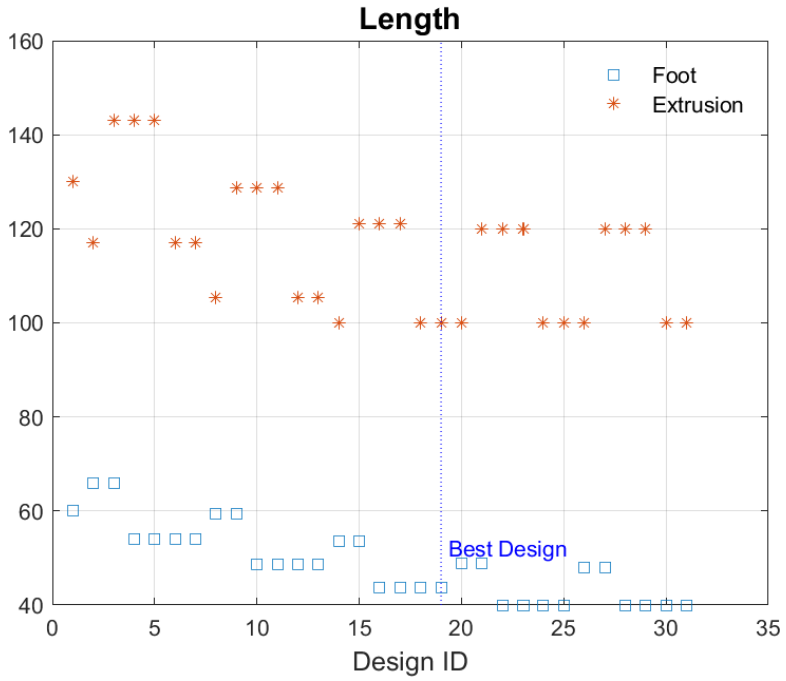

Figure 52 *Length parameter values of each design point.*

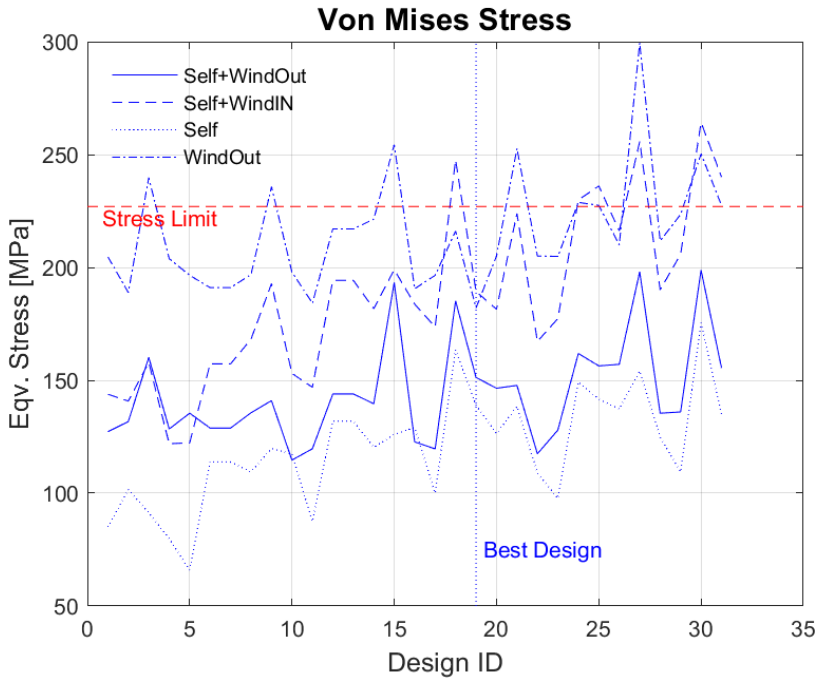

Figure 53 *Max von Mises stress result of each design point.*

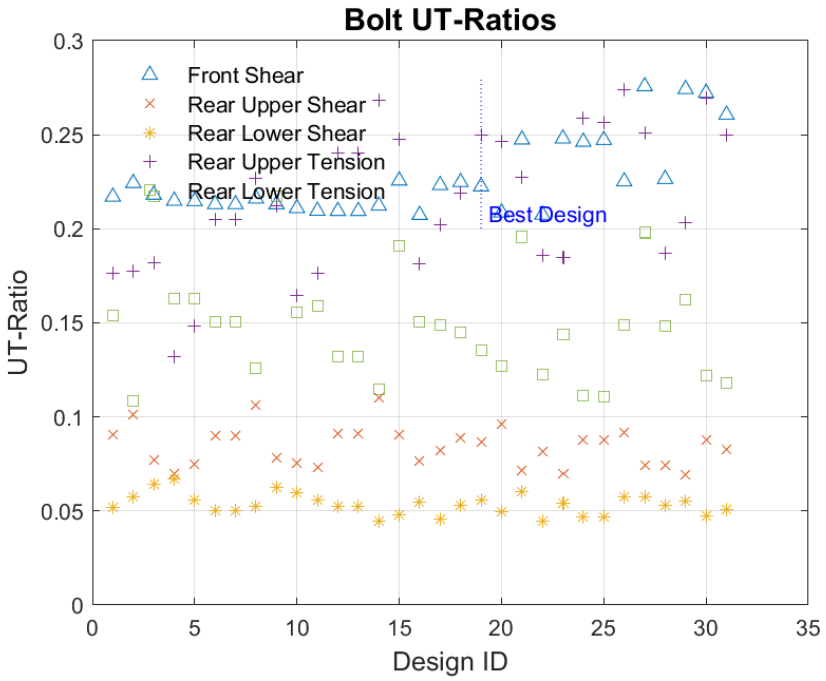

Figure 54 *Bolt UT-Ratios of each design point.*

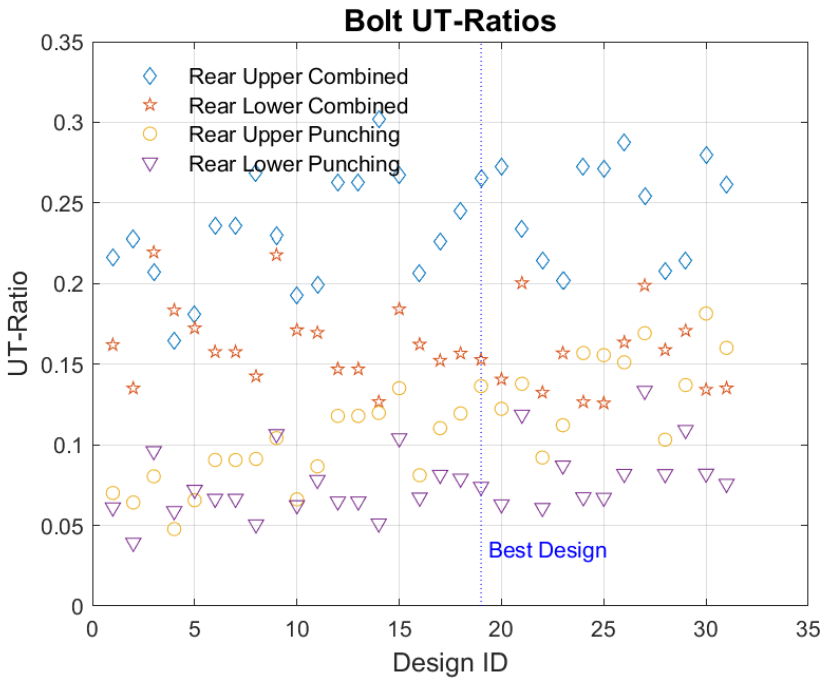

Figure 55 *Bolt UT-Ratios of each design point.*

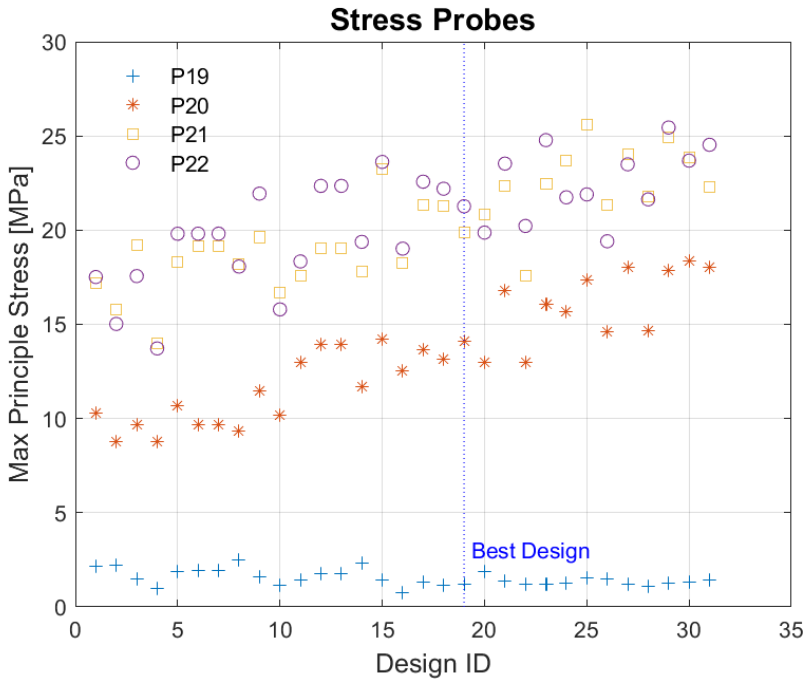

Figure 56 *Principle stress values at probe points for each design point.*

APPENDIX 3: FINAL DESIGN DRAWINGS

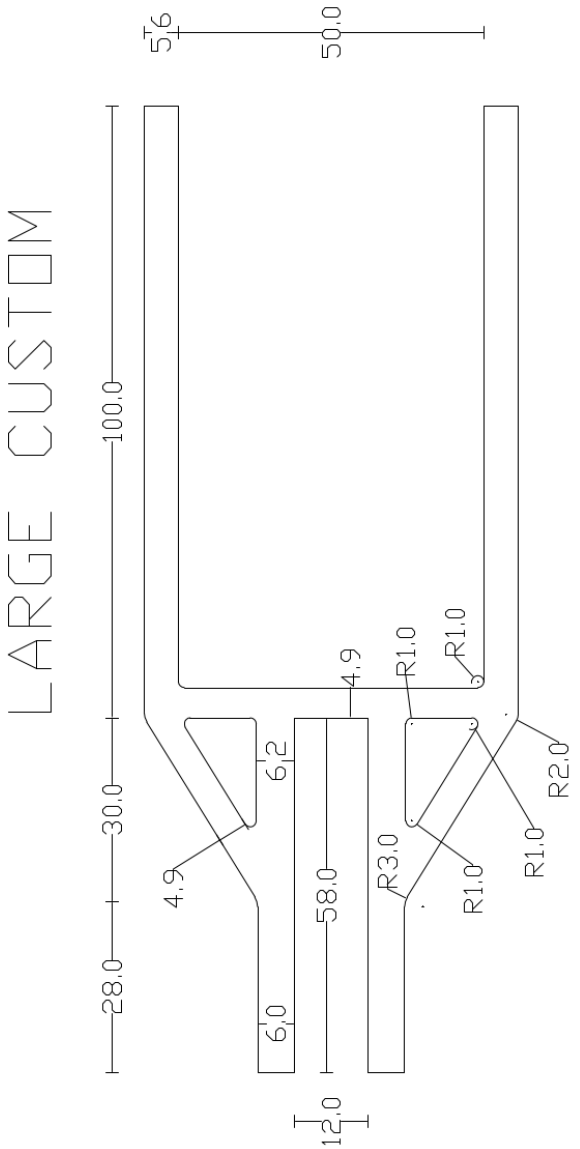

Figure 1 *Large custom profile final design. Dimensions in mm.*

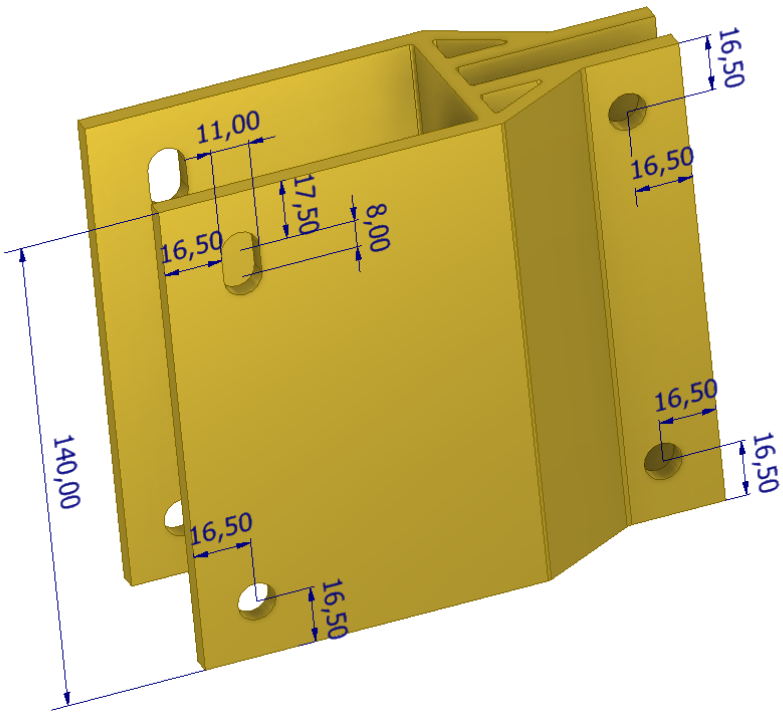

Figure 2 *Bolt hole placement and extrusion length for large custom self-weight + wind profile. All bolts size M10. Dimensions in mm.*

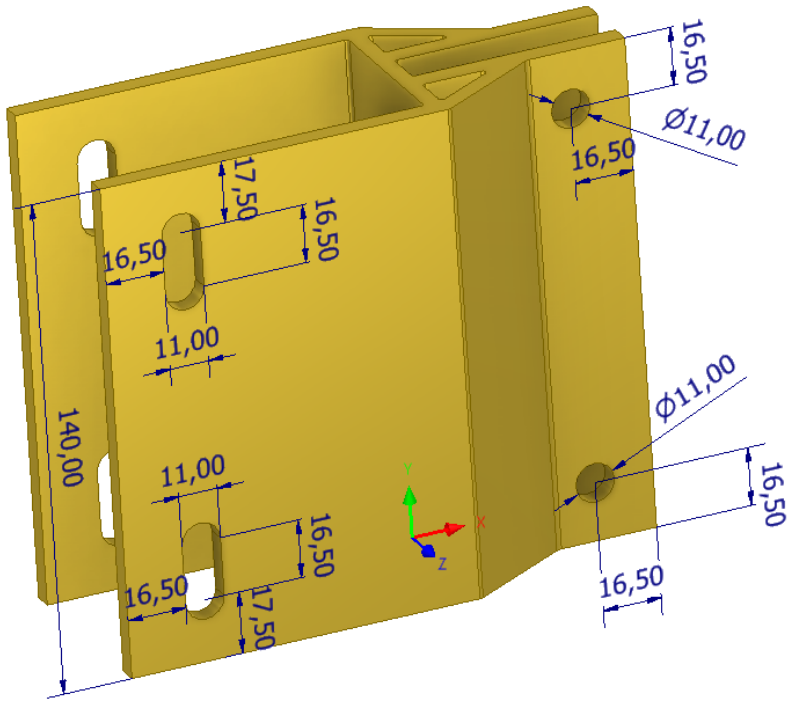

Figure 3 *Bolt hole placement and extrusion length for large custom wind profile. All bolts size M10. Dimensions in mm.*

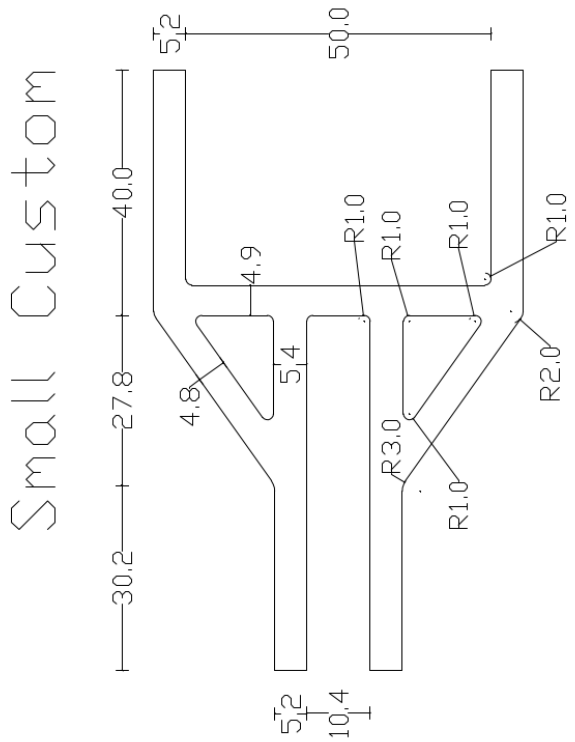

Figure 4 *Small custom profile final design. Dimensions in mm.*

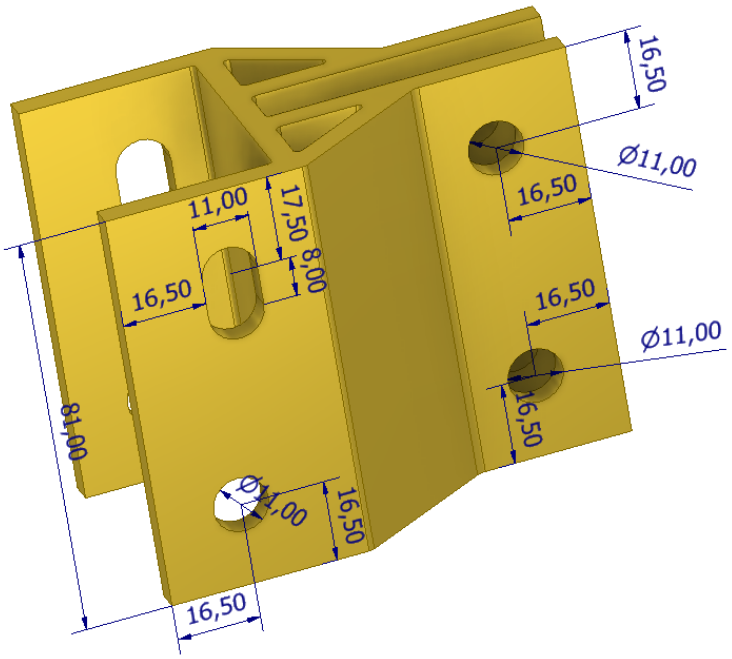

Figure 5 *Bolt hole placement and extrusion length for small custom self-weight + wind profile. All bolts size M10. Dimensions in mm.*

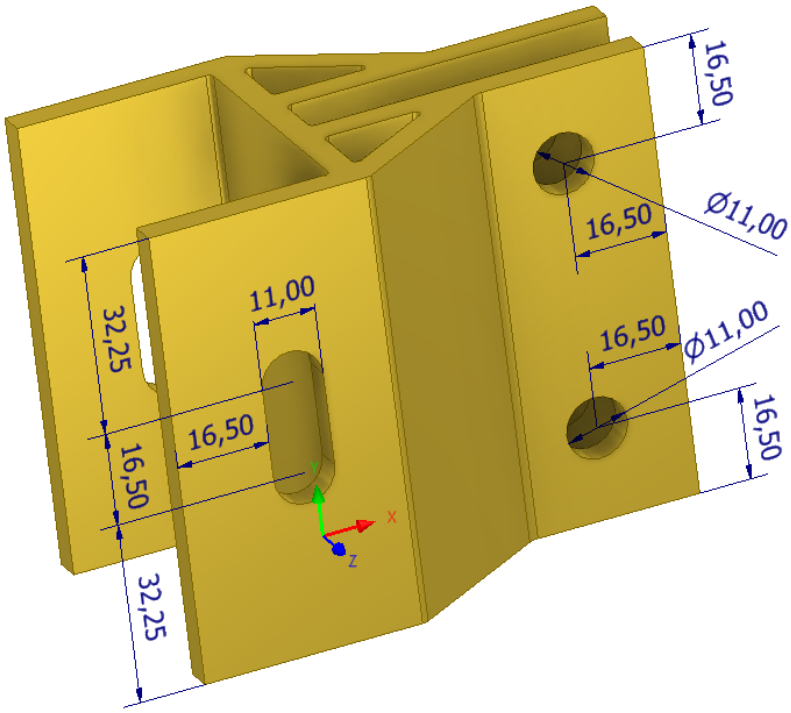

Figure 6 *Bolt hole placement and extrusion length for small custom wind profile. All bolts size M10. Dimensions in mm.*

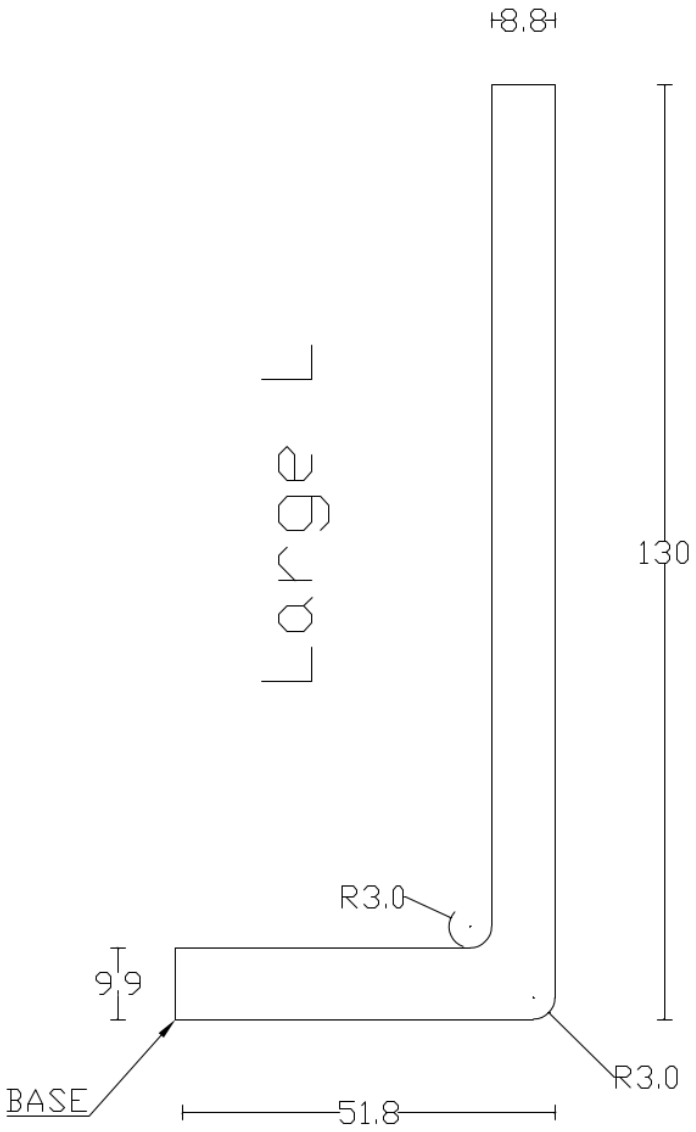

Figure 7 *Large L-profile final design. Dimensions in mm.*

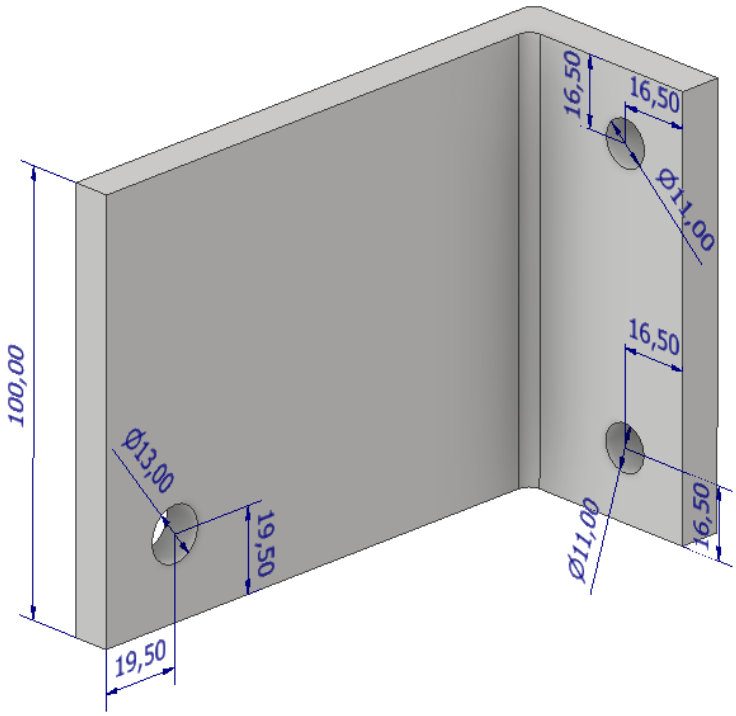

Figure 8 *Bolt hole placement and extrusion length for large self-weight + wind L-profile. Rear bolts are size M10, front bolt is size M12. Dimensions in mm.*

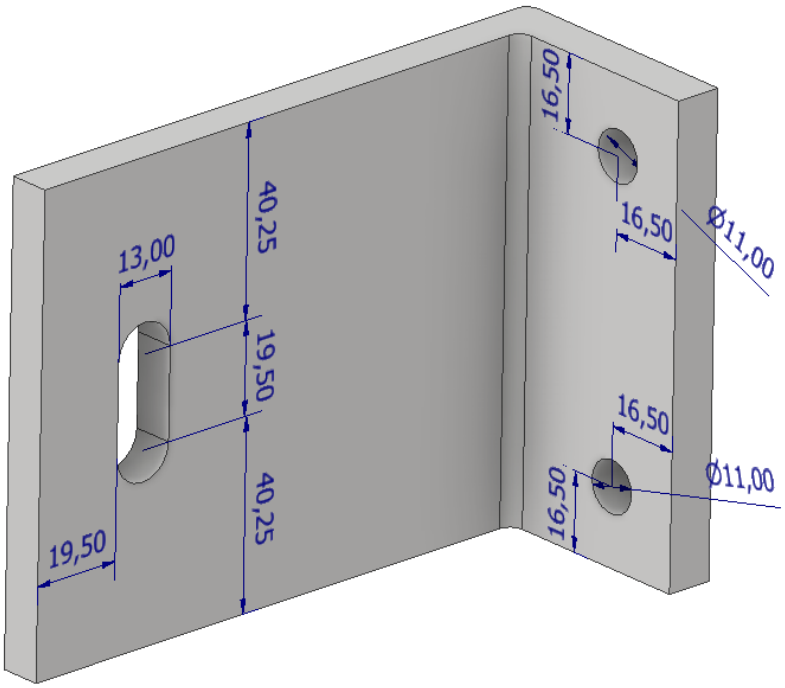

Figure 9 *Bolt hole placement and extrusion length for large wind L-profile. Rear bolts are size M10, front bolt is size M12. Dimensions in mm.*

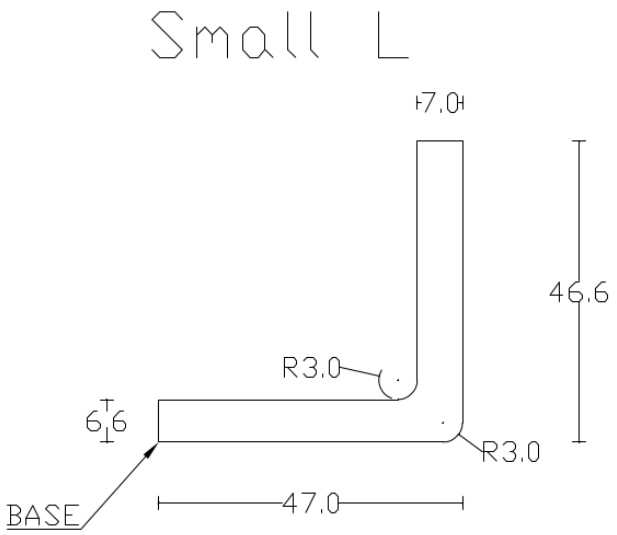

Figure 10 *Small L-profile final design. Dimensions in mm.*

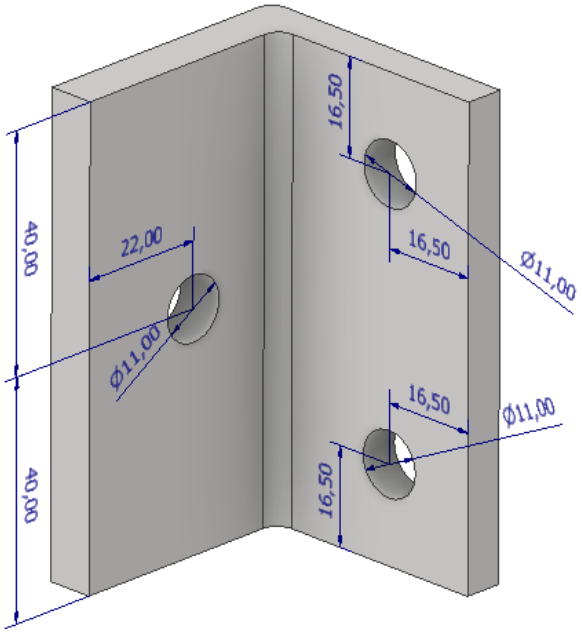

Figure 11 *Bolt hole placement and extrusion length for small self-weight + wind L-profile. All bolts are size M10. Dimensions in mm.*

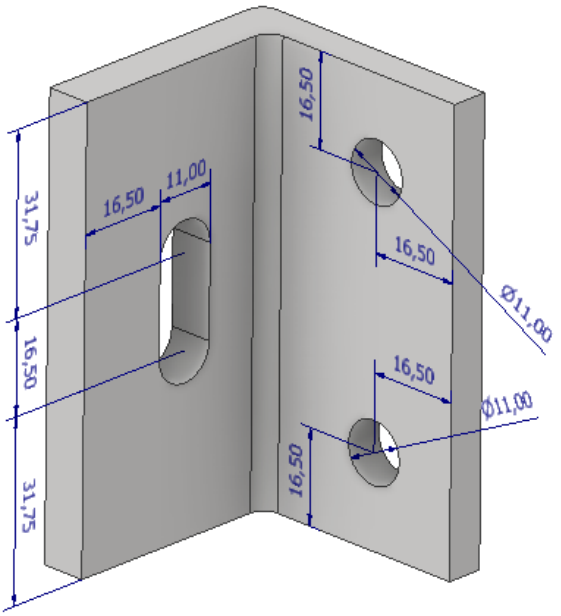

Figure 12 *Bolt hole placement and extrusion length for small wind L-profile. All bolts are size M10.*